



저작자표시-비영리-변경금지 2.0 대한민국

이용자는 아래의 조건을 따르는 경우에 한하여 자유롭게

- 이 저작물을 복제, 배포, 전송, 전시, 공연 및 방송할 수 있습니다.

다음과 같은 조건을 따라야 합니다:



저작자표시. 귀하는 원저작자를 표시하여야 합니다.



비영리. 귀하는 이 저작물을 영리 목적으로 이용할 수 없습니다.



변경금지. 귀하는 이 저작물을 개작, 변형 또는 가공할 수 없습니다.

- 귀하는, 이 저작물의 재이용이나 배포의 경우, 이 저작물에 적용된 이용허락조건을 명확하게 나타내어야 합니다.
- 저작권자로부터 별도의 허가를 받으면 이러한 조건들은 적용되지 않습니다.

저작권법에 따른 이용자의 권리는 위의 내용에 의하여 영향을 받지 않습니다.

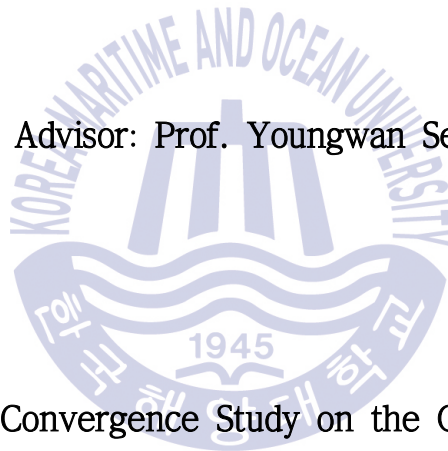
이것은 [이용허락규약\(Legal Code\)](#)을 이해하기 쉽게 요약한 것입니다.

[Disclaimer](#)

Thesis for Master Degree

An exploratory study on bioactive constituents
from the sponge *Coscinoderma* sp.

Advisor: Prof. Youngwan Seo



Department of Convergence Study on the Ocean Science and
Technology

School of Ocean Science and Technology

Korea Maritime and Ocean University

Hui Jeong Jeong

February. 2017

Approved by the Committee of the Ocean Science and Technology
School of Korea Maritime and Ocean University in Fulfillment of the
Requirements for the Degree of Master of Science

Dissertation Committee :

Prof. Sun-Young Lim, Chair

Prof. In-Seok Park , Advisor

Prof. Youngwan Seo, Advisor



2017. 12. 15

Department of Convergence Study on
the Ocean Science and Technology School
of Ocean Science and Technology Korea Maritime and Ocean University

Hui Jeong Jeong

Index

List of Schemes -----	i
List of Tables -----	ii
List of Figures -----	iii
List of Abbreviations -----	vii
Korean Abstract (국문 요약) -----	1
1. Introduction -----	3
2. Materials and Methods -----	7
2.1. Materials -----	7
2.2. General experimental procedures -----	8
2.3. Extraction and fractionation, and isolation -----	9
2.4. Antioxidant activity -----	16
2.4.1. DPPH radical scavenging activity -----	16
2.4.2. Peroxynitrite scavenging activity -----	19
2.4.3. Ferric reducing antioxidant power (FRAP) assay -----	22
2.4.4. Cell culture and measurement of cell viability by MTT assay -----	22
2.4.5. Determination of intracellular formation of reactive oxygen species (ROS) using DCFH-DA labelling -----	23
2.5. Antiproliferative activity assay against human cancer cells -----	26
2.5.1. Cell cultures and inhibition of cancer cell proliferation -----	26
2.6. Anti-inflammatory activity assay -----	27
2.6.1. Cell culture and determination of nitric oxide (NO) production ---	27

2.6.2 Reverse transcription-polymerase chain reaction (RT-PCR) -	29
2.7. Statistical analysis -----	29
3. Results and discussion -----	31
3.1. Isolation and structure determination of compounds -----	31
3.2. Antioxidant effects of crude extract and its solvent fractions ----	42
3.2.1. DPPH radical scavenging activity -----	42
3.2.2. Peroxynitrite scavenging activity -----	44
3.2.3. Ferric reducing antioxidant power (FRAP) assay -----	46
3.2.4. Intracellular ROS scavenging activity in HT-1080 cells-----	48
3.2.4.1. Assessment of cell viability by crude extract and its solvent fractions in HT-1080 cells -----	48
3.2.4.2. Determination of intracellular formation of ROS using DCFH-DA labeling -----	49
3.3. Antiproliferation effects of crude extract and its solvent fractions on human cancer cells -----	52
3.3.1. Antiproliferation effect against the growth of HT-1080 cells -	52
3.3.2. Antiproliferation effect against the growth of AGS cells ----	52
3.3.3. Antiproliferation effect against the growth of HT-29 cells --	52
3.3.4. Antiproliferation effect against the growth of MCF-7 cells --	53
3.4. Anti-inflammatory effects of crude extract and its solvent fractions -----	56
3.4.1. Measurement of cell viability by crude extract and its solvent fractions in Raw 264.7 cells -----	56
3.4.2. Determination of nitric oxide (NO) production -----	58
3.4.3. Reverse transcription-polymerase chain reaction (RT-PCR) -	60

3.5. Antioxidant effects of compounds 1-9 -----	63
3.5.1. DPPH radical scavenging activity -----	63
3.5.2. Peroxynitrite scavenging activity -----	65
3.5.3. Ferric reducing antioxidant power (FRAP) assay -----	68
3.5.4. Antioxidant effects of compounds 1-9 intracellular -----	70
3.5.4.1. Measurement of cell viability by compounds 1-9 in HT-1080 cells -----	70
3.5.4.2. Determination of intracellular formation of ROS using DCFH-DA labeling -----	72
3.6. Antiproliferative effects of compounds 1-9 -----	76
3.6.1. Antiproliferative effect against the growth of HT-1080 cells	76
3.6.2. Antiproliferative effect against the growth of AGS cells ----	76
3.6.3. Antiproliferative effect against the growth of HT-29 cells --	77
3.6.4. Antiproliferative effect against the growth of MCF-7 cells --	77
3.7. Antiinflammatory effects of compounds 1-9 -----	82
3.7.1. Measurement of cell viability by compounds 1-9 in Raw 264.7 cells -----	82
3.7.2. Determination of nitric oxide (NO) production -----	84
 4. Conclusion -----	 86
 Reference -----	 88
 Appendix -----	 91

List of Schemes

Scheme 1. Flow diagram for extraction and fractionation of the sponge <i>Coscinoderma</i> sp. -----	10
Scheme 2. Isolation procedure of compound 1 from the sponge <i>Coscinoderma</i> sp. -----	12
Scheme 3. Isolation procedure of compound 2 from the sponge <i>Coscinoderma</i> sp. -----	13
Scheme 4. Isolation procedure of compounds 3, 4, 5 and 6 from the sponge <i>Coscinoderma</i> sp. -----	14
Scheme 5. Isolation procedure of compounds 7, 8 and 9 from the sponge <i>Coscinoderma</i> sp. -----	15
Scheme 6. Measurement of DPPH radical scavenging effect -----	18
Scheme 7. Measurement of the ONOO ⁻ scavenging effect -----	21

List of Tables

Table 1.	Sequences of primes used for RT-PCR -----	30
Table 2.	^1H and ^{13}C NMR spectral data for compound 1 isolated from the sponge <i>Coscinoderma</i> sp. -----	34
Table 3.	^1H and ^{13}C NMR spectral data for compound 2 isolated from the sponge <i>Coscinoderma</i> sp. -----	35
Table 4.	^1H and ^{13}C NMR spectral data for compound 3 isolated from the sponge <i>Coscinoderma</i> sp. -----	36
Table 5.	^1H and ^{13}C NMR spectral data for compound 4 isolated from the sponge <i>Coscinoderma</i> sp. -----	37
Table 6.	^1H and ^{13}C NMR spectral data for compound 5 isolated from the sponge <i>Coscinoderma</i> sp. -----	38
Table 7.	^1H and ^{13}C NMR spectral data for compound 6 isolated from the sponge <i>Coscinoderma</i> sp. -----	39
Table 8.	^1H NMR spectral data for compounds 7 , 8 and 9 isolated from the sponge <i>Coscinoderma</i> sp. -----	40

List of Figures

Fig. 1.	Compounds isolated from the sponge <i>Coscinoderma</i> sp. ----	6
Fig. 2.	Photographs of the sponge <i>Coscinoderma</i> sp. -----	7
Fig. 3.	Scavenging of the DPPH radical by phenol -----	17
Fig. 4.	Peroxynitrite (ONOO ⁻) mediated oxidation of DHR123 -----	20
Fig. 5	Metabolization of MTT to a MTT formazan by viable cells -	24
Fig. 6.	Degradation pathway of DCFH-DA in an oxidation-induced cellular system -----	25
Fig. 7.	Coloring reaction of NO ₂ ⁻ detection -----	28
Fig. 8.	Chemical structure of compounds 1-9 from the sponge <i>Coscinoderma</i> sp. -----	41
Fig. 9.	DPPH radical scavenging effect of crude extract and its solvent fractions from the sponge <i>Coscinoderma</i> sp. -----	43
Fig. 10.	Scavenging effects of crude extract and its solvent fractions from the sponge <i>Coscinoderma</i> sp. on authentic ONOO (% of control) -----	45
Fig. 11.	Scavenging effects of crude extract and its solvent fractions from the sponge <i>Coscinoderma</i> sp. on ONOO ⁻ from SIN-1 (% of control) -----	45
Fig. 12.	Ferric reducing antioxidant power assay of crude extract and its solvent fractions from the sponge <i>Coscinoderma</i> sp. -	47
Fig. 13.	Effect of crude extract and its solvent fractions from the sponge <i>Coscinoderma</i> sp. on viability of HT-1080 cells ----	48

Fig. 14.	Scavenging effects of crude extract and its solvent fractions from the sponge <i>Coscinoderma</i> sp. on intracellular ROS levels induced by hydrogen peroxide in HT-1080 cells -----	50
Fig. 15.	Antiproliferative effect of crude extract and its solvent fractions from the sponge <i>Coscinoderma</i> sp. on viability of cancer cells -----	54
Fig. 16.	Effect of crude extract and its solvent fractions from the sponge <i>Coscinoderma</i> sp. on viability of Raw 264.7 cells -	57
Fig. 17.	Effects of crude extract and its solvent fractions from the sponge <i>Coscinoderma</i> sp. on nitrite production in Raw 264.7 cells -----	59
Fig. 18.	Effects of crude extract and its solvent fractions from the sponge <i>Coscinoderma</i> sp. on mRNA levels -----	60
Fig. 19.	DPPH radical scavenging effect of compounds 1-9 from the sponge <i>Coscinoderma</i> sp. -----	64
Fig. 20.	Scavenging effects of compounds 1-9 from the sponge <i>Coscinoderma</i> sp. on authentic ONOO (% of control) ----	66
Fig. 21.	Scavenging effects of compounds 1-9 from the sponge <i>Coscinoderma</i> sp. on ONOO ⁻ from SIN-1 (% of control) -	67
Fig. 22.	Ferric reducing antioxidant power assay of compounds 1 and 2 from the sponge <i>Coscinoderma</i> sp. -----	69
Fig. 23.	Effect of compounds 1-9 from the sponge <i>Coscinoderma</i> sp. on viability of HT-1080 cells -----	71

Fig. 24.	Scavenging effects of compounds 1-9 from the sponge <i>Coscinoderma</i> sp. on intracellular ROS levels induced by hydrogen peroxide in HT-1080 cells -----	73
Fig. 25.	Antiproliferative effect of compounds 1-9 from the sponge <i>Coscinoderma</i> sp. on viability of HT-1080 cells --	78
Fig. 26.	Antiproliferative effect of compounds 1-9 from the sponge <i>Coscinoderma</i> sp. on viability of AGS cells -----	79
Fig. 27.	Antiproliferative effect of compounds 1-9 from the sponge <i>Coscinoderma</i> sp. on viability of HT-29 cells ----	80
Fig. 28.	Antiproliferative effect of compounds 1-9 from the sponge <i>Coscinoderma</i> sp. on viability of MCF-7 cells ---	81
Fig. 29.	Effect of compounds 1-9 from the sponge <i>Coscinoderma</i> sp. on viability of Raw 264.7 cells -----	83
Fig. 30.	Effect of compounds 1-9 from the sponge <i>Coscinoderma</i> sp. on nitrite production in Raw 264.7 cells -----	85
Fig. 31	¹ H and ¹³ C NMR spectrum of compound 1 isolated from the sponge <i>Coscinoderma</i> sp. in CD ₃ OD -----	91
Fig. 32.	¹ H and ¹³ C NMR spectrum of compound 2 isolated from the sponge <i>Coscinoderma</i> sp. in CD ₃ OD -----	92
Fig. 33	¹ H and ¹³ C NMR spectrum of compound 3 isolated from the sponge <i>Coscinoderma</i> sp. in CDCl ₃ -----	93
Fig. 34	¹ H COSY and TOCSY spectrum of compound 3 isolated from the sponge <i>Coscinoderma</i> sp. in CDCl ₃ -----	94
Fig. 35	gHMQC and gHMBC spectrum of compound 3 isolated from the sponge <i>Coscinoderma</i> sp. in CDCl ₃ -----	95

Fig. 36	^1H and ^{13}C NMR spectrum of compound 4 isolated from the sponge <i>Coscinoderma</i> sp. in CDCl_3 -----	96
Fig. 37	^1H and ^{13}C NMR spectrum of compound 5 isolated from the sponge <i>Coscinoderma</i> sp. in CD_3OD -----	97
Fig. 38	gHMBC spectrum of compound 5 isolated from the sponge <i>Coscinoderma</i> sp. in CD_3OD -----	98
Fig. 39	^1H and ^{13}C NMR spectrum of compound 6 isolated from the sponge <i>Coscinoderma</i> sp. in benzene- d_6 -----	99
Fig. 40	^1H NMR spectrum of compound 7 isolated from the sponge <i>Coscinoderma</i> sp. in D_2O -----	100
Fig. 41	^1H NMR spectrum of compound 8 isolated from the sponge <i>Coscinoderma</i> sp. in D_2O -----	101
Fig. 42	^1H NMR spectrum of compound 9 isolated from the sponge <i>Coscinoderma</i> sp. in D_2O -----	102
Fig. 43	Chemical structure of compounds 1-9 from the sponge <i>Coscinoderma</i> sp. -----	103

List of Abbreviations

Benzene- d_6	: deuterated benzene
BHA	: butylated hydroxyanisole
BHT	: butylated hydroxytoluene
$CDCl_3$: deuterated chloroform
CD_3OD	: deuterated methanol
CH_2Cl_2	: dichloromethane (methylene chloride)
^{13}C NMR	: carbon 13 nuclear magnetic resonance
D_2O	: deuterated water
DPPH	: 1,1-diphenyl-2-picryl-hydrazyl
EtOAc	: ethyl acetate
Fig.	: figure
H_2O	: water
1H NMR	: proton nuclear magnetic resonance
Hz	: herz (sec^{-1})
MeOH	: methanol
<i>n</i> -BuOH	: normal-butanol
$NO \cdot$: nitric oxide radical
$\cdot O_2^-$: superoxide anion radical
$\cdot OH$: hydroxyl radical
$ONOO^-$: peroxyxynitrite
ROS	: reactive oxygen species
RP	: reversed phase
TLC	: thin layer chromatography
UV	: ultraviolet

해면동물 *Coscinoderma* sp.로부터 생리활성 성분의 탐색

정 희 정

한국해양대학교 해양과학기술전문대학원

해양과학기술융합학과

요 약

해면동물 *Coscinoderma* sp. 시료를 methylene chloride와 methanol로 추출하여 조추출물을 얻었으며 이 조추출물을 용매 극성도에 따라 분획하여 4가지 용매분획층들인 *n*-hexane, 85% aqueous methanol (85% aq.MeOH), *n*-butanol (*n*-BuOH), water 분획층을 얻었다. 이렇게 얻어진 조추출물과 용매분획층에 대한 항산화활성, 암세포 증식억제 활성, 그리고 항염증활성을 검색하였다.

항산화활성 검색은 DPPH radical, peroxyntirite (ONOO⁻), 그리고 세포내 ROS (reactive oxygen species)에 대한 소거효과와 ferric ion에 대한 환원력을 측정하였다. 전반적으로 85% aq.MeOH과 *n*-BuOH 분획층에서 유의한 항산화효과가 관측되었다. DPPH radical 소거활성은 85% aq.MeOH과 *n*-BuOH 분획층이 유의적인 소거효과를 보여주었으나 *n*-BuOH 분획층이 좀 더 높은 소거효과를 나타내었다. Peroxyntirite에 대해서도 85% aq.MeOH과 *n*-BuOH 분획층이 높은 소거효과를 보여 주었다 하지만 ferric ion에 대한 환원력 측정에 있어서는 85% aq.MeOH과 *n*-BuOH 분획층이 농도의존적인 환원력을 나타내었으나 효과가 뛰어나지는 못하였다. HT-1080 세포내에 생성된 ROS의 소거활성실험에서는 water층을 제외한 모든 용매분획층들이 높은 소거능을 보여주었으나 그 중에서

n-BuOH 분획층이 가장 좋은 소거능을 나타내었다. 이 뿐만 아니라 lipopolysaccharide (LPS)로 자극된 Raw 264.7 cells에서 생성되는 nitric oxide (NO·)에 대해서도 모든 용매분획들이 농도의존적으로 억제효과를 나타내었으나 그 중에서 *n*-BuOH 분획층이 가장 좋은 NO 생성억제 효과를 나타내었다. 또한 염증매개인자들인 iNOS, COX-2, IL-1 β , IL-6, TNF- α 의 mRNA 발현측정에서 85% aq.MeOH과 *n*-BuOH 분획층이 좋은 발현 억제효과를 나타내었다. 인체 암세포들에 대한 증식억제실험에서 모든 용매분획들이 모든 암세포들(HT-1080, AGS, HT-29 및 MCF-7)에 대해 농도의존적인 증식억제효과를 나타내었으나 그 효과는 높지 않았으며 *n*-BuOH 분획층이 상대적으로 비교적 좋은 효과를 나타내었다.

생리활성 스크리닝 결과가 가장 좋은 *n*-BuOH 분획층으로부터 sesterterpene 유도체인 Halisulfate 1 (1)과 3개의 nucleoside인 2'-Deoxyadenosine (7), 2'-Deoxyuridine (8), Thymidine (9)을 분리하였으며 85% aq.MeOH 분획층에서는 sesterterpene 유도체인 Halisulfate 2 (2)를 분리하였다. 또 *n*-hexane 분획층으로부터는 epidioxysteroide 유도체들인 (24S)-5,8-epidioxy-24-methylcholest-6-en-3 β -ol (3), 5 α ,8 α -epidioxycholesta-6,22-dien-3 β -ol (4), 5 α ,8 α -epidioxy-cholesta-6-en-3 β -ol (5) 그리고 5 α ,8 α -epidioxy-24-methylcholest-6,9(11)-dien-3 β -ol (6)이 분리되었다.

분리된 화합물들(1-9)에 대한 항산화, 항염증, 암세포 증식억제 활성을 측정하였으며 halisulfates 1 (1)과 2 (2)가 비교적 좋은 항산화 활성을 나타내었다. 하지만 항염증이나 암세포 증식억제에 있어서는 농도의존적인 억제효과는 관측되었지만 주목할만한 유의적인 활성을 보여주지는 못하였다.

주제어: 해면동물 *Coscinoderma* sp; antioxidant activity 항산화 효과; secondary metabolism 2차 대사산물

1. Introduction

From the ancient time, people have used terrestrial natural products such as herbs, in treating wounds and diseases. However, as the development of drugs from terrestrial organisms, a traditional repository of natural products has stagnated over the years, marine organisms can be emphasized as a new potential source.

In 1951, from the sponge *Cryptotethya crypta*, Werner and Bergmann reported isolation of arabinopentosyl and ribopentosyl nucleosides which are structurally very different from the conventional ones (Molinski et al., 2009). This finding led to increased interest in natural marine products, with more than 25,000 isolated by 2012.

Marine is a vast new field to be explored, expected to serve as a new source material, given that only less than 1% of marine natural products have been studied so far. Approximately 300,000 species are distributed throughout the oceans, with their primary productivity being five to seven times higher than that of terrestrial organisms. In addition, recent technological developments enabled us to more easily collect marine organisms from deep sea, leading to much more attention to them.

With this focus on marine natural products, coastal nations are strongly claiming exclusive rights for living resources inhabiting in their territorial waters. Due to the increasing conflicts over the allocation of profits between countries studying the living resources and those providing them, the Nagoya Protocol was signed in 2010 to

mediate the issue.

According to the treaty, countries doing the research on other territorial waters should notify the providing nations in advance to gain approval for samples collection. Furthermore, profits due to development of bioresources should be distributed between them according to the terms of the protocol. Therefore, the acquisition of domestic and foreign living resources have become increasingly important.

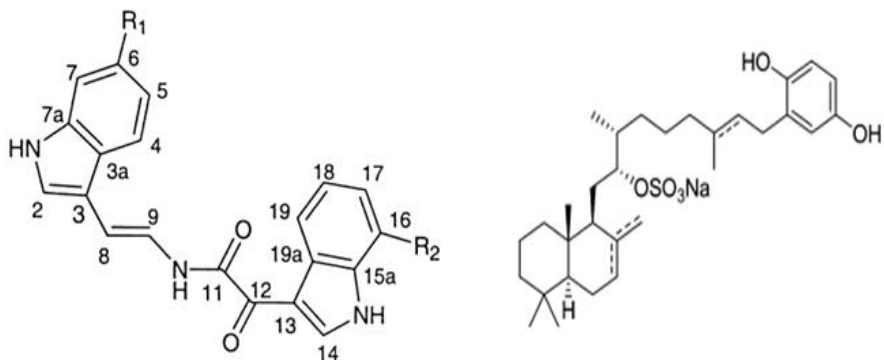
In a recent search for bioactivity of marine organisms, researchers have isolated substances that are much more potent and effective than terrestrial organisms. The marine organism to have received the highest level of attention is sponge, one of the marine colonial animals. This is the sticky multicellular animal that ingests nutrients by filtering water. Knowledge of sponge biodiversity is still incomplete and about 11,000 species have been formally described to date. however, more than 15,000 species are thought to exist on earth.

Sponges, which are sessile animal, have little movement and thus are unable to protect themselves from predation. Therefore, sponges possess a powerful and diverse array of secondary metabolites (natural products) for chemical defense. In other words, sponges produce unique secondary metabolites in order to adapt to the harsh environment. Much attention was paid to these metabolites as attractive potential sources of new materials with unique structures and strong biological activities. It has also been known that marine organisms in tropical waters are more likely to contain secondary metabolites that have more

unusual carbon skeleton and more potent bioactivity than those living in other waters. This can be ascribed to intense competition between species under the stable physical environment of tropical waters.

Many bioactive compounds, potential candidates for the treatment of diseases were isolated from sponges. These include the following compounds: ara-A (vidarabine) as the antiviral agent; discodermide and discodermolide as the antifungal, anti-cancer and immunosuppressive agents; manoalide as the potent anti-inflammatory agent; topsentins as the anti-cancer and anti-inflammatory agents; manzamine as the antimalaria, antituberculosis, and anti-AIDS agents. In addition, the polyketides PM050489 and PM060184, isolated from the sponge *Lithoplocamia lithistoides* in Madagascar, have been shown to have strong anticancer effects, and are therefore currently in clinical trials (Martin et al., 2013; Newman & Cragg, 2016). In particular, eribulin, a synthetic derivative of halichondrin B isolated as a potent anticancer agent from *Halichondria okakai* and *Lissodendryx* sp., has been developed as a drug for the treatment of breast cancer and liposarcoma and is already marketed under the tradename Halaven (E7389) (Silva & Scheuer, 1980; Hirata & Uemura, 1986; Zabriskie et al, 1986; Crews et al., 1986).

In our search for bioactive substances from marine resources, we collected the sponge *Coscinoderma* sp. from coastal area of Chuuk state, Federated States of Micronesia. Herein we report the isolation of the secondary metabolites from *Coscinoderma* sp., and their antioxidant, anti-inflammatory, and anticancer activities.



- (1) $R_1 = \text{Br}$, $R_2 = \text{H}$ (4) $17E$, Δ^7
 (2) $R_1 = R_2 = \text{H}$ (5) $17E$, $\Delta^{8,22}$
 (3) $R_1 = \text{Br}$, $R_2 = \text{OH}$ (6) $17Z$, Δ^7

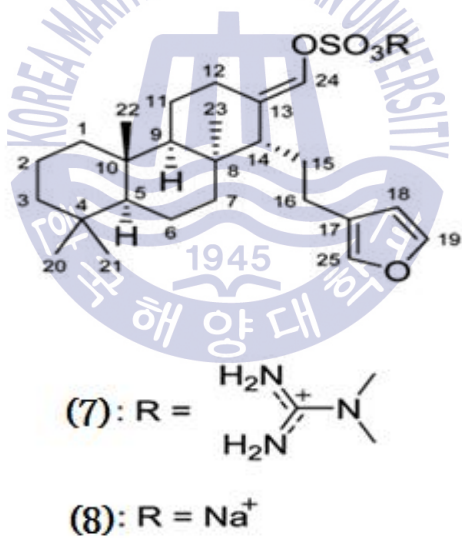


Fig. 1. Compounds isolated from the sponge *Coscinoderma* sp..

2. Materials and Methods

2.1. Materials

The specimens of the sponge were collected off the shore of chuuk Island, Federated States of Micronesia, using scuba. They were kept in -25°C until chemically investigated (Fig. 2).



Fig. 2. Photograph of the sponge *Coscinoderma* sp..

2.2. General experimental procedures

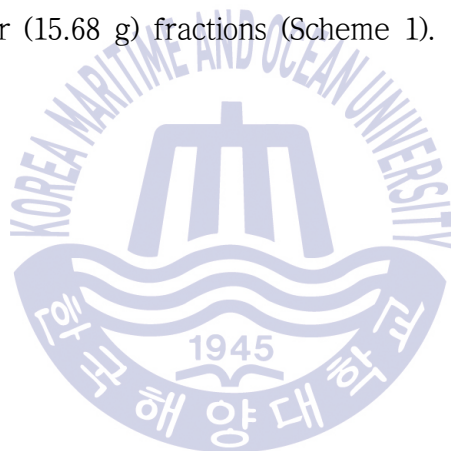
RP-18 (YMC-Gel ODS-A, 12 mm, S-75 μm) was used as column packing material, and TLC was carried out on Silica gel 60 F₂₅₄ plate (Merck). HPLC was performed on column (YMC pack ODS-A, 250 \times 10 mm, S 5 μm , 12 mm) and the guard column (7.5 \times 4.6 mm, Alltech).

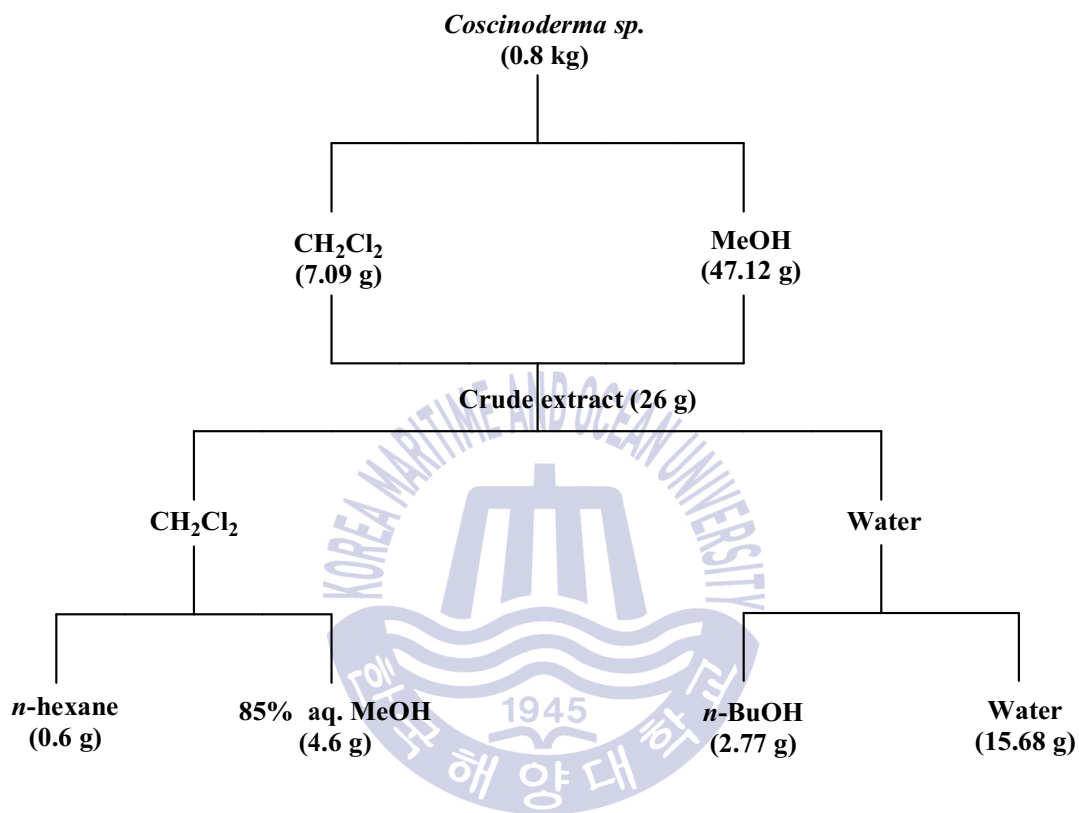
1,1-Diphenyl-2-picrylhydrazyl radical (DPPH), 3-morpholinsydnonimine (SIN-1), dihydrorhodamine 123 (DHR 123), and DL-2-amino-3-mercaptopropanoic acid (DL-penicillamine) were purchased from Sigma aldrich (St Louis, MO, USA). Fetal Bovine Serum (FBS), penicillin-streptomycin, phosphate buffered saline (PBS), and 0.05% trypsin-0.02% EDTA were purchased from Gibco (Grand Island, NY, USA). RPMI 1640 required for cell culture, peroxyntirite (ONOO⁻), and DCFH-DA were purchased from Hyclone (Logan, Utah, USA), Cayman (Ann Arbor, MI, USA), and Molecular Probes Inc. (Eugan, OR, USA), respectively.

NMR spectra were recorded on a Varian NMR 300 spectrometer (300 MHz for ¹H and 75.5 MHz for ¹³C). Chemical shifts were referenced to the respective residual solvent peaks, recorded in δ values, and expressed in ppm. High performance liquid chromatography (HPLC) was performed with a Dionex P580 with a Varian 350 RI detector. Antioxidant, antiproliferation activity, and anti-inflammation activities were measured by UV-Vis spectrophotometer (Thermo Spectronic, England) and Multi-detection microplate fluorescence spectrophotometer Synerge HT (Bio-TEK instruments, USA).

2.3. Extraction and fractionation, and isolation

The freeze-dried sponge materials (0.8 kg) were chopped into small pieces. They were extracted twice for 24 h with methylene chloride (CH_2Cl_2) at room temperature, and then twice with methanol (MeOH), in turn. The extracted solution was evaporated to dryness under reduced pressure (EYELA, N-N series, Japan). The residue was partitioned between methylene chloride and water. The organic layer was further partitioned between *n*-hexane and 85% aq.MeOH and then the aqueous layer was fractionated with *n*-BuOH and water, successively, to afford *n*-hexane (600 mg), 85% aq.MeOH (4.6 g), *n*-BuOH (2.77 g), water (15.68 g) fractions (Scheme 1).





Scheme 1. Flow diagram for extraction and fractionation of the sponge *Coscinoderma sp.*.

A portion of *n*-BuOH fraction (1.30 g) was separated into 7 subfractions by C-18 chromatography eluting with stepwise gradient mixtures of MeOH/water (50%, 60%, 70%, 80%, 90% aq.MeOH, and 100% MeOH). The fourth fraction (0.31 g) was subjected to preparative TLC on a Silica gel with the solvent MeOH/CH₂Cl₂ (1:3) to yield compound **1** (15 mg) (Scheme 2). The first fraction (0.41 g) was also subjected to preparative TLC on a Silica gel with elution by EtOAc/MeOH (9:1). Further purification of the mixture was made by reversed-phase HPLC (YMC ODS-A, 20% aq.MeOH) to yield compound **7** (3.1 mg), **8** (6.3 mg), and **9** (7.8 mg) (Scheme 5).

A portion of the 85% aq.MeOH fraction (2.45 g) was subjected to C-18 chromatography using gradient mixtures of MeOH and H₂O (elution order: 50, 60, 70, 80, 90% aq.MeOH, 100% MeOH). Further purification of the fourth fraction (100 mg) by preparative TLC on a Silica gel column with MeOH/CH₂Cl₂/water (5:25:1) as eluent followed by reversed-phase HPLC (YMC ODS-A, 75% aq.MeOH) to afford (5 mg) of compound **2** (Scheme 3).

The *n*-hexane fraction (0.6 g) was chromatographed on a silica gel eluting with stepwise gradient mixtures of *n*-hexane/EtOAc (100% *n*-hexane, 5%, 10%, 20%, 30%, 40%, 50%, 60%, 70% EtOAc in *n*-hexane, and 100% EtOAc). The fifth fraction (62 mg) was separated by reversed-phase HPLC (YMC ODS-A, MeOH:AcCN=1:3) to yield compound **3** (14 mg) and a mixture. Further purification of the mixture was made by reversed-phase HPLC (YMC ODS-A, 95% aq.MeOH) to give compound **4** (4.6 mg), compound **5** (6.3 mg), **6** (1.8 mg).

Compound **6**: ¹H NMR (benzene-d₆, 800 MHz) δ 6.40 (1H, d, *J*=8.5 Hz, H-7), 6.01 (1H, d, *J*=8.5 Hz, H-6), 5.24 (1H, dd, *J*=5.8 Hz, H-11), 3.94 (1H, m, H-3), 0.94 (1H, s, H-19) 0.94 (3H, d, *J*=6.4 Hz, H-26/27), 0.93 (3H, d, *J*=6.4, H-26/27), 0.86 (3H, d, *J*=6.4, H-21), 0.62 (3H, s, H-18); ¹³C NMR (benzene-d₆, 800 MHz) δ 144.4, 136.3, 131.2, 119.2, 82.8, 78.4, 66.5, 56.6, 48.8, 44.2, 42.0, 40.2, 38.7, 36.9, 36.7, 36.0, 33.4, 31.5, 30.6, 28.7, 25.9, 24.6, 23.4, 23.1, 21.6, 18.9, 13.33.

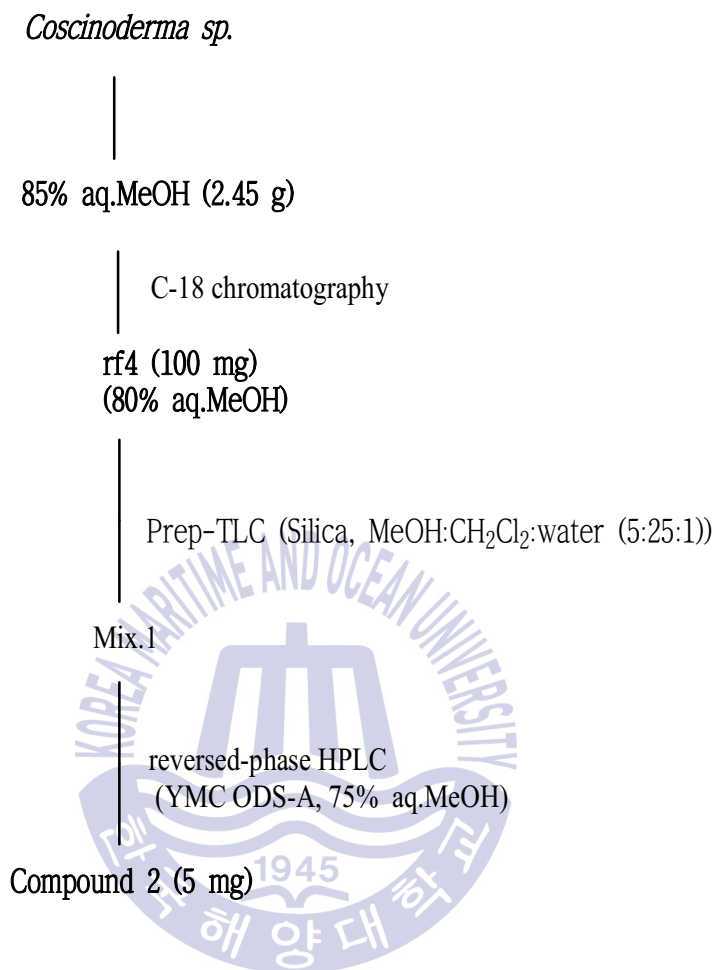
Coscinoderma sp.

|
n-BuOH (1.30 g)

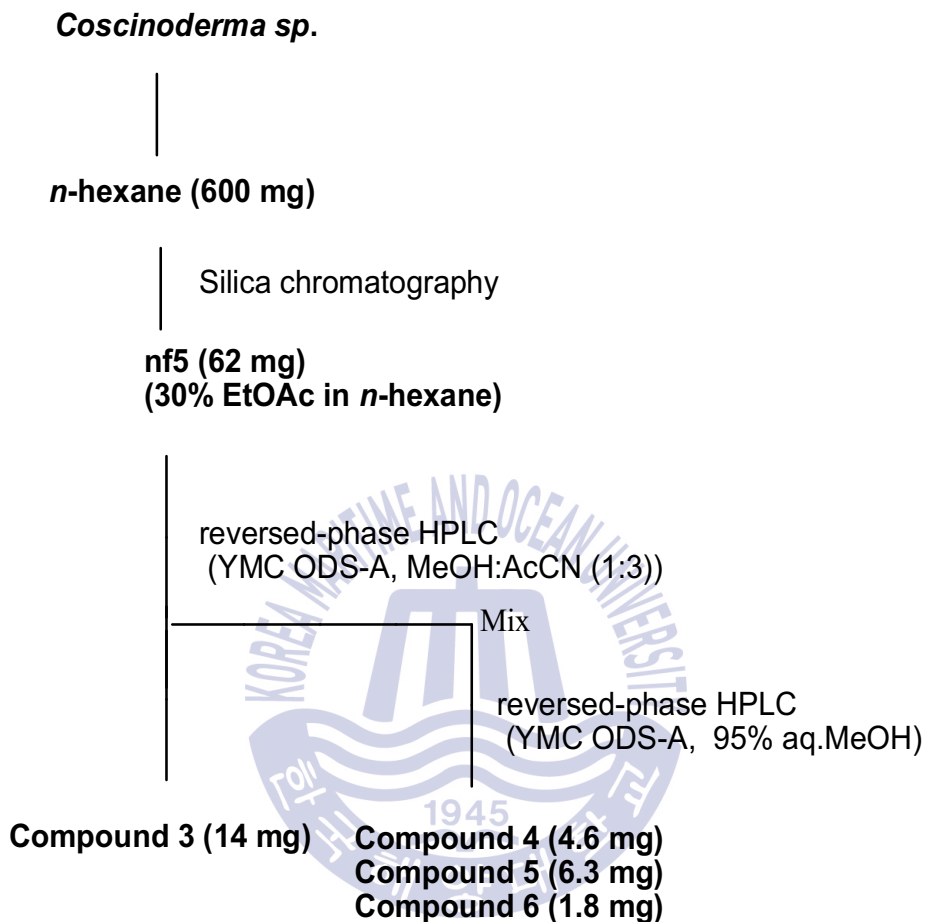
| C-18 chromatography
rf4 (310 mg)
(80% aq.MeOH)

| Prep-TLC (Silica, MeOH/CH₂Cl₂ (1:3))
Compound 1 (15 mg)

Scheme 2. Isolation procedure of compound 1 from the sponge *Coscinoderma* sp..



Scheme 3. Isolation procedure of compound **2** from the sponge *Coscinoderma* sp..



Scheme 4. Isolation procedure of compounds 3, 4, 5, and 6 from the sponge *Coscinoderma* sp..

Coscinoderma sp.

|
n-BuOH (1.30 g)

| C-18 chromatography
rf1 (410 mg)
(50% aq.MeOH)

| Prep-TLC (Silica, EtOAc/MeOH (9:1))
Compounds 7 (3.1 mg), 8 (6.3 mg), 9 (7.8 mg)

Scheme 5. Isolation procedure of compounds 7, 8, and 9 from the sponge
Coscinoderma sp..

2.4. Antioxidant activity

2.4.1. DPPH radical scavenging activity

1,1-Diphenyl-2-picryl-hydrazyl (DPPH) radical scavenging activity was determined using the method employed by Blois. (1958). To 1.0 mL of DPPH methanol solution (1.5×10^{-1} M), 4 mL of MeOH solution of various sample concentrations was added. After mixing gently and leaving for 10 min at room temperature, the optical density was measured at 518 nm using a spectrophotometer.



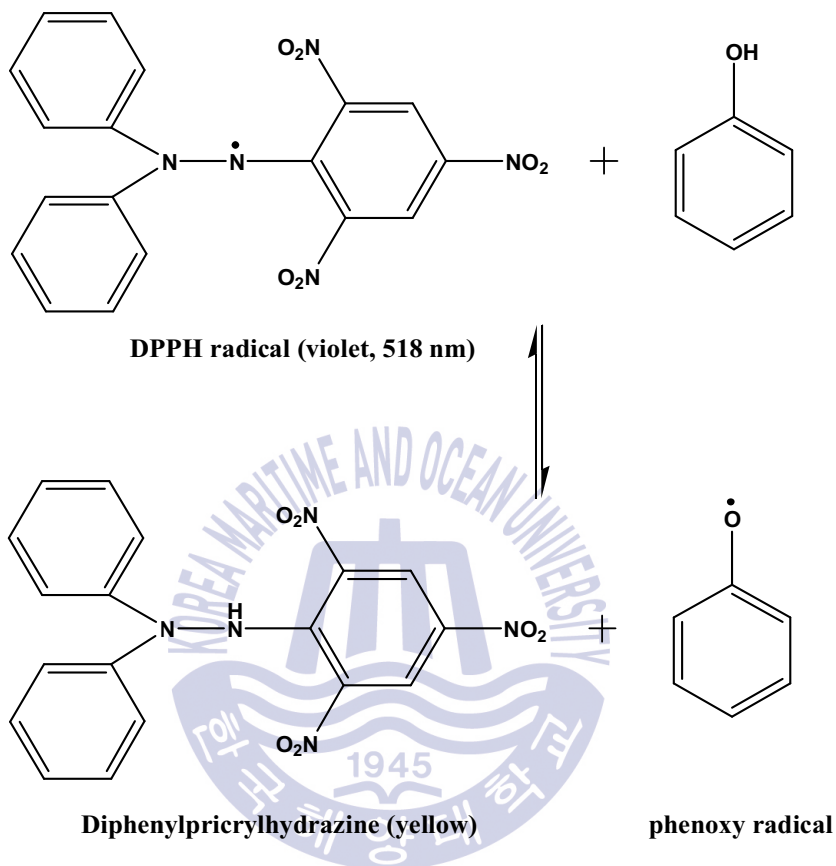
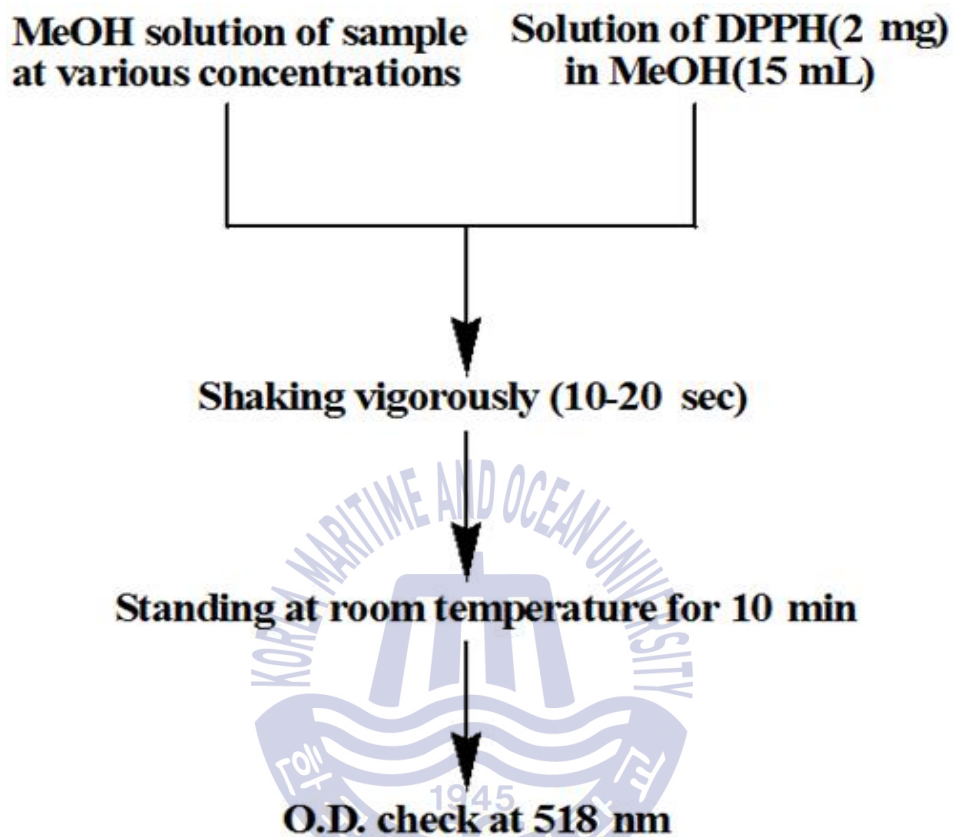


Fig. 3. Scavenging of the DPPH radical by phenol.



Scheme 6. Measurement of DPPH radical scavenging effect.

2.4.2. Peroxynitrite scavenging activity

The peroxynitrite (ONOO^-) scavenging activity was determined by monitoring the oxidation of dihydrorhodamine 123 (DHR 123) to rhodamine123 according to a modified version of the method of Kooy et al. (1994). The peroxynitrite reacts with DHR 123, causing oxidized DHR 123 to form, and its converted chemical structure is capable of emitting fluorescence. A stock solution of DHR 123 (5 mM) in dimethylformamide (DMF) was purged with nitrogen and kept at -80°C . A working solution of DHR 123 (final conc. 5 M) diluted from the stock solution was placed on ice in the dark immediately prior to the determinations. The buffer of 90 mM sodium chloride, 50 mM sodium phosphate (pH 7.4) and 5 mM potassium chloride was purged with nitrogen and placed on ice before use. At the beginning step of the experiments, diethylenetriaminepentaacetic acid (DTPA) (final conc. 100 mM) was added to the buffer. The fluorescence intensity of the oxidized DHR 123 was measured by a microplate fluorescence reader at excitation and emission wavelengths of 485 and 530 nm. The background and final fluorescent intensities were measured 5 min after treatment with or without SIN-1 (final conc. 10 mM) or authentic ONOO^- (final conc. 10 mM) in 0.3 M sodium hydroxide. L-ascorbic acid and penicillamine were used as a positive control.

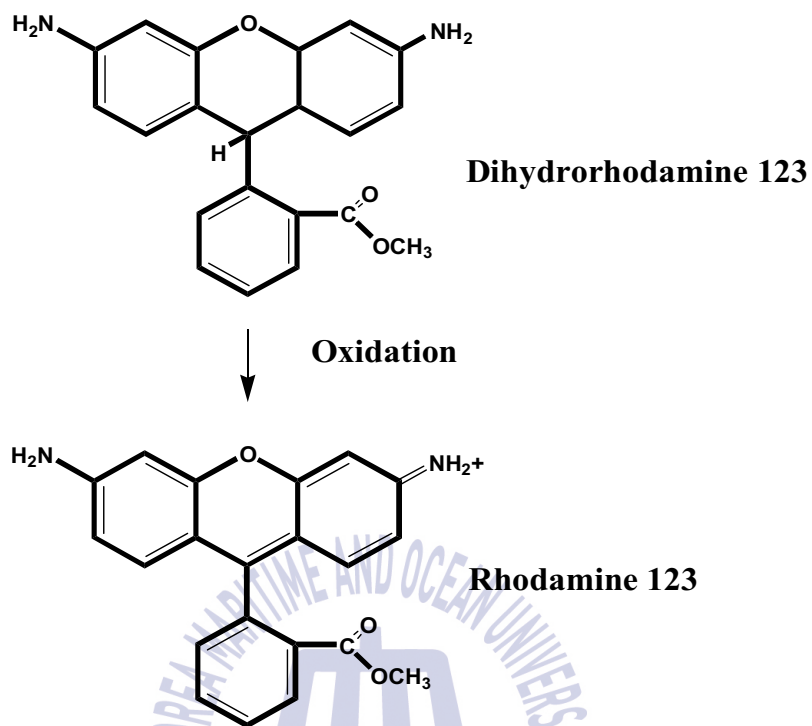


Fig. 4. Peroxynitrite (ONOO^-) mediated oxidation of DHR123.

Diethylenetriaminepentaacetic acid (DTPA) 100 μ M



Dihydrorhodamine 123 5 μ M



Incubation at 37°C for 1 min



Sample



Peroxyntirite 5 μ M or SIN-1 200 μ M



Measurement of fluorescence intensity

Excitation wavelength at 480 nm

Emission wavelength at 525 nm

Scheme 7. Measurement of the ONOO⁻ scavenging effect.

2.4.3. Ferric reducing antioxidant power (FRAP) assay

0.2 mL of sodium phosphate (pH 6.6) and 0.2 mL of 1% potassium ferricyanide were mixed with 0.2 mL of sample and the mixture was reacted at 50°C for 20 min. After adding 0.2 mL of 10% trichloroacetic acid, the mixture was centrifuged 10,000 rpm for 10 min, then 0.5 mL of the supernatant was reacted with 0.5 mL of 0.1% ferric chloride, and the absorbance was measured at 700 nm using a spectrophotometer. L-ascorbic acid was used as a control (Oyaizu, 1986).

2.4.4. Cell culture and measurement of cell viability by MTT assay

The HT-1080 cells were grown as monolayer in culture flasks with 5% CO₂ at 37°C in a humidified atmosphere supplemented with 10% fetal bovine serum (FBS), 2 mM glutamine and 100 µg/mL penicillin-streptomycin (Gibco Co.). RPMI was used as the culture mediums for HT-1080 cells. The medium was changed 5-6 times each week.

Cell viability of the tested samples on cultured cells was measured using 3-(4,5-dimethylthiazol-2-yl)-2,5-diphenyl-tetrazolium bromide (MTT) assay, which is based on the conversion of MTT to MTT-formazan by mitochondrial enzyme (Hansen et al., 1989). The cells were grown in 96-well plates at a density of 5×10^4 cells/well. After 24 h, the cells were washed with fresh medium and were treated with control medium or the medium supplemented with each solvent extract. After incubation for 24 h, the cells were rewashed and 100 µL of MTT solution (1 mg/mL) was added and incubated for 4 h. Finally, 100 µL of DMSO was added to solubilize the formed formazan crystals. The amount of formazan crystal was determined by measuring the absorbance at 540 nm using a multidetection microplate fluorescence spectrophotometer synergy HT (Bio-Tek instruments Inc., Wicooski, VT, USA). Relative cell viability was determined by the amount of MTT converted into a

formazan. Viability of cells was quantified as a percentage in comparison with the control (Fig. 5).

2.4.5. Determination of intracellular formation of reactive oxygen species (ROS) using DCFH-DA labelling

Intracellular formation of reactive oxygen species (ROS) was assessed using oxidation sensitive dye 2',7'-dichlorodihydrofluorescein-diacetate (DCFH-DA) as the substrate (Okimoto et al., 2000). The HT-1080 cells growing in fluorescence microtiter 96-well plates were loaded with 20 μ M DCFH-DA in HBSS and incubated for 20 min in the dark. Nonfluorescent DCFH-DA dye, which freely penetrates into cells, gets hydrolyzed by intracellular esterases to 2',7'-dichlorodihydrofluorescein (DCFH), and traps inside the cells. After treatment with the different concentrations of sample, the HT-1080 cells were incubated for 1 h. The culture medium was removed, the cells were washed three times with PBS, and 500 μ M H₂O₂ dissolved in HBSS was added to cells. The formation of 2',7'-dichlorofluorescein (DCF), a fluorescent compound ($\lambda_{\text{excitation}}=485$ nm; $\lambda_{\text{emission}}=528$ nm), due to oxidation of DCFH in the presence of various ROS, was read after every 30 min using a multidetection microplate fluorescence spectrophotometer synergy HT (Bio-Tek instruments, USA). Time-dependent effects of the sample groups were plotted and compared with fluorescence intensity of control and blank groups (Fig. 6).

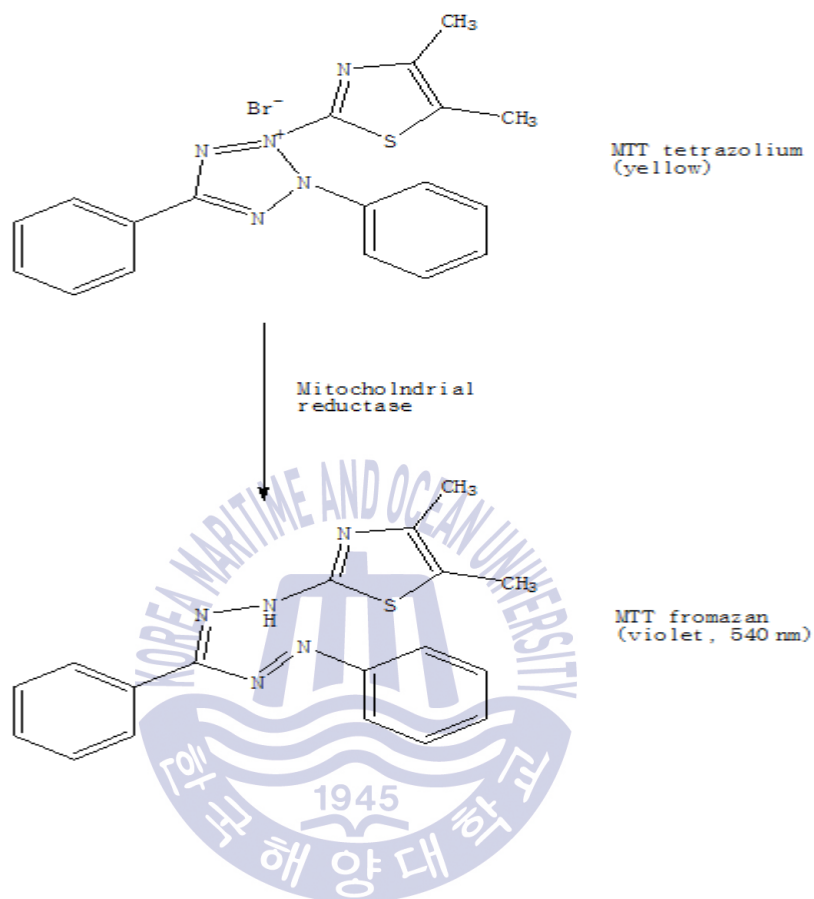


Fig. 5. Metabolization of MTT to a MTT formazan by viable cells.

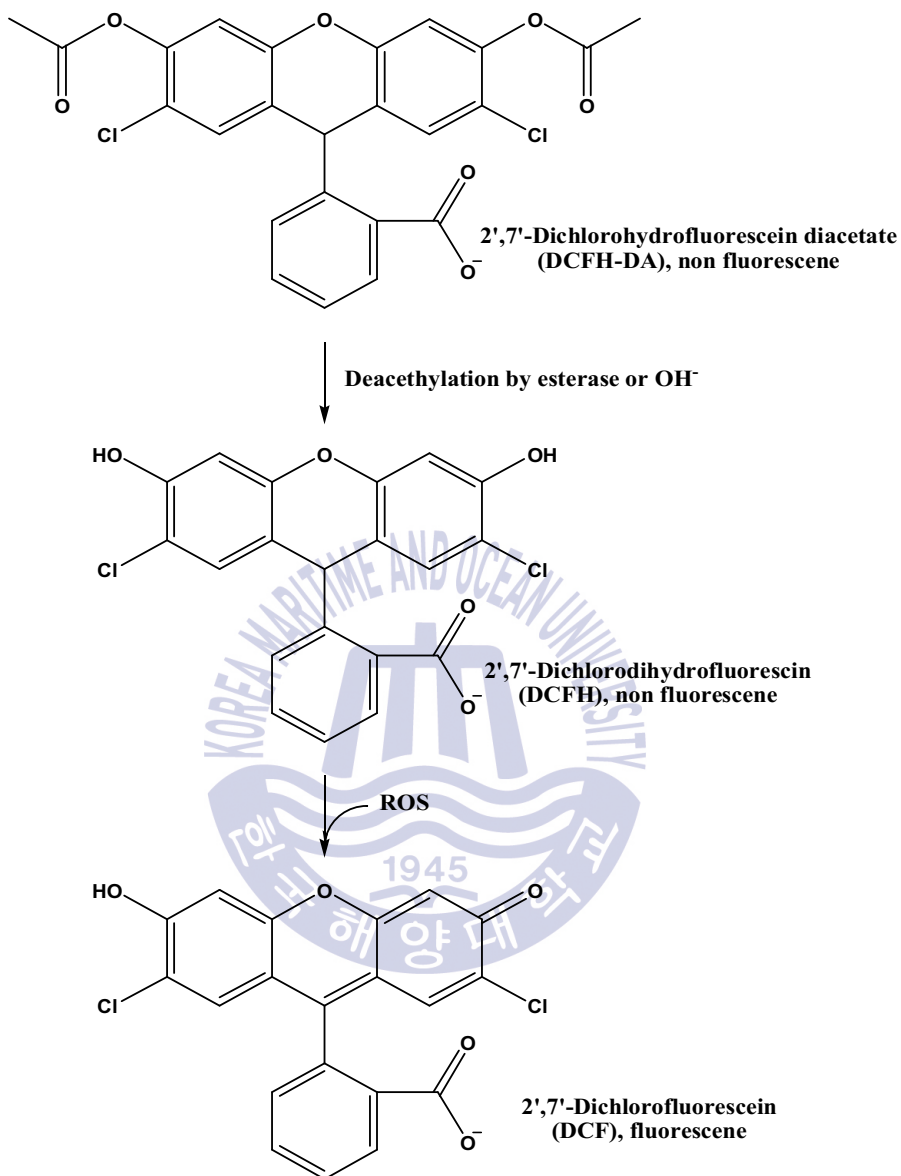


Fig. 6. Degradation pathway of DCFH-DA in an oxidation-induced cellular system.

2.5. Antiproliferative activity assay against human cancer cells

2.5.1. Cell cultures and inhibition of cancer cell proliferation

The HT-1080, AGS, HT-29 and MCF-7 cells were separately grown as monolayer in culture flask with 5% CO₂ and 37°C in a humidified atmosphere. The anti-cancer effect of the crude extract and its solvent fractions on cultured cells were determined using MTT assay. The cell number was adjusted to 5×10^3 cells/well in 96-well plates, for 24 h. After cells were treated with different concentrations of sample, they were incubated for 24 h. 100 μ L of MTT solution (1 mg/mL) was added and incubated for 4 h. Finally, the medium was removed and 100 μ L of DMSO was added to solubilize the formed formazan crystals, and absorbance was measured at 540 nm using a multidetection microplate fluorescence spectrophotometer synergy HT (Bio-Tek instruments Inc., Wicooski, VT, USA). The control medium was added with 1XPBS instead of the sample. Viability of cells was quantified as a percentage in comparison with the control (Twentyman & Luscombe, 1987).

2.6. Anti-inflammatory activity assay

2.6.1. Cell culture and determination of nitric oxide (NO) production

Macrophage Raw 264.7 cells grown as monolayers in T-75 tissue culture flasks (Nunc, Roskilde, Denmark) in a humidified atmosphere of 95% air with 5% CO₂ at 37 °C using appropriate media supplemented with 10% fetal bovine serum (FBS), 2 mM glutamine, and 100 μg/mL penicillin-streptomycin. Dulbecco's modified eagle medium (DMEM) was used as the culture mediums for Raw 264.7 cells. The medium was changed 5-6 times each week.

To determine the effects of samples on the NO production in the cultured media, the Raw 264.7 cells were seeded at densities of 2×10^5 cells/well in 96-well plates using DMEM without phenol red and allowed to adhere overnight with pre-treated test samples for 1 h. Cells were stimulated by adding 1 μg/mL final concentration of LPS and further incubated for 48 h. After incubation, the production of NO was determined based on the Griess reaction (Green et al., 1982). Each of the 50 μL of cultured medium was added onto a 96-well microtiter plate. The 50 μL of Griess reagent was added to each well and stand for 15 min at room temperature. The absorbance of the mixture at 550 nm was measured by using a multidetection microplate fluorescence spectrophotometer synergy HT (Bio-Tek instruments Inc., Wicooski, VT, USA). The concentrations of nitrite were calculated from regression analysis, using serial dilutions of sodium nitrite as a standard (Beda & Nedospasov, 2005) (Fig. 7).

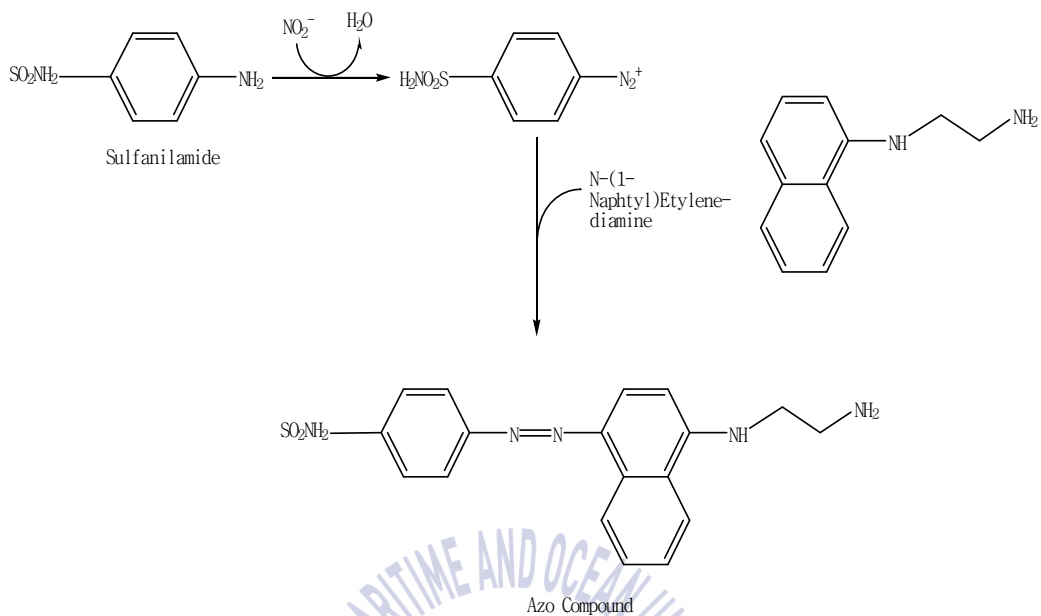
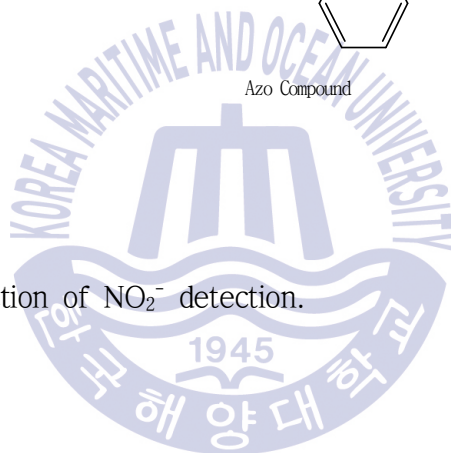


Fig. 7. Coloring reaction of NO_2^- detection.



2.6.2. Reverse transcription-polymerase chain reaction (RT-PCR)

The levels of tumor necrosis factor alpha (TNF- α), inducible nitric oxide synthase (iNOS), cyclooxygenase-2 (COX-2), interleukin-1 beta (IL-1 β), and interleukin 6 (IL-6) mRNA were determined by RT-PCR using the Raw 264.7 cells. Total RNA was isolated with Trizol reagent (Ambion, Life Technologies™, USA) according to manufacturer's recommendations. cDNA was synthesized from 2 μ g total RNA by incubation at 37°C for 1 h with AMV reverse transcriptase (Amersham) with random hexanucleotide.

The cDNA synthesized by the PCR PreMix was reacted with TNF- α , iNOS, COX-2, IL-1 β , and IL-6 primers (Table 1).

Amplification was performed in a master-cycle (Eppendorf, Hamburg, Germany) with cycles of predenaturation at 94°C for 5 min, denaturation at 94°C for 30 sec, annealing at 50–54°C for 30 sec and extension at 72°C for 1 min, respectively. The PCR products were visualized by electrophoresis through a 1.0% agarose gel stained with ethidium bromide (EtBr). The degree of mRNA expression was quantified using a UV Davinch-Chemi imager™ (CAS-400SM, Davinch-K, Seoul, Korea).

2.7. Statistical analysis

The data were presented as mean \pm SD. Differences between the means of the individual groups were assessed by one-way ANOVA with Duncan's multiple range tests. Differences were considered significant at $p < 0.05$. The statistical software package, SAS v9.1 (SAS Institute Inc., NC, USA), was used for these analyses.

Table 1. Sequences of primes used for RT-PCR

Gene	Direction	Sequence
iNOS	Forward	5'-TTC-CAG-AAT-CCC-TGG-ACA-AG-3'
	<u>Reverse</u>	5'-TGG-TCA-AAC-TCT-TGG-GGT-TC-3'
COX-2	Forward	5'-AGA-AGG-AAA-TGG-CTG-CAG-AA-3'
	<u>Reverse</u>	5'-GCT-CGG-CTT-CCA-GTA-TTG-AG-3'
IL-1 β	Forward	5'-GGG-CCT-CAA-AGG-AAA-GAA-TC-3'
	<u>Reverse</u>	5'-TAC-CAG-TTG-GGG-AAC-TCT-GC-3'
IL-6	Forward	5'-AGT-TGC-CTT-CTT-GGG-ACT-GA-3'
	<u>Reverse</u>	5'-CAG-AAT-TGC-CAT-TGC-ACA-AC-3'
β -Actin	Forward	5'-CCA-CAG-CTG-AGA-GGG-AAA-TC-3'
	<u>Reverse</u>	5'-AAG-GAA-GGC-TGG-AAA-AGA-GC-3'



3. Results and discussion

3.1. Isolation and structure determination of compounds

Compound **1** was isolated as a colorless gum. The presence of 2-alkyl-1,4-hydroquinone ring was readily recognized by an occurrence of proton signals for a trisubstituted aromatic ring (δ 6.56, d, $J = 8.4$ Hz; 6.52, d, $J=3.0$ Hz; 6.41, dd, $J=8.4, 3.0$ Hz) and a benzylic methylene group (δ 3.22, d, $J=7.2$ Hz) in the ^1H NMR spectrum. Olefinic proton signals were observed at δ 5.32 (1H, br s) and 5.30 (1H, br t, $J=7$ Hz). The corresponding olefinic carbon signals in ^{13}C NMR spectrum appeared at δ 150.8, 148.6, 136.8, 136.7, 130.1, 124.8, 123.9, 118.0, 117.5, and 114.8 that were assigned to the aromatic ring and two trisubstituted double bonds. In addition, carbon signal at δ 84.6 in ^{13}C NMR spectrum and proton signals at δ 4.50 in the ^1H NMR spectrum indicated the presence of one oxygenated methine carbon. Six methyl signals were also observed and two of them were the allylic methyl signals (δ_{H} 1.68, 6H, s; δ_{C} 16.3, 23.0) on a trisubstituted double bond (Table 2). With this information, literature survey revealed that compound **1** was halisulfate **1**, previously isolated from a sponge of the family *Halichondriidae*. Comparison of the spectral data of **1** showed very good correlation with published data for this compound (Kernan & Faulkner, 1988).

Compound **2** was isolated as a colorless gum. The existence of mono-substituted furan ring part was shown by proton signals at δ 6.28, 7.34 and 7.24 in the ^1H NMR spectrum and carbon signals at δ 111.8, 126.2, 139.9 and 143.7 in the ^{13}C NMR spectrum. ^1H NMR spectrum also revealed proton

signals of two trisubstituted double bonds (δ 5.40, 1H; 5.08, 1H), two vinylic methyl groups (δ 1.60, 6H), and an oxygen-bearing methylene (δ 3.92, 2H) (Table 3). With the aid of these informations, comparison of its ^1H and ^{13}C NMR spectroscopic data with those of Halisulfate 2, previously isolated from a sponge of the family *Halichondriidae* indicated that it was the same compound. Its NMR spectral data measured in the same NMR solvent were in good agreement with the reported data (Kernan & Faulkner, 1988).

Four epidioxy steroids (**3-6**) were isolated as white solids. The stereochemistry of their epidioxy centers at C-5 and C-8 was determined by careful examination of chemical shifts of the adjacent protons. According to the literature survey, chemical shifts of the H-6, H-7, H-18 and H-19 protons were significantly influenced by the stereochemistry at C-5 and C-8 (Greca et al., 1990). That is, the orientations of oxygens attached to the epidioxy centers influence the chemical shifts of the H-18 and H-19 methyl protons which in turn would change those of the H-6 and H-7 olefinic protons. In the case of a 5β , 8β -epidioxide, due to the spatial proximity with oxygens, the H-18 and H-19 methyl protons would be shifted downfield. In contrast, the H-6 and H-7 protons would be shifted upfield because the interactions with the H-18 and H-19 methyls disappeared. This phenomenon would be reversed in a 5α , 8α -epidioxide in that the olefinic protons would be shifted downfield by the spatial proximity with the methyl protons which were shifted upfield by the disappearance of the interaction with the oxygens. As a result, the chemical shifts of the H-6, H-7, H-18 and H-19 protons in a 5α , 8α -epidioxide were observed at δ 6.25, 6.51, 0.82, 0.89, respectively, while signals of the same protons were found at δ 5.57, 5.89, 1.18 and 0.93, respectively, in the corresponding 5β , 8β -epidioxysterols. Since chemical shifts of H-6, H-7, H-18 and H-19 protons of compounds **3-6** were very similar to those observed for the 5α , 8α -epidioxide, stereochemistry of compounds **3-6**

was assigned as $5\alpha, 8\alpha$. The chemical structures of compounds **3-6** were readily determined $5\alpha, 8\alpha$ -epidioxycholesta-6-en- 3β -ol (3), $5\alpha, 8\alpha$ -epidioxycholesta-6,22-dien- 3β -ol (4), $5\alpha, 8\alpha$ -epidioxycholesta-6-en- 3β -ol (5), and $5\alpha, 8\alpha$ -epidioxycholesta-6,9(11)-dien- 3β -ol (6) by combinations of spectroscopic analysis and comparison with reported data for these compounds (Gunatilaka et al., 1981; Kazuo et al., 1993; Sera et al., 1999; Ioannou et al., 2009) (Table 4-7). Nucleosides **7-9** were isolated from *n*-BuOH fraction. Similarly, their identities were also established to be 2-deoxyadenosine, 2-deoxyuridine and thymidine by comparison of its spectral data with those reported (Anderson et al., 2005; Qiu et al., 2007) (Table 8).



Table 2. ^1H and ^{13}C NMR spectral data for compound **1** isolated from the sponge *Coscinoderma* sp.

Position	δH	δC
1	1.22 (1H, m), 1.77 (1H)	39.8
2	1.39 (1H, m), 1.49(1H, m)	19.9
3	1.23 (1H, m), 1.37 (1H, m)	43.3
4	-	33.6
5	1.29 (1H, dd, $J=11.3$)	52.0
6	1.95 (1H, br dd, $J=13.8$), 1.85 (1H, br dd, $J=15.7$)	24.9
7	5.32 (1H, m)	123.9
8	-	136.8
9	2.28 (1H, m)	49.3
10	-	37.4
11	1.24 (1H, m), 1.61 (1H, m)	27.7
12	4.50 (1H, dd, $J=10.5, 2.5$ Hz)	85.7
13	2.27 (1H, m)	38.2
14	1.15 (1H, m), 1.38 (1H, m)	34.3
15	1.44 (1H, m), 1.57 (1H, m)	27.4
16	2.03 (2H, t, $J=7.3$ Hz)	41.0
17	-	136.7
18	5.30 (1H, m)	124.8
19	3.22 (2H, d, $J=7.1$ Hz)	29.2
20	0.84 (3H, s,)	33.7
21	0.89 (3H, s)	22.5
22	1.68 (3H, s)	23.0
23	0.75 (3H, s)	14.2
24	0.93 (3H, d, $J=6.9$ Hz)	13.7
25	1.68 (3H, s)	16.3
1'	-	130.1
2'	-	148.6
3'	6.56 (1H, d, $J = 8.4$ Hz)	117.5
4'	6.41 (1H, dd, $J = 8.4, 3.0$ Hz)	114.8
5'	-	150.8
6'	6.52 (1H, d, $J = 3.0$ Hz)	118.0

Measured in CD_3OD at 300MHz.

Table 3. ^1H and ^{13}C NMR spectral data for compound **2** isolated from the sponge *Coscinoderma* sp.

Position	δH	δC
1	1.50 (1H, br, s)	26.6
2	1.96, 1.40 (2H)	28.2
3	5.40 (1H, br s)	124.9
4	-	140.6
5	-	41.6
6	1.95 (2H)	34.5
7	1.5 (2H)	35.5
8	1.95 (2H)	36.4
9	-	137.1
10	5.08 (1H, t, $J=6.6$ Hz)	125.1
11	1.98 (2H)	26.1
12	1.33 (2H)	32.3
13	1.48 (1H)	38.5
14	1.35 (2H)	31.7
15	1.56 (2H)	28.4
16	2.41 (2H, t, $J=7.3$ Hz)	25.9
17	-	126.2
18	6.28 (1H, br s)	111.8
19	7.34 (1H, t, $J = 1.5$ Hz)	139.9
20	1.60 (3H, s)	16.4
21	0.86(3H, s)	19.6
22	0.87 (3H, d, $J = 7.2$ Hz)	21.5
23	1.60 (3H, s)	16.3
24	3.92 (2H, d, $J=5.5$ Hz)	71.2
25	7.24 (1H, br s)	143.7

Measured in CD_3OD at 300MHz.

Table 4. ^1H and ^{13}C NMR spectral data for compound **3** isolated from the sponge *Coscinoderma* sp.

Position	δH	δC
1	1.93, 1.67 (2H, m)	34.7
2	1.82, 1.51 (2H, m)	30.2
3	3.96 (1H, m)	66.5
4	2.09, 1.89 (2H, m)	35.7
5	-	79.4
6	6.23 (1H, d, J=8.5 Hz)	135.3
7	6.49 (1H, d, J=8.5 Hz)	130.7
8	-	82.1
9	1.46 (1H, m)	51.6
10	-	35.8
11	1.48, 1.19 (2H, m)	20.6
12	1.96, 1.20 (2H, m)	39.0
13	-	44.8
14	1.54 (1H, m)	51.1
15	1.61, 1.40(2H, m)	23.5
16	1.90, 1.37(2H, m)	28.3
17	1.16 (1H, m)	56.3
18	0.79 (3H, s)	12.8
19	0.88 (3H, s)	18.3
20	1.36 (1H, m)	39.4
21	0.90 (3H, d, J=6.6 Hz)	20.7
22	1.30, 1.02 (2H, m)	33.5
23	1.35, 1.01 (2H, m)	30.6
24	1.81 (1H, m)	37.0
25	1.50 (1H, m)	15.6
26	0.85 (3H, d, J=6.8 Hz)	32.5
27	0.78 (3H, d, J=6.6Hz)	18.8
28	0.77 (3H, d, J = 6.9 Hz)	17.6

Measured in CDCl_3 at 300 MHz.

Table 5. ^1H and ^{13}C NMR spectral data for compound **4** isolated from the sponge *Coscinoderma* sp.

Position	δH	δC
1	1.94, 1.67 (2H, m)	34.7
2	1.83, 1.52 (2H, m)	30.2
3	3.96 (1H, m)	66.5
4	2.09, 1.89 (2H, m)	36.9
5	-	82.1
6	6.23 (1H, d, $J=8.5$ Hz)	135.3
7	6.49 (1H, d, $J=8.5$ Hz)	130.6
8	-	79.4
9	1.48 (1H, m)	51.0
10	-	37.0
11	1.49, 1.21 (2H, m)	23.5
12	1.95, 1.22 (2H, m)	39.4
13	-	44.8
14	1.54 (1H, m)	51.6
15	1.62, 1.42 (2H, m)	20.7
16	1.92, 1.38 (2H, m)	28.3
17	1.20 (1H, m)	56.2
18	0.80 (3H, s)	12.7
19	0.88 (3H, s)	18.6
20	1.40 (1H, m)	35.2
21	0.93 (3H, d, $J=6.3$ Hz)	18.3
22	1.55, 1.14 (2H, m)	34.4
23	2.06, 1.90 (2H, m)	31.0
24	-	156.4
25	2.19 (1H, m)	33.8
26	1.02 (3H, d, $J=6.9$ Hz)	21.8
27	1.02 (3H, d, $J=6.9$ Hz)	22.1
28	4.70 (brs), 4.63 (brs)	106.0

Measured in CD_3OD at 300MHz.

Table 6. ^1H and ^{13}C NMR spectral data for compound **5** isolated from the sponge *Coscinoderma* sp.

Position	δH	δC
1	1.93, 1.67 (2H, m)	34.7
2	1.82, 1.51 (2H, m)	30.2
3	3.8 (1H, m)	66.5
4	2.09, 1.89 (2H, m)	36.9
5	-	82.1
6	6.24 (1H, d, $J=8.4$ Hz)	135.3
7	6.52 (1H, d, $J=8.4$ Hz)	130.6
8	-	79.4
9	1.47 (1H, m)	51.0
10	-	37.0
11	1.48, 1.19 (2H, m)	23.5
12	1.96, 1.20 (2H, m)	39.4
13	-	44.8
14	1.53 (1H, m)	51.6
15	1.61, 1.40 (2H, m)	20.7
16	1.89, 1.35 (2H, m)	28.3
17	1.15 (1H, m)	56.2
18	0.84 (3H, s)	12.7
19	0.90 (3H, s)	18.6
20	1.40 (1H, m)	35.2
21	0.94 (3H, d, $J=6.6$ Hz)	18.3
22	1.55, 1.14 (2H, m)	36.0
23	2.06, 1.90 (2H, m)	23.8
24	1.09 (2H, m)	39.4
25	2.19 (1H, m)	28.0
26	0.88 (3H, d, $J=6.3$ Hz)	21.8
27	0.88 (3H, d, $J=6.5$ Hz)	22.1

Measured in CD_3OD at 300MHz.

Table 7. ^1H and ^{13}C NMR spectral data for compound **6** isolated from the sponge *Coscinoderma* sp.

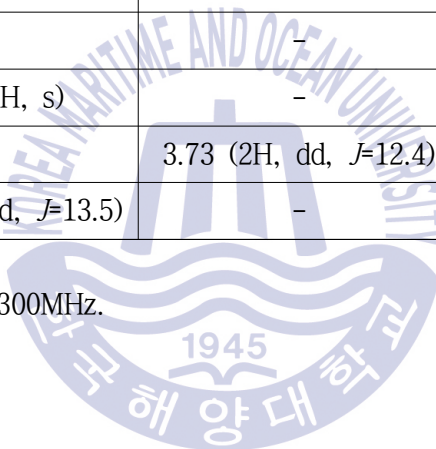
Position	δH	δC
1	1.93, 1.67 (2H, m)	34.7
2	1.82, 1.51 (2H, m)	30.2
3	3.90 (1H, m)	66.5
4	2.09, 1.89 (1H, m)	36.9
5	-	82.1
6	6.18 (1H, d, J=8.4 Hz)	135.3
7	6.42 (1H, d, J=8.4 Hz)	130.6
8	-	79.4
9	-	51.0
10	-	37.0
11	5.46 (1H, dd, J=5.9 Hz)	23.5
12	1.96, 1.20 (2H, m)	39.4
13	-	44.8
14	1.53 (1H, m)	51.6
15	1.61, 1.40 (2H, m)	20.7
16	1.89, 1.35 (2H, m)	28.3
17	1.15 (1H, m)	56.2
18	0.73 (3H, s)	12.7
19	1.10 (3H, s)	18.6
20	1.40 (1H, m)	35.2
21	0.83 (3H, d, J=6.6 Hz)	18.3
22	1.55, 1.14 (2H, m)	34.4
23	2.06, 1.90 (2H, m)	31.0
24	1.09 (2H, m)	156.4
25	2.19 (1H, m)	33.8
26	0.80 (3H, d, J=6.3 Hz)	21.8
27	0.79 (3H, d, J=6.5Hz)	22.1

Measured in CD_3OD at 300MHz.

Table 8. ^1H NMR spectral data for compounds **7**, **8** and **9** isolated from the sponge *Coscinoderma* sp.

Position	compound 7 δH	compound 8 δH	compound 9 δH
1	6.43(1H, t, $J=13.8$)	6.25 (1H, t, $J=16.0$)	6.27 (1H, t, $J=13.5$)
2	2.59 (2H, m)	2.25 (2H, m)	2.22 (2H, m)
3	4.54 (1H, m)	4.37 (1H, m)	4.38 (1H, m)
4	4.02 (1H, q, $J=14.3$)	3.91 (1H, q, $J=10.2$)	3.89 (1H, q, $J=10.2$)
5	8.32 (1H, s)	7.97 (1H, d, $J=8.0$)	7.80 (1H, d, $J=1.37$)
6	-	5.68 (1H, d, $J=10.7$)	-
7	-	-	1.87 (3H, d, $J=1.4$)
8	8.03 (1H, s)	-	-
9	-	3.73 (2H, dd, $J=12.4$)	-
10	3.76 (2H, dd, $J=13.5$)	-	3.75 (2H, dd, $J=10.3$)

Measured in D_2O at 300MHz.



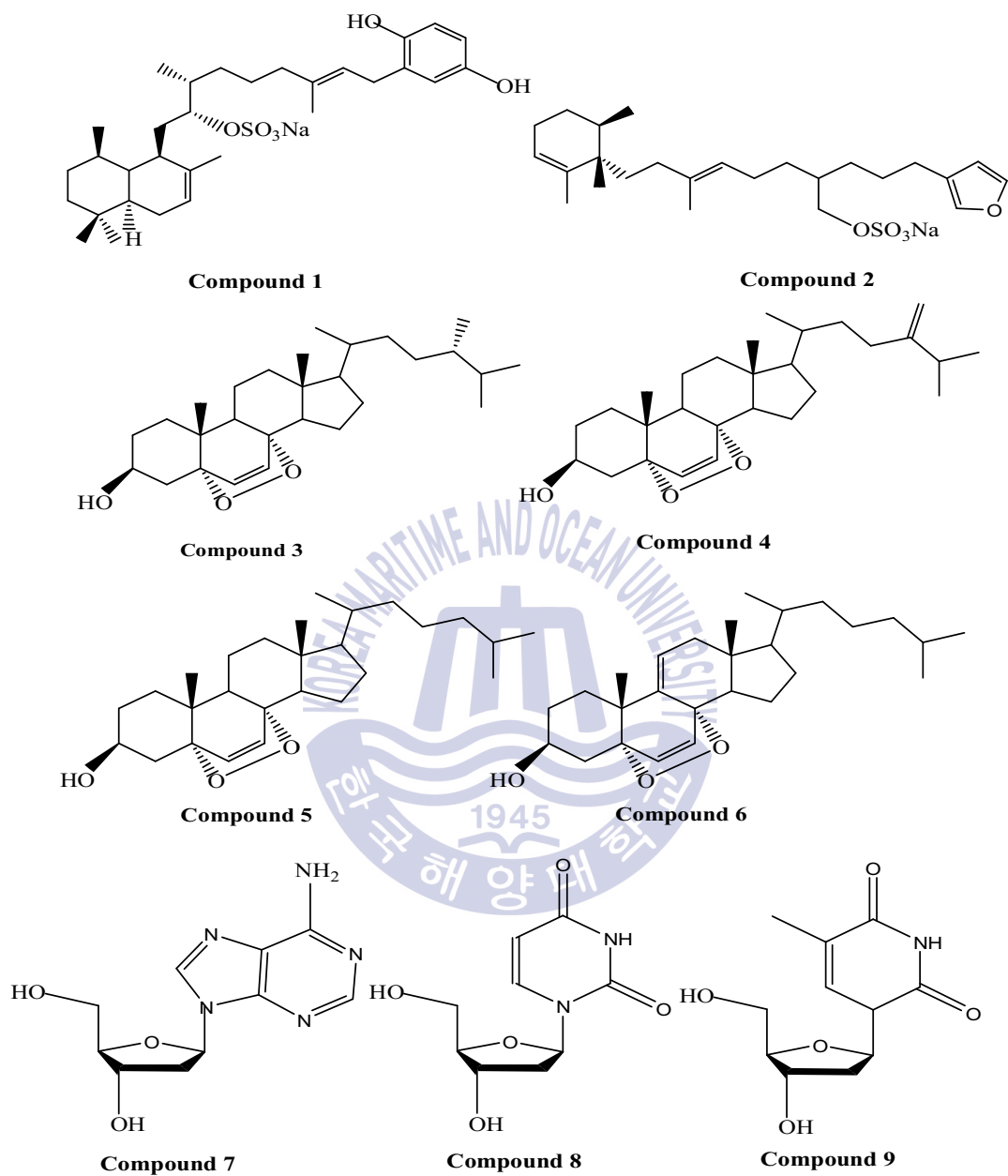


Fig. 8. Chemical structure of compounds 1-9 from the sponge *Coscinoderma* sp..

3.2. Antioxidant effects of crude extract and its solvent fractions

3.2.1. DPPH radical scavenging activity

DPPH radical scavenging activity was measured at the different concentrations (200, 100, 50, 10 and 1 $\mu\text{g/mL}$) of each of crude extract and its four solvent fractions (*n*-hexane, 85% aq.MeOH, *n*-BuOH and water), and compared with butylated hydroxyanisol (BHA) and L-ascorbic acid (Vitamin C). A significant antioxidant effect was observed in crude extract, 85% aq.MeOH, and *n*-BuOH fractions. Among samples tested, *n*-BuOH fraction showed the highest scavenging activity, showing 60.9%, 43.0%, 28.1%, 8.7% and 5.3% at the concentrations of 200, 100, 50, 10 and 1 $\mu\text{g/mL}$ in its scavenging ratio, respectively (Fig. 9).



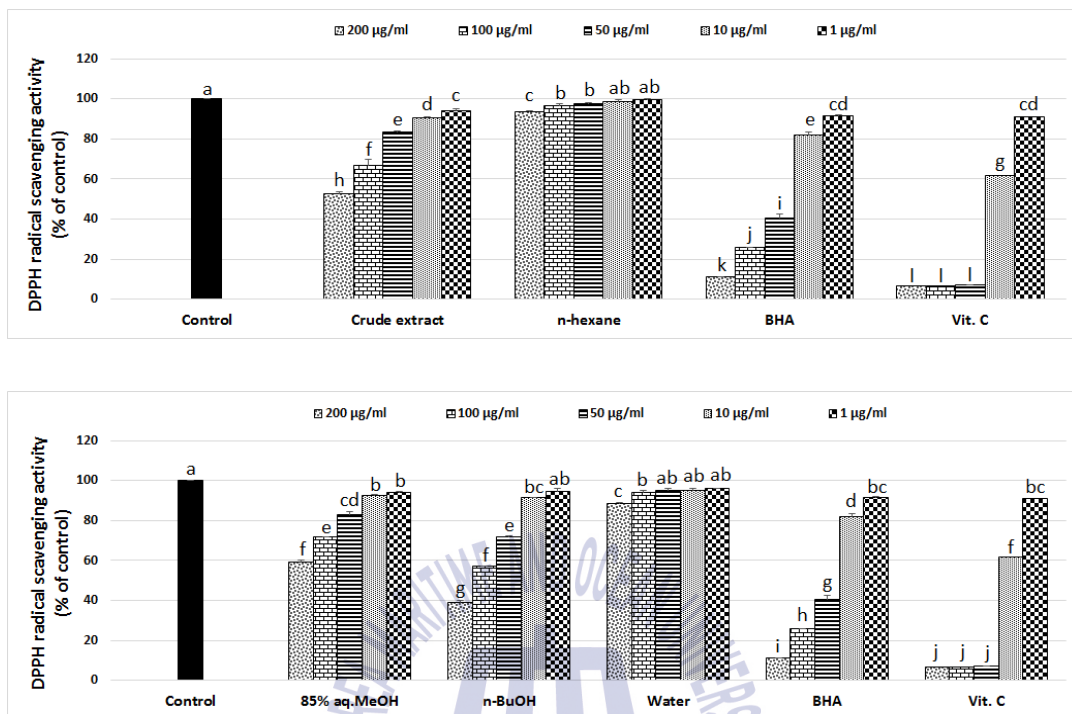
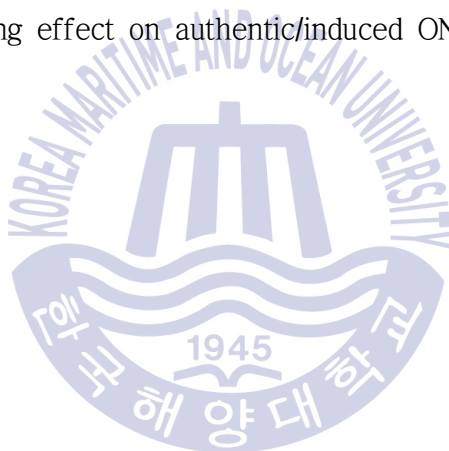


Fig. 9. DPPH radical scavenging effect of crude extract and its solvent fractions from the sponge *Coscinoderma* sp. ^{a-l}Means with the different letters are significantly different ($p < 0.05$) by Duncan's multiple range test.

3.2.2. Peroxynitrite scavenging activity

The scavenging activity of crude extract and its four solvent fractions on authentic/induced ONOO⁻ from SIN-1 is shown in figures 10 and 11. For authentic peroxynitrite, the scavenging activities of solvent fractions increased in the order of 85% aqueous MeOH \approx *n*-BuOH > *n*-hexane > H₂O fractions, showing the scavenging ratios of 87.9%, 87.8%, 38.0%, and 7.3% respectively, at a concentration of 10 μ g/mL. However, the inhibitory activities against the generation of ONOO⁻ increased in the order of *n*-BuOH, 85% aq.MeOH, water, and *n*-hexane fractions with 59.4%, 62.6%, 47.9%, and 5.0% in scavenging ratios, respectively, at a concentration of 10 μ g/mL. *n*-BuOH fraction showed the strongest scavenging effect on authentic/induced ONOO⁻ from SIN-1.



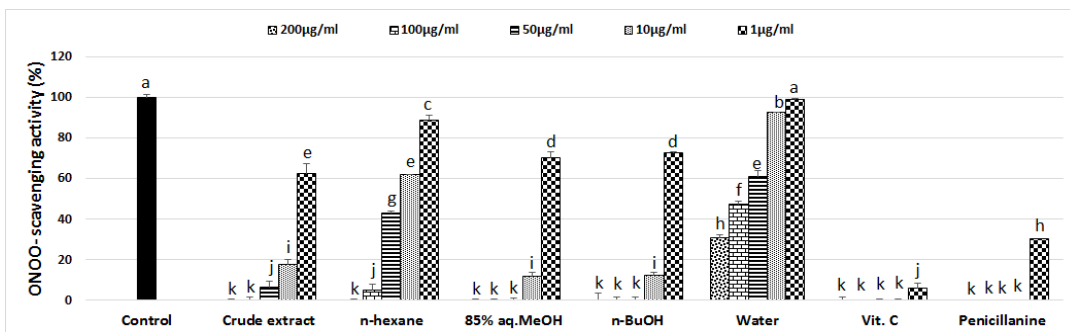


Fig. 10. Scavenging effects of crude extract and its solvent fractions from the sponge *Coscinoderma* sp. on authentic ONOO (% of control). ^{a-k}Means with different letters are significantly different ($p < 0.05$) by Duncan's multiple range test.

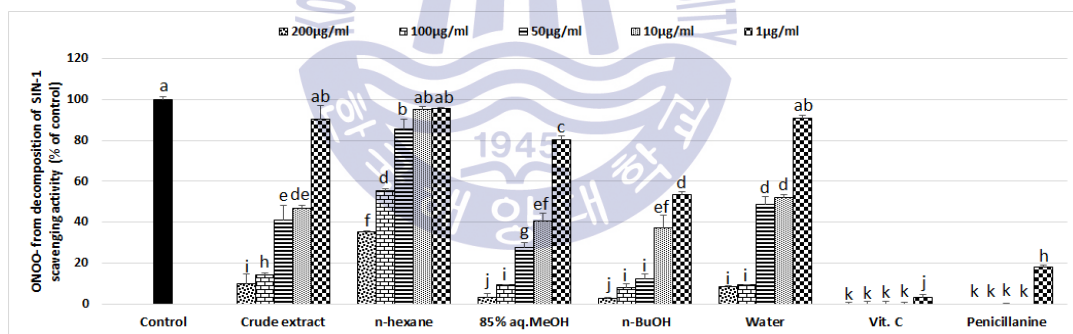


Fig. 11. Scavenging effects of crude extract and its solvent fractions from the sponge *Coscinoderma* sp. on ONOO⁻ from SIN-1 (% of control). ^{a-k}Means with different letters are significantly different ($p < 0.05$) by Duncan's multiple range test.

3.2.3. Ferric reducing antioxidant power (FRAP) assay

The close relationship between reducing power and antioxidant activity has been well-known. The FRAP assay is to measure the ability of samples to reduce Fe^{+3} to Fe^{+2} and to produce blue color of ferrous form. Antioxidant components exert their reducing power by donating electron to ferric complex and thus breaking the radical chain reaction (Kim et al., 2011). *n*-BuOH fraction exhibited the highest reducing power followed by 85% aqueous MeOH fraction. However, their reducing powers were weak, compared with ascorbic acid as the positive control. The 85% aq.MeOH and *n*-BuOH fractions exhibited 24.9% and 33.5% reducing powers, respectively, at 100 $\mu\text{g/mL}$ (Fig. 12).



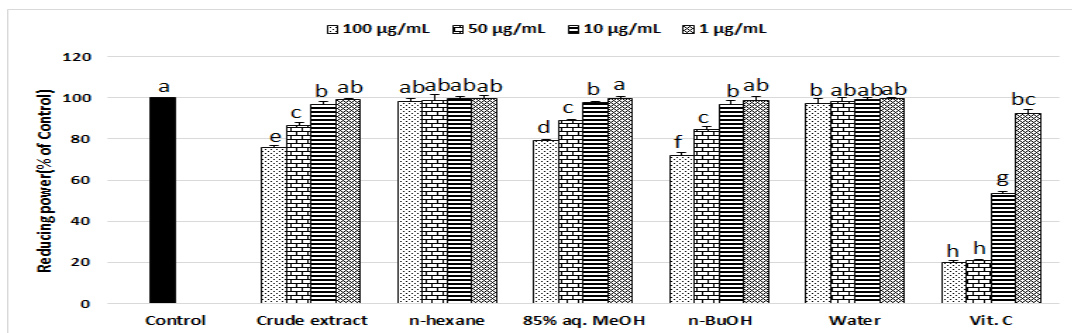


Fig. 12. Ferric reducing antioxidant power assay of crude extract and its solvent fractions from the sponge *Cosinoderma* sp.. ^{a-h}Means with different letters are significantly different ($p < 0.05$) by Duncan's multiple range test.



3.2.4 Intracellular ROS scavenging activity in HT-1080 cells

3.2.4.1. Assessment of cell viability by crude extract and its solvent fractions in HT-1080 cells

To avoid cytotoxic interference of crude extract and its solvent fractions, the influence of the sample on cell viability of HT-1080 cells was determined using MTT assay. The cells were treated with wide-range of concentrations (200, 100, 50 and 10 $\mu\text{g/mL}$) of the sample for 1 h. The cell viabilities of HT-1080 cells were 70.1%, 66.5%, 74.3%, 76.1% and 75.5% for crude extract, *n*-hexane, 85% aq.MeOH, *n*-BuOH and water fractions, respectively, at a concentration of 200 $\mu\text{g/mL}$ as shown in Fig. 13. According to the cell viability assay, 100 $\mu\text{g/mL}$ was chosen as the highest dose to treat as the first concentration shows significant cell viability loss (<80% cell viability).

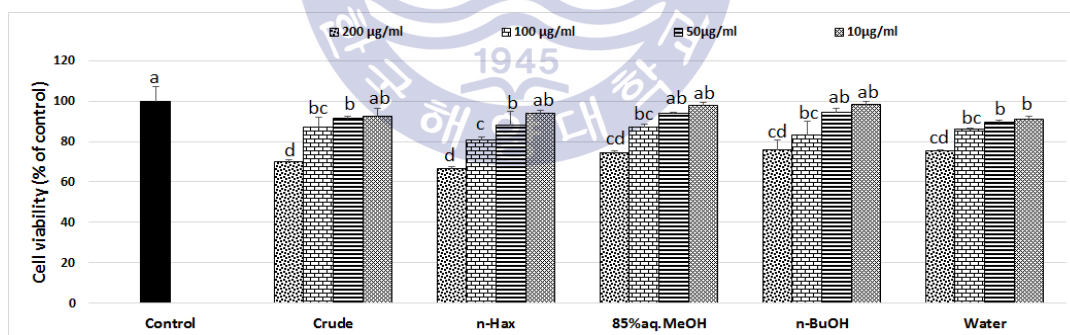
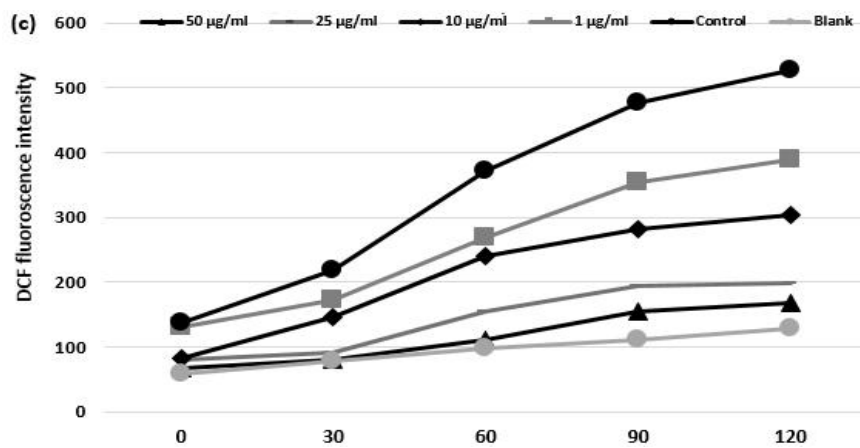
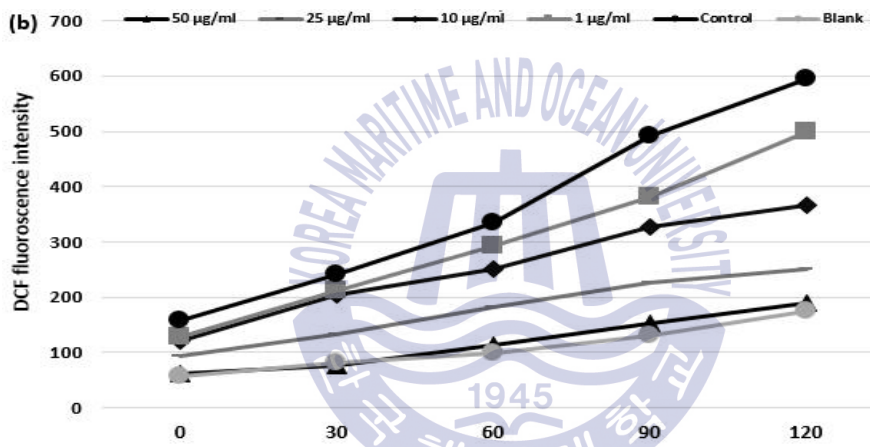
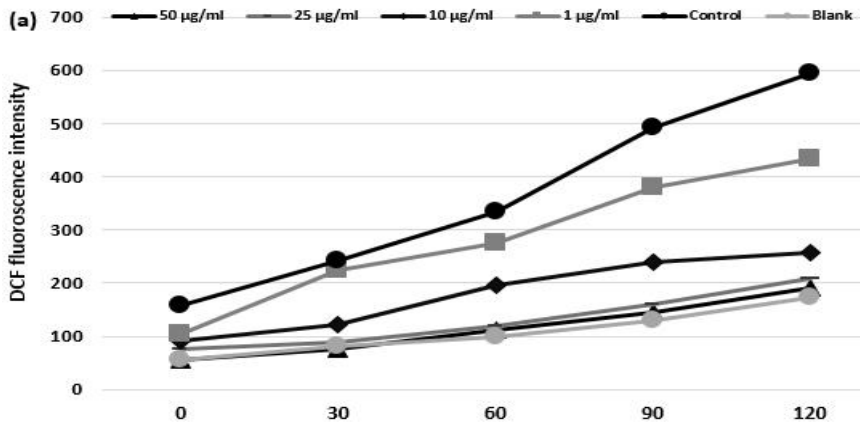


Fig. 13. Effect of crude extract and its solvent fractions from the sponge *Coscinoderma* sp. on viability of HT-1080 cells. ^{a-d}Means with the different letters are significantly different ($p < 0.05$) by Duncan's multiple range test.

3.2.4.2. Determination of intracellular formation of ROS using DCFH-DA labeling

The radical scavenging effect of Crude extract and its fractions on the intracellular ROS was investigated on HT-1080 cells using DCFH-DA. DCFH-DA crosses cell membranes, and it is then outed off acetate group by intracellular esterase to non-fluorescein diacetate DCFH (2',7'-Dichlorodihydro fluorescein). It was oxidized through active oxygen and turned into fluorescent DCF. The radical scavenging effects were compared to the control that was treated 1×PBS instead of sample and treated with 500 μ M H₂O₂ and blank that wasn't treated both sample and H₂O₂. The degree of DCF fluorescence was determined at 0, 30, 60, 90 and 120 min.

All samples concentration-dependently inhibited production of ROS in HT-1080 cells. The intracellular ROS scavenging ratios of crude extract, *n*-hexane, 85% aq.MeOH and *n*-BuOH fractions were observed to be 95.9%, 96.4%, 90.3% and 99.4 %, respectively, after incubation for 2 h at a concentration of 50 μ g/mL, compared to control. *n*-BuOH fraction showed the most potent radica-scavenging effect of them, and its radical scavenging ratios compared to the control were 99.4%, 94.9%, 56.0% and 26.2% as shown in Fig. 14.



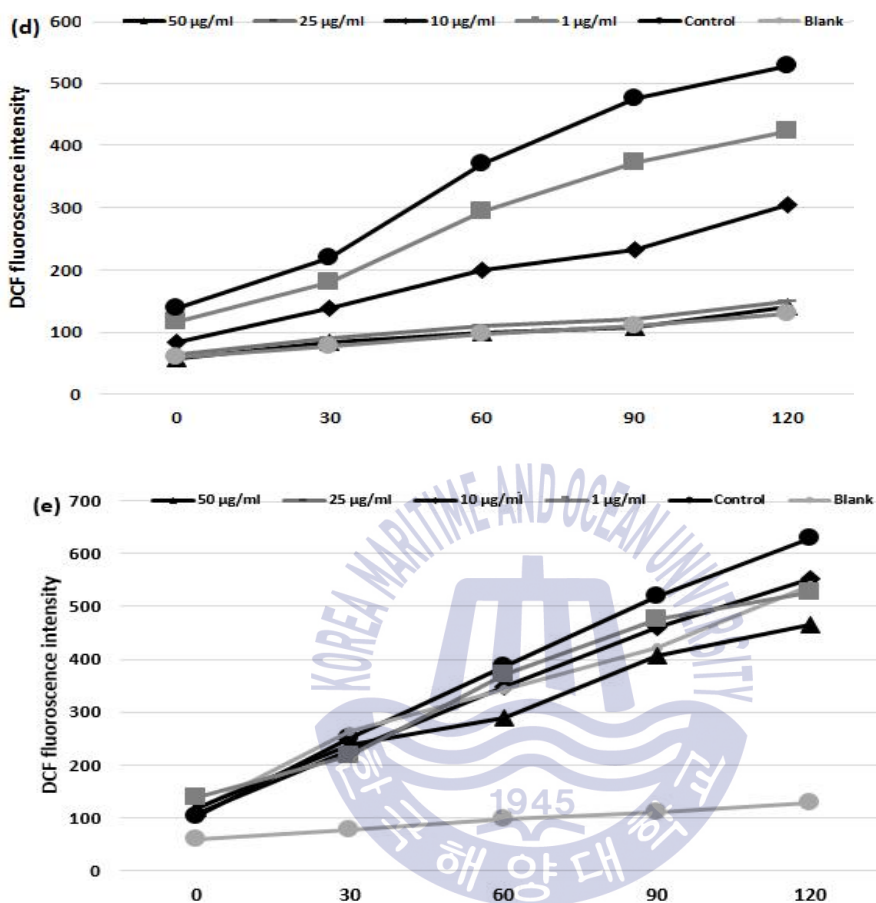


Fig. 14. Scavenging effects of crude extract and its solvent fractions from the sponge *Coscinoderma* sp. on intracellular ROS levels induced by hydrogen peroxide in HT-1080 cells. (a) crude extract; (b) *n*-hexane; (c) 85% aq.MeOH; (d) *n*-BuOH; (e) water.

3.3 Antiproliferative effects of crude extract and its solvent fractions on human cancer cells

The antiproliferative effects of crude extract and its solvent fractions (*n*-hexane, 85% aq.MeOH, *n*-BuOH and water) were investigated against four human cancer cell lines: HT-1080, AGS, HT-29 and MCF-7.

3.3.1. Antiproliferative effect against the growth of HT-1080 cells

Human fibrosarcoma cells (HT-1080) were treated with four different concentrations of the same sample for 24 h, and the antiproliferative effect was assessed using MTT assay. The 85% aq.MeOH and *n*-BuOH fractions showed a relatively significant effect on HT-1080. Growth inhibitory rates of 85% aq.MeOH and *n*-BuOH fractions against the HT-1080 cells were 41.4% and 40.4%, respectively, at a concentration of 100 μ g/mL. This result is shown in Fig. 15.

3.3.2. Antiproliferative effect against the growth of AGS cells

Human gastric carcinoma cells (AGS) were treated with four different concentrations of the same sample for 24 h, and the antiproliferative effect was assessed using MTT assay. Among the samples tested, *n*-BuOH fraction had a comparatively high antiproliferative effect on AGS cells, exhibiting the inhibitory rates of 31.7% against them at a concentration of 100 μ g/mL. This result is shown in Fig. 15.

3.3.3. Antiproliferative effect against the growth of HT-29 cells

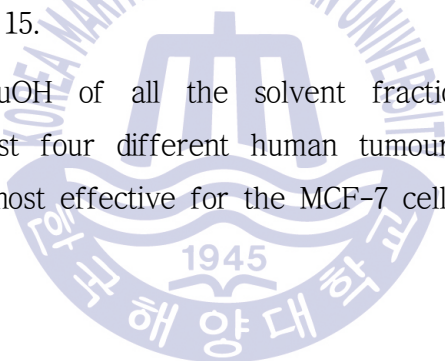
Human colon cancer cells (HT-29) were treated with four different concentrations of the same sample for 24 h, and antiproliferative effect was assessed using MTT assay. The 85% aq.MeOH and *n*-BuOH fractions showed

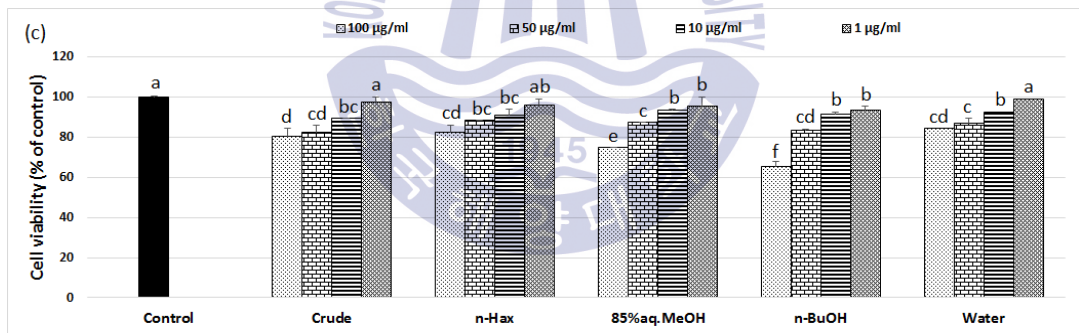
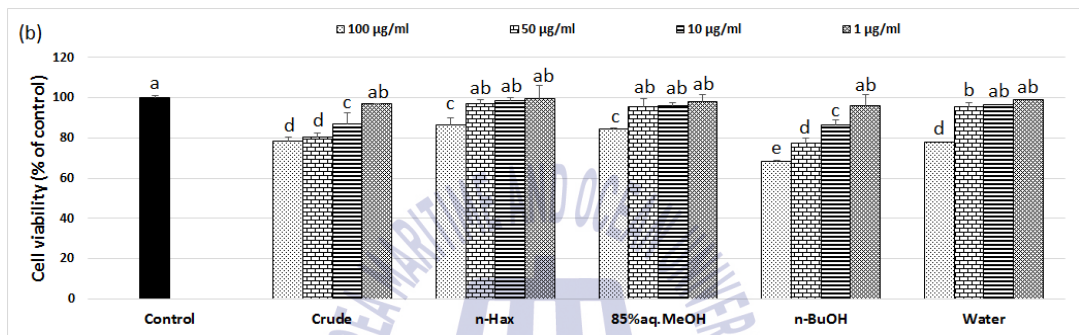
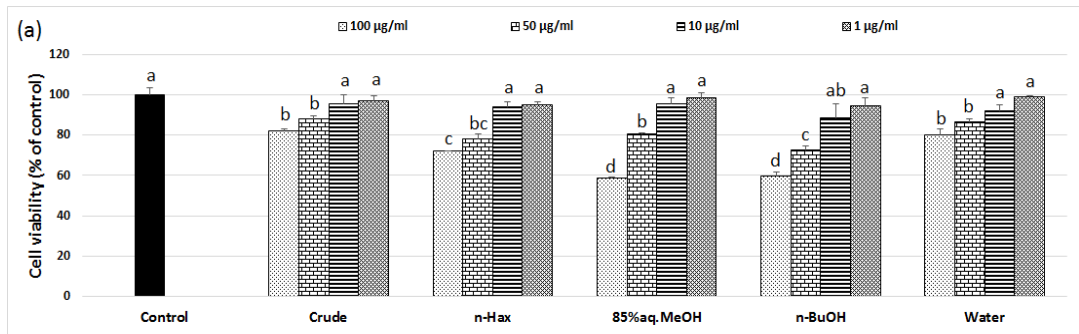
relatively significant effects on HT-29. *n*-BuOH fraction exhibited the inhibitory rates of 34.7% against HT-29 cells, at a concentration of 100 μ g/mL. This result is shown in Fig. 15.

3.3.4. Antiproliferative effect against the growth of MCF-7 cells

Human breast cancer cells (MCF-7) were treated with four different concentrations of the same sample for 24 h, and the antiproliferative effect was assessed using MTT assay. *n*-Hexane, 85% aq.MeOH and *n*-BuOH fractions showed growth inhibitory rates of 34.8%, 35.9% and 43.1%, respectively, against the MCF-7 cell, at a concentration of 100 μ g/mL. This result is shown in Fig. 15.

To summarize, *n*-BuOH of all the solvent fractions showed the most inhibitory effect against four different human tumour cell lines. Especially, *n*-BuOH fraction was most effective for the MCF-7 cells.





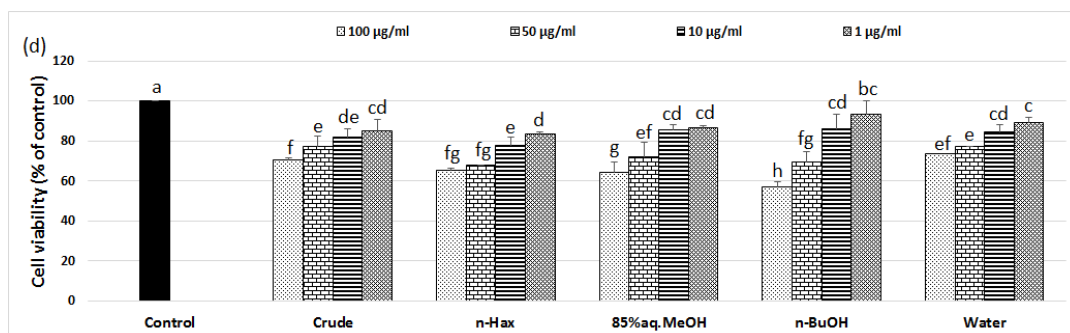
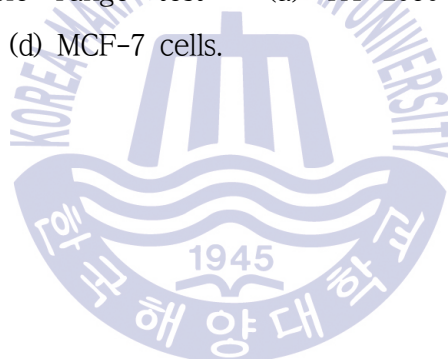


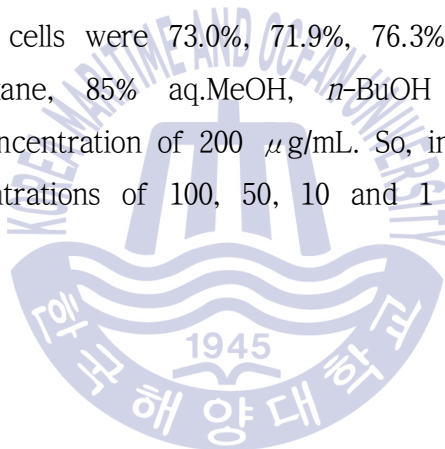
Fig. 15. Antiproliferative effect of crude extract and its solvent fractions from the sponge *Coscinoderma* sp. on viability of cancer cells. ^{a-h}Means with the different letters are significantly different ($p < 0.05$) by Duncan's multiple range test : (a) HT-1080 cells; (b) AGS cells; (c) HT-29 cells; (d) MCF-7 cells.



3.4. Anti-inflammatory effects of crude extract and its solvent fractions

3.4.1. Measurement of cell viability by crude extract and its solvent fractions in Raw 264.7 cells

To avoid cytotoxic interference of crude extract and its solvent fractions, the influence of the sample on cell viability of Raw 264.7 cells was determined using MTT assay. The cells were treated with four different concentrations (200, 100, 50 and 10 $\mu\text{g/mL}$) of the sample for 1 h. The cell viabilities of HT-1080 cells were 73.0%, 71.9%, 76.3%, 78.5% and 79.4% for crude extract, *n*-hexane, 85% aq.MeOH, *n*-BuOH and water fractions, respectively, at the concentration of 200 $\mu\text{g/mL}$. So, in this study, the sample was diluted to concentrations of 100, 50, 10 and 1 $\mu\text{g/mL}$. This result is shown in Fig. 16.



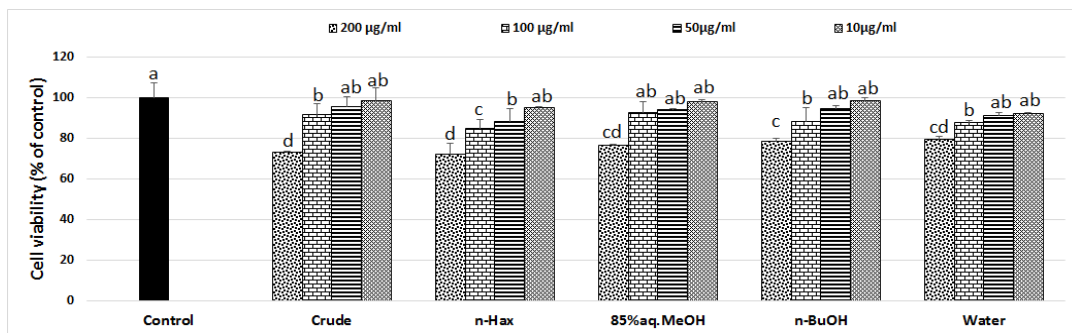


Fig. 16. Effect of crude extract and its solvent fractions from the sponge *Coscinoderma* sp. on viability of Raw 264.7 cells. ^{a-d}Means with the different letters are significantly different ($p < 0.05$) by Duncan's multiple range test.



3.4.2 Determination of nitric oxide (NO) production

The anti-inflammatory effect of crude extract and its solvent fractions on NO production was investigated in LPS-treated Raw 264.7 cells. LPS is the cell envelope constituents of gram-negative *bacillus* and has a strong stimulating effect on various cells such as monocytic cells and macrophages. In particular, macrophages are easily activated by LPS stimulation and then release inflammatory mediators, such as NO. Excessive secretion of NO causes production of a reactive peroxyne nitrite by the reaction with superoxide (O_2^-) in vivo, which leads to oxidative stress and DNA damage and then generates an inflammatory disease (Kim & Son, 2014).

Among the samples tested, 85% aq.MeOH and *n*-BuOH fractions had a comparatively significant inhibition of NO production: for 85% aq.MeOH fraction, inhibition ratios of 55.5%, 42.1%, 29.3% and 15.5% at the concentrations of 100, 50, 10 and 1 μ g/mL, respectively; for *n*-BuOH fraction, inhibition ratios of 73.8%, 57.5%, 32.7% and 19.0% at the same concentrations. This result is shown in Fig. 17.

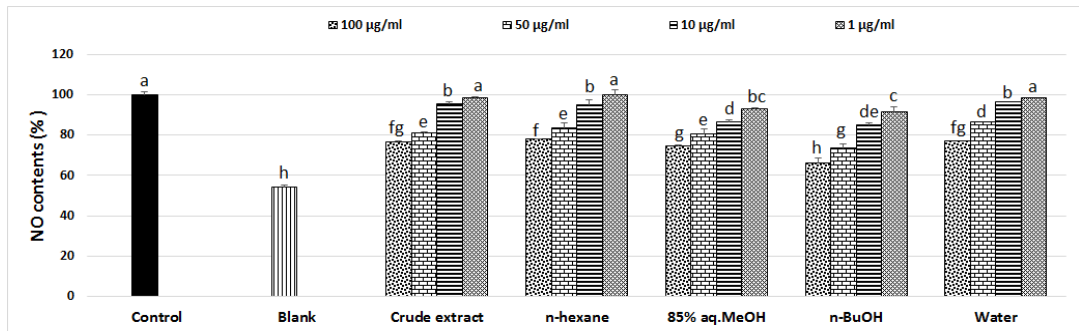
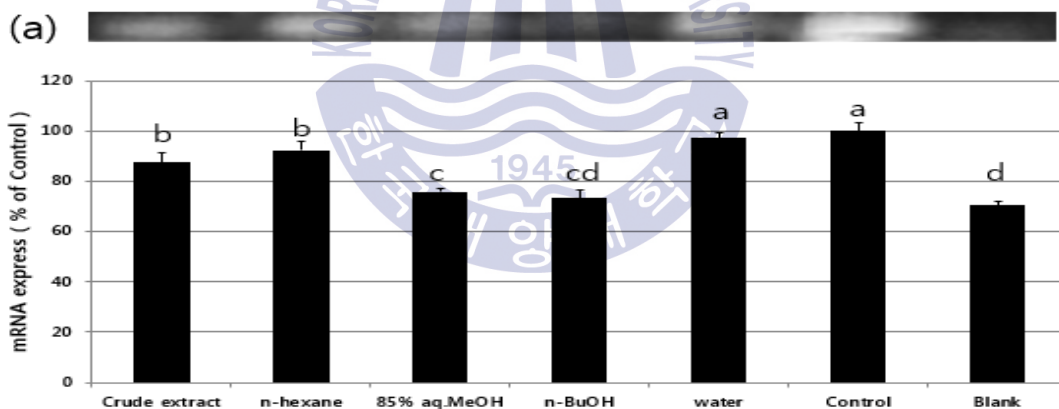


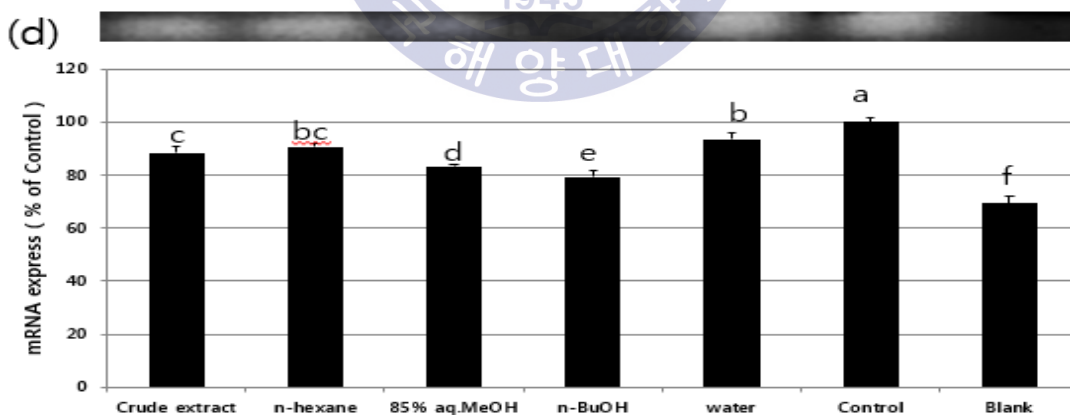
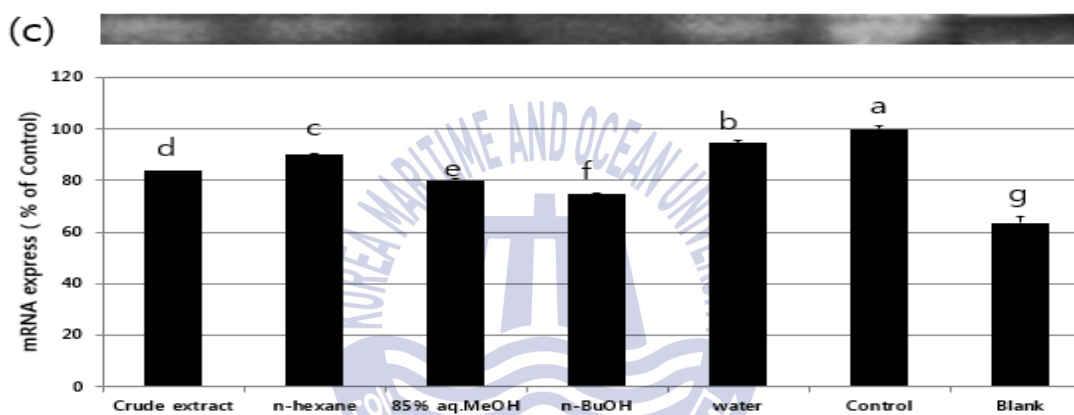
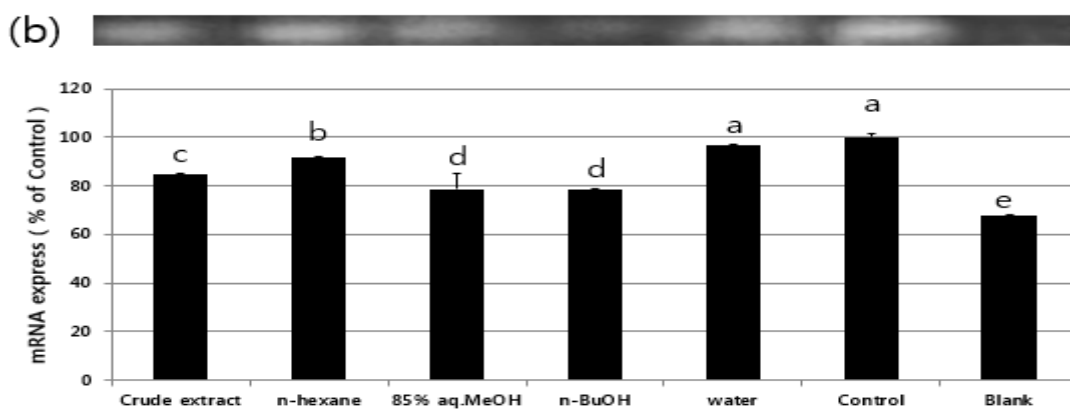
Fig. 17. Effects of crude extract and its solvent fractions from the sponge *Coscinoderma* sp. on nitrite production in Raw 264.7 cells. ^{a-h}Means with the different letters are significantly different ($p < 0.05$) by Duncan's multiple range test.



3.4.3 Reverse transcription–polymerase chain reaction (RT-PCR)

iNOS and COX-2 are expressed by proinflammatory agents, and induce inflammatory responses via the activation of immune cells. During an inflammatory event, iNOS and COX-2 induce the production of inflammatory mediators such as NO. Additionally, IL-1 β and IL-6, which are representative proinflammatory cytokines, are known to be overexpressed in activated macrophages and to promote fever, tissue damage, and inflammatory responses. When comparing the degrees of expression for the fractions at the intracellular transcription level, the inhibition rates of expression were higher in 85% aq.MeOH and *n*-BuOH fractions than in the *n*-hexane and water fraction, at a concentration of 100 μ g/mL. This result is showed in Fig. 18.





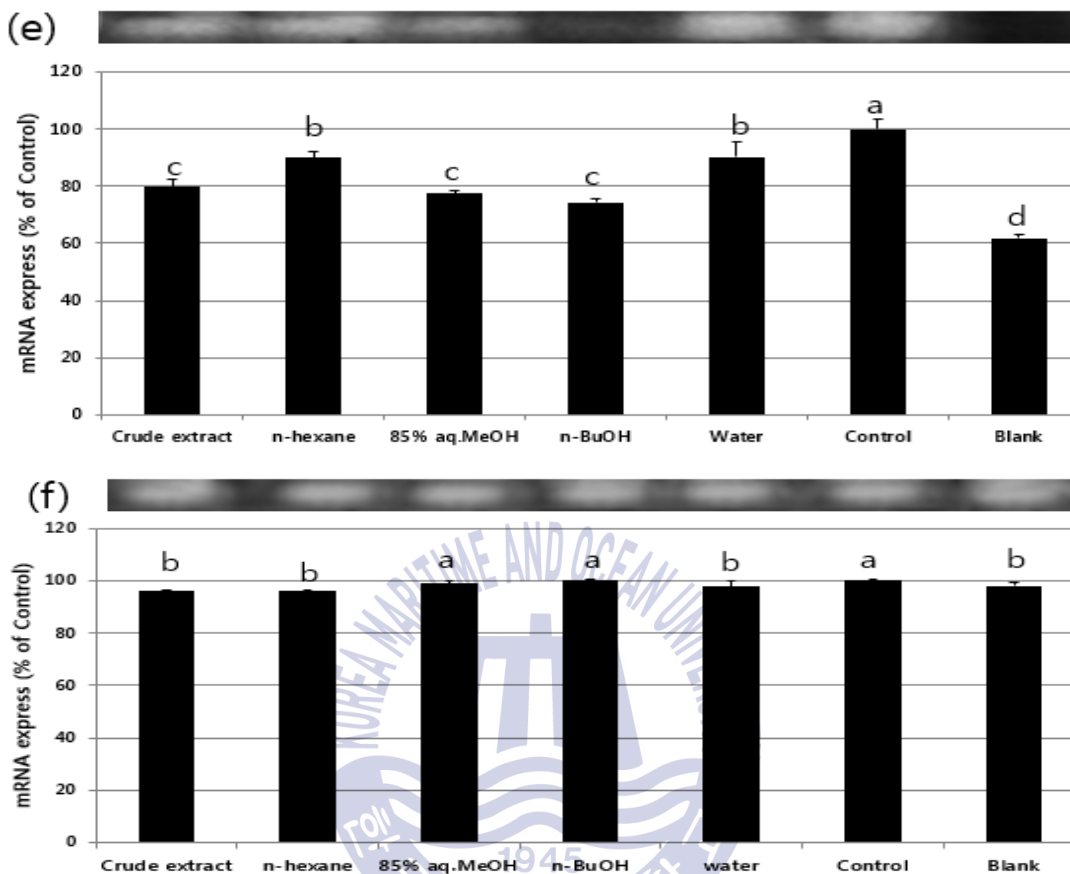


Fig. 18. Effects of crude extract and its solvent fractions from the sponge *Coscinoderma*. sp. on mRNA levels of (a) iNOS, (b) COX-2, (c) IL-1 β , (d) IL-6, (e) TNF- α and (f) β -actin in LPS-stimulated Raw 264.7 cells, at a concentration of 100 μ g/mL. ^{a-g}Means with the different letters are significantly different ($p < 0.05$) by Duncan's multiple range test.

3.5 Antioxidant effects of compounds 1-9

3.5.1 DPPH radical scavenging activity

DPPH radical scavenging activity of compounds **1-9** was measured at the four different concentrations: for **1, 2, 7, 8** and **9**, 100, 50, 10 and 1 μM ; for **3, 4, 5** and **6**, 50, 25, 10 and 1 μM . BHA and L-ascorbic acid of the same concentration as the sample were used as the positive controls. Compounds **1** and **2** showed relatively significant effects. Their scavenging activity are 42.2% and 43.2% at a concentration of 100 μM , respectively, compared with control. This is shown in Fig. 19.



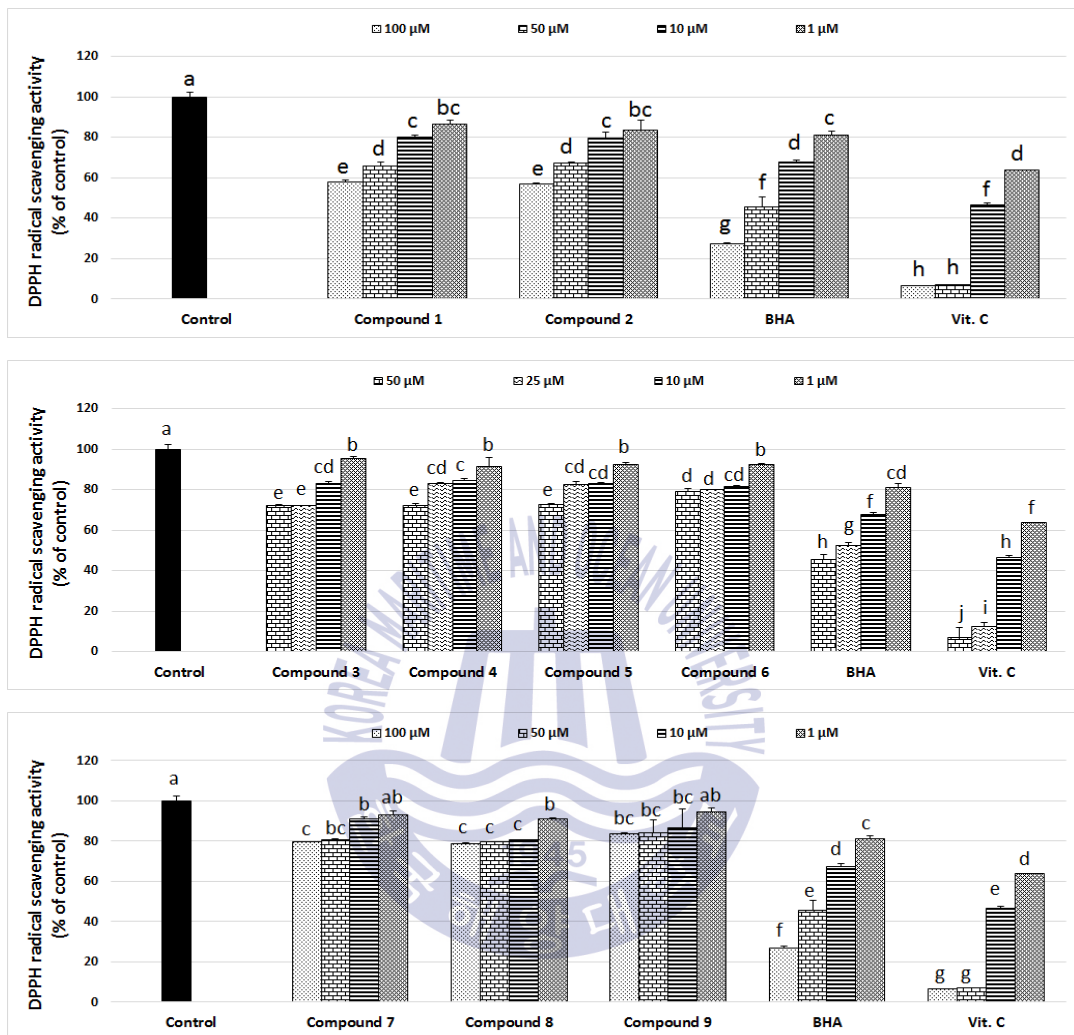


Fig. 19. DPPH radical scavenging effect of compounds 1-9 from the sponge *Coscinoderma* sp. ^{a-j}Means with the different letters are significantly different ($p < 0.05$) by Duncan's multiple range test.

3.5.2 Peroxynitrite scavenging activity

The inhibitory effects of compounds **1**, **2**, **7**, **8** and **9** against peroxynitrite were measured at the four different concentrations (100, 50, 10 and 1 μ M). However, for compounds **3**, **4**, **5** and **6**, concentrations of 50, 25, 10 and 1 μ M were used for the measurement.

The results are shown in Figs. 20 and 21. Compounds **1** and **2** showed 65.7% and 70.4% on authentic peroxynitrite in their scavenging ratio at a concentration of 100 μ M, respectively and 72.3% and 62.4% on the induced peroxynitrite from SIN-1 at the same concentration. These scavenging effects were comparable with those of L-ascorbic acid and penicillamine.



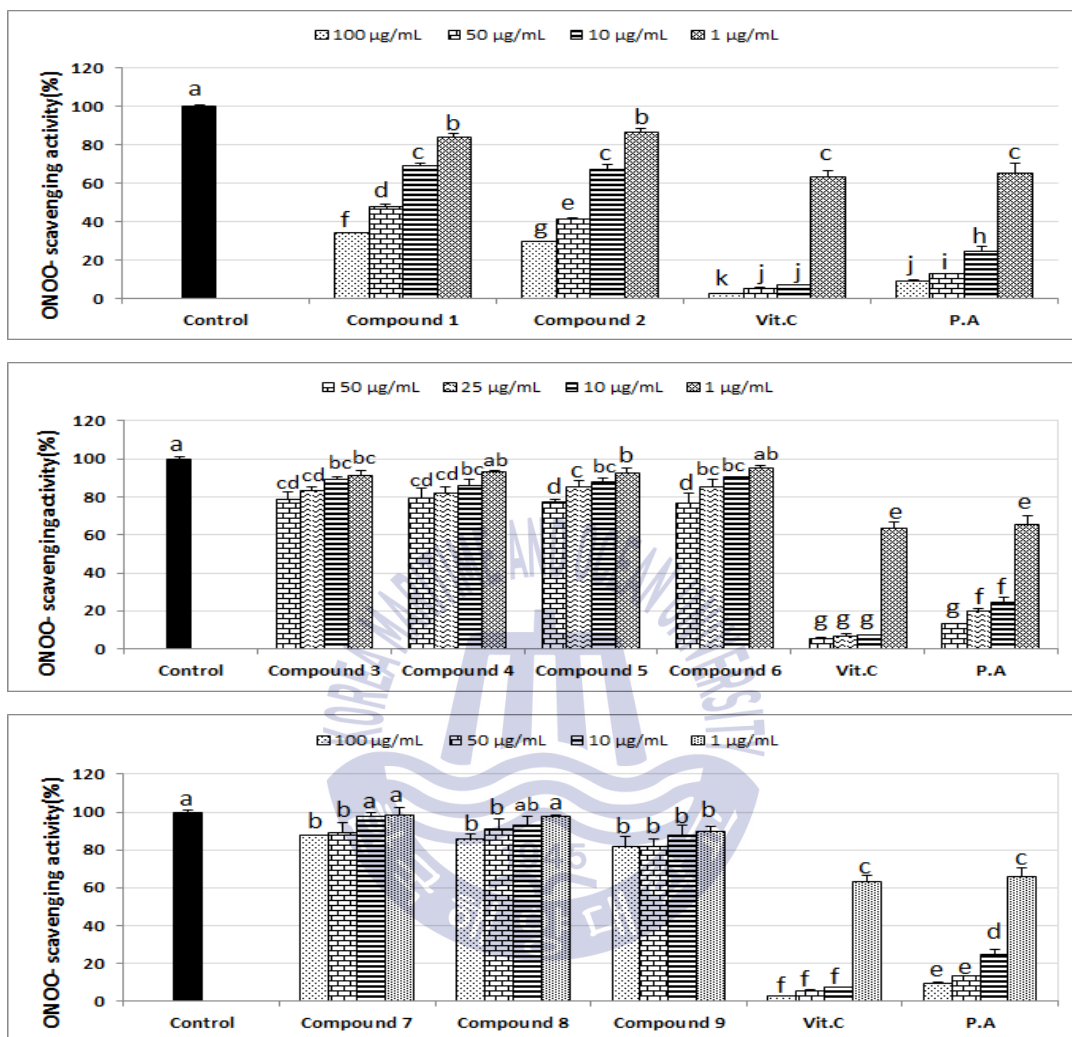


Fig. 20. Scavenging effects of compounds 1-9 from the sponge *Coscinoderma* sp. on authentic ONOO (% of control). ^{a-k}Means with different letters are significantly different ($p < 0.05$) by Duncan's multiple range test.

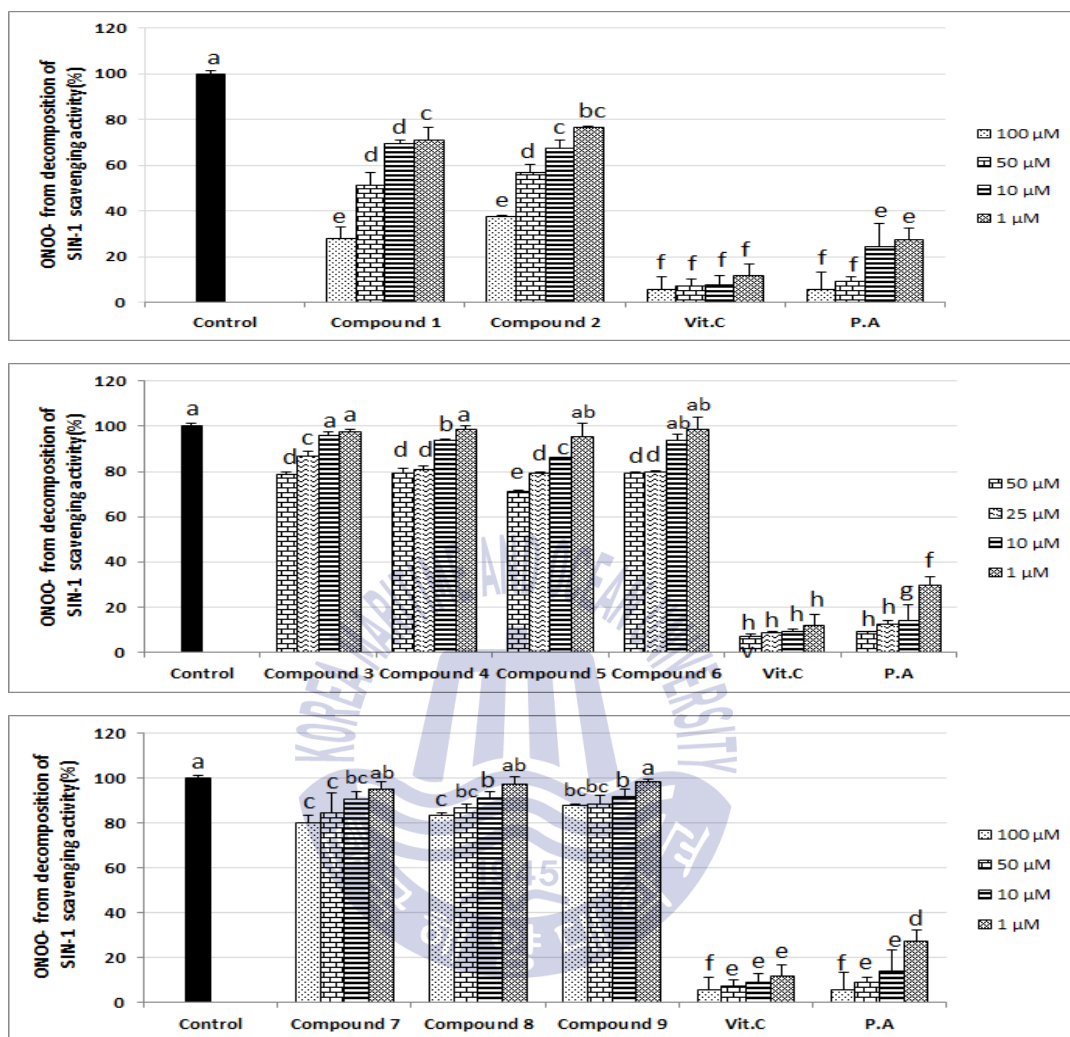


Fig. 21. Scavenging effects of compounds 1-9 from the sponge *Coscinoderma* sp. on ONOO⁻ from SIN-1 (% of control). ^{a-h}Means with different letters are significantly different ($p < 0.05$) by Duncan's multiple range test.

3.5.3 Ferric reducing antioxidant power (FRAP) assay

The close relationship between reducing power and antioxidant activity is well-known. The reducing power is capacity to reduces the Fe^{3+} ion present in the yellow ferricyanide complex (potassium ferricyanide) to Fe^{2+} ion. Concentration of Perl' s prussian blue generated in the redox reaction was measured at 700 nm. Compounds **1** and **2** exhibited the high reducing power of 92.3% and 90.8%, compared with the control Vitamin C, respectively, at a concentration of 100 μM . This result is shown in Fig. 22.



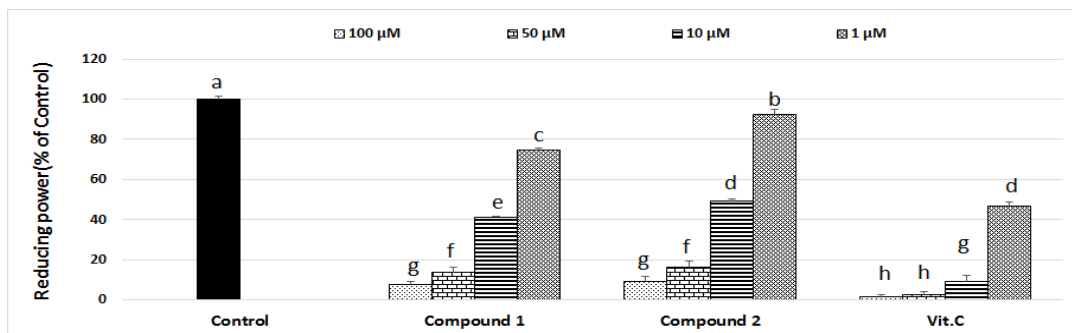
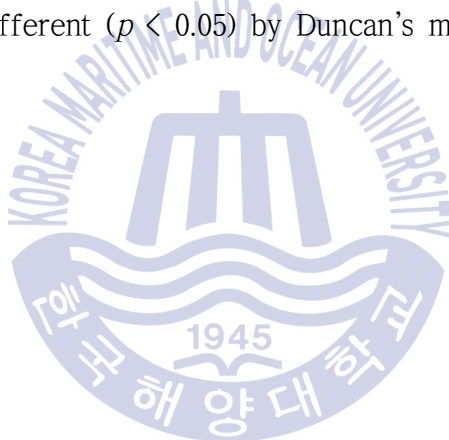


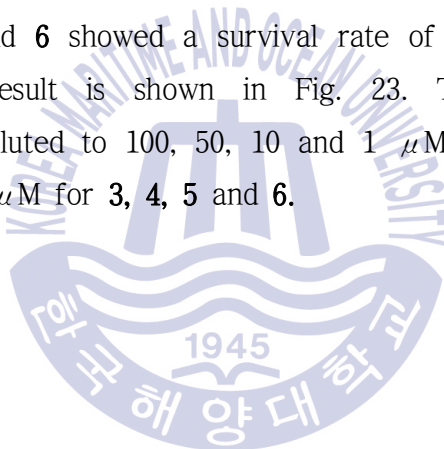
Fig. 22. Ferric reducing antioxidant power assay of compounds 1 and 2 from the sponge *Consinoderma* sp.. ^{a-h}Means with different letters are significantly different ($p < 0.05$) by Duncan's multiple range test.



3.5.4. Antioxidant effects of compounds 1-9 intracellular

3.5.4.1. Measurement of cell viability by compounds 1-9 in HT-1080 cells

To avoid cytotoxic interference of compounds **1-9**, the influence of the sample on cell viability of HT-1080 cells was determined using MTT assay. The cells were treated with four different concentrations (100 and 50 μ M) of the same sample for 1 h. In HT-1080 cells, compounds **1, 2, 7, 8** and **9** showed a survival rate of 80% or more, at 100 μ M, concentration but compounds **3, 4, 5** and **6** showed a survival rate of 80% more, at 50 μ M concentration. This result is shown in Fig. 23. Therefore, the sample concentrations were diluted to 100, 50, 10 and 1 μ M for **1, 2, 7, 8** and **9**, and 50, 25, 10 and 1 μ M for **3, 4, 5** and **6**.



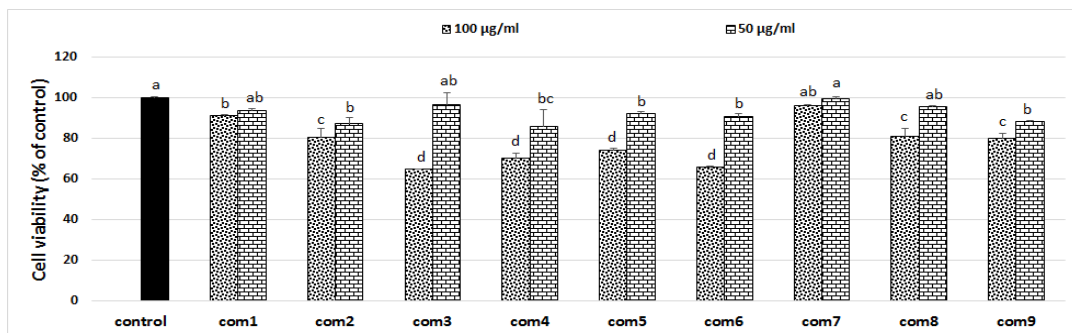


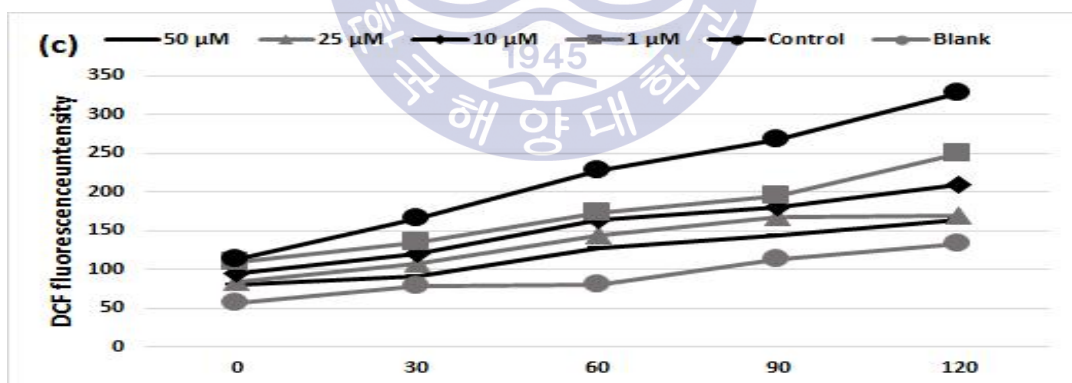
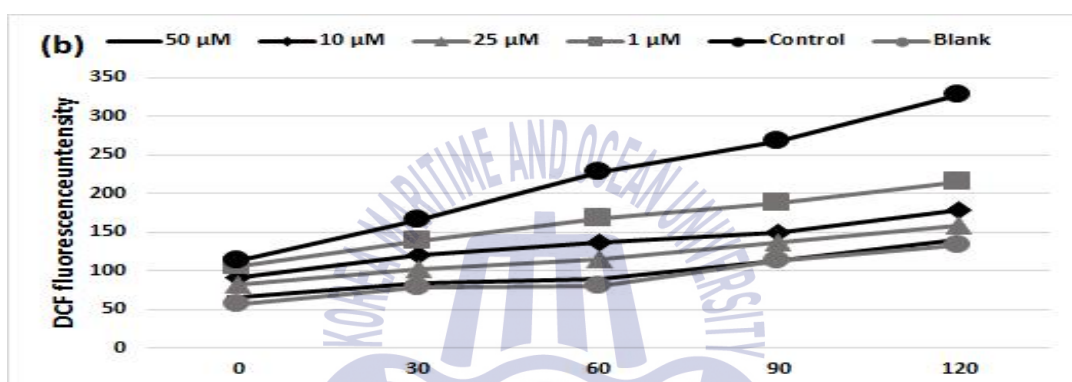
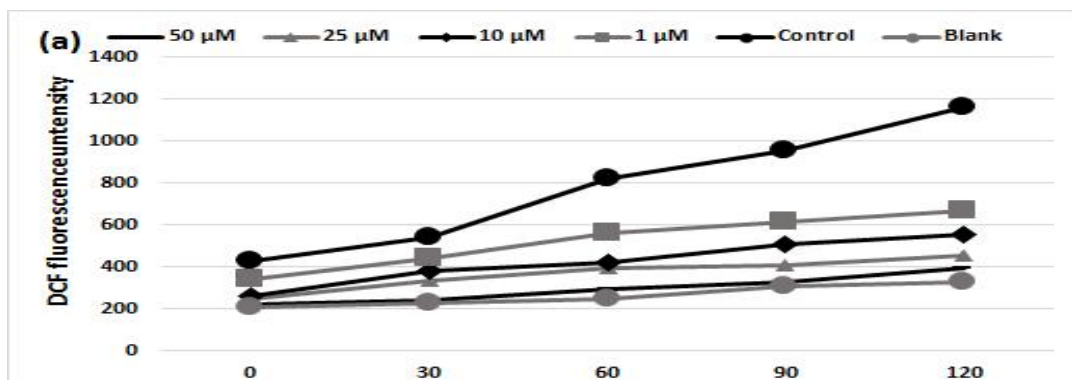
Fig. 23. Effect of compounds 1-9 from the sponge *Coscinoderma* sp. on viability of HT-1080 cells. ^{a-d}Means with the different letters are significantly different ($p < 0.05$) by Duncan's multiple range test.

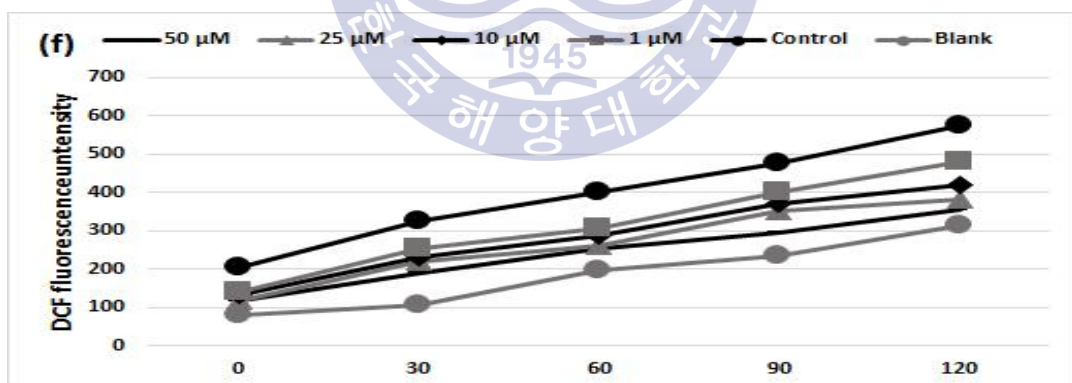
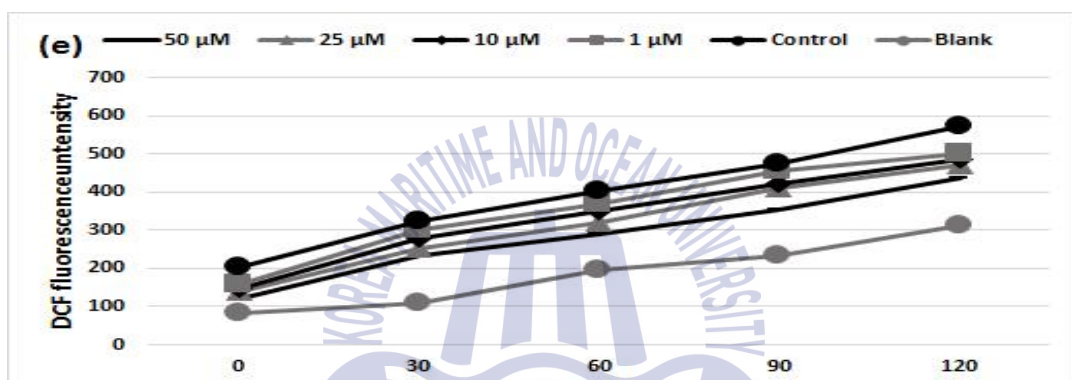
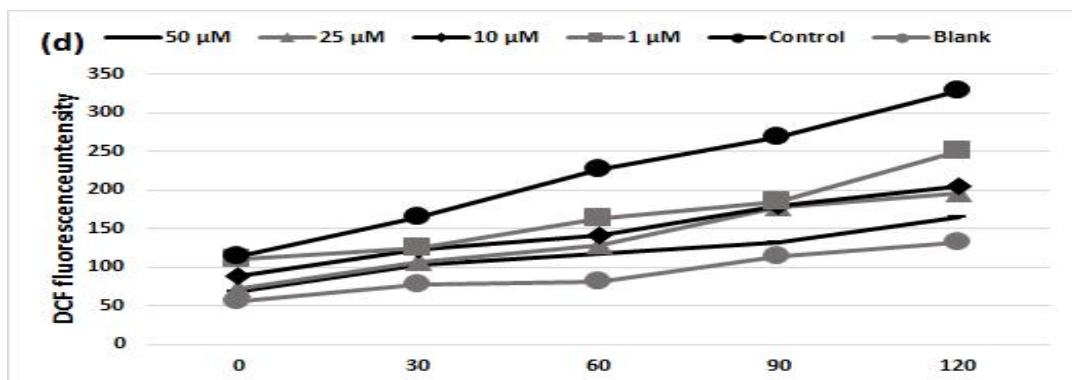


3.5.4.2. Determination of intracellular formation of ROS using DCFH-DA labeling

The radical scavenging effect of crude extract and its solvent fractions on the intracellular ROS was investigated in HT-1080 cells using DCFH-DA. DCFH-DA crosses cell membranes, and it is then outed off acetate group by intracellular esterase to non-fluorescein diacetate DCFH. It was oxidized through reactive oxygen and turned into fluorescent DCF. The radical scavenging effects were compared to the control that was treated $1 \times$ PBS instead of sample and treated with $500 \mu\text{M H}_2\text{O}_2$ and blank that wasn't treated with both sample and H_2O_2 . The degree of DCF fluorescence was determined at 0, 30, 60, 90 and 120 min. In the control, the degree of DCF fluorescence continued to increase whereas, in the blank, the degree of DCF fluorescence almost remained with time. All samples concentration-dependently inhibited the production of ROS.

The intracellular ROS scavenging ratios of compounds **1-6** were observed to be 91.9%, 96.4%, 84.4%, 83.1%, 52.0% and 83.9%, respectively, after incubation for 2 h at a concentration of $50 \mu\text{M}$, compared to control. The intracellular ROS scavenging ratios of compounds **7-9** were observed to be 68.2%, 79.9% and 79.6%, respectively, under the same condition but at a concentration of $100 \mu\text{M}$. Compounds **1** and **2** showed the good scavenging effect, and this result is shown in Fig. 24.





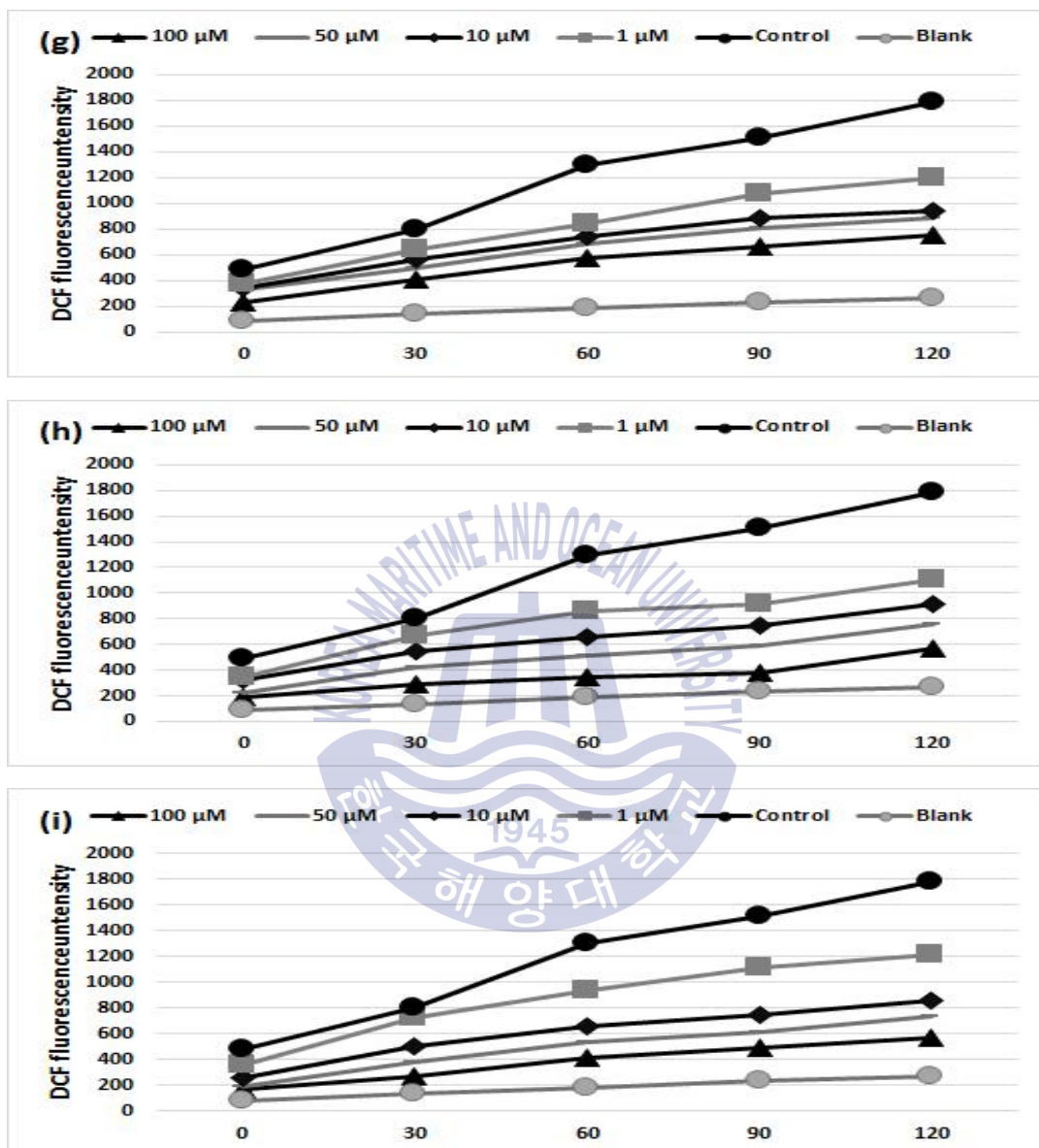


Fig. 24. Scavenging effects of compounds 1-9 from the sponge *Coscinoderma* sp. on intracellular ROS levels induced by hydrogen peroxide in HT-1080 cells. (a) compound 1; (b) compound 2; (c) compound 3; (d) compound 4; (e) compound 5; (f) compound 6; (g) compound 7; (h) compound 8; (i) compound 9.

3.6. Antiproliferative effects of compounds 1-9 on human cancer cells

Antiproliferative effects of compounds on the human tumour cell lines (HT-1080, AGS, HT-29 and MCF-7) were measured at the four different concentrations: for **1, 2, 7, 8** and **9**, 100, 50, 10 and 1 μM ; for **3, 4, 5** and **6**, 50, 25, 10 and 1 μM .

3.6.1 Antiproliferative effect against the growth of HT-1080 cells

HT-1080 (human fibrosarcoma) cells were treated with four different concentrations of the same sample for 24 h, and the antiproliferative effect was assessed using MTT assay. Compounds **1, 2, 3, 4, 6** and **8** showed a relatively significant effect on HT-1080 cells. Growth inhibitory rates of compounds **1, 2** and **8** were 42.9%, 43.4% and 38.7% against the HT-1080 cells, respectively, at a concentration of 100 μM . Also, growth inhibitory rates of compounds **3, 4** and **6** were 37.2%, 38.4% and 38.0% against the HT-1080 cells, respectively, at a concentration of 50 μM . This result is shown in Fig. 25. Of them, compound **1** showed the strongest antiproliferative effect.

3.6.2 Antiproliferative effect against the growth of AGS cells

AGS (human gastric carcinoma) cells were treated with four different concentrations of the same sample for 24 h, and the antiproliferative effect was assessed using MTT assay. Compound **2** exhibited the inhibitory rates of 36.0% against AGS cells at a concentration of 100 μM . Compound **4** exhibited the inhibitory rates of 32.3% against AGS cell at a concentration of 50 μM . This result is shown in Fig. 26

3.6.3 Antiproliferative effect against the growth of HT-29 cells

HT-29 (human colon cancer) cells were treated with four different concentrations of the same sample for 24 h, and the antiproliferative effect was assessed using MTT assay. Compounds **1** and **2** exhibited the inhibitory rates of 37.4% and 32.9% against the HT-29 cells, at a concentration of 100 μ M. Compound **4** exhibited the inhibitory rates of 39.4% against the HT-29 cells, at a concentration of 50 μ M. This result is shown in Fig. 27.

3.6.4 Antiproliferative effect against the growth of MCF-7 cells

MCF-7 (human breast cancer) cells were treated with four different concentrations of the same sample for 24 h, and the antiproliferative effect was assessed using MTT assay. Compounds **1** and **2** showed growth inhibitory rates of 40.2% and 39.5%, respectively, against the MCF-7 cells, at a concentration of 100 μ M. Among the sample tested, compound **1** had comparatively high antiproliferative effect on MCF-7 cells. This result was shown in Fig. 28.

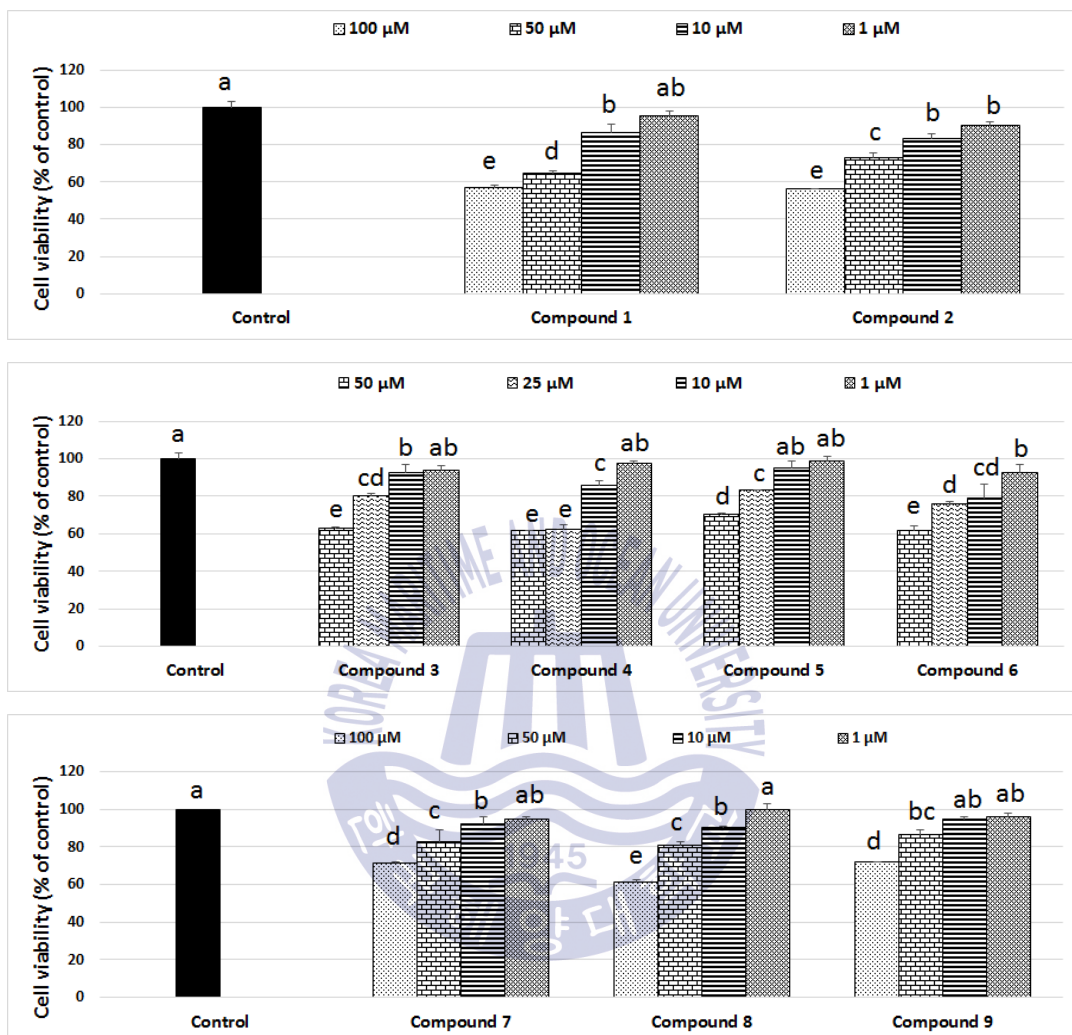


Fig. 25. Antiproliferative effect of compounds 1-9 from the sponge *Coscinoderma* sp. on viability of HT-1080 cells. ^{a-e}Means with the different letters are significantly different ($p < 0.05$) by Duncan's multiple range test.

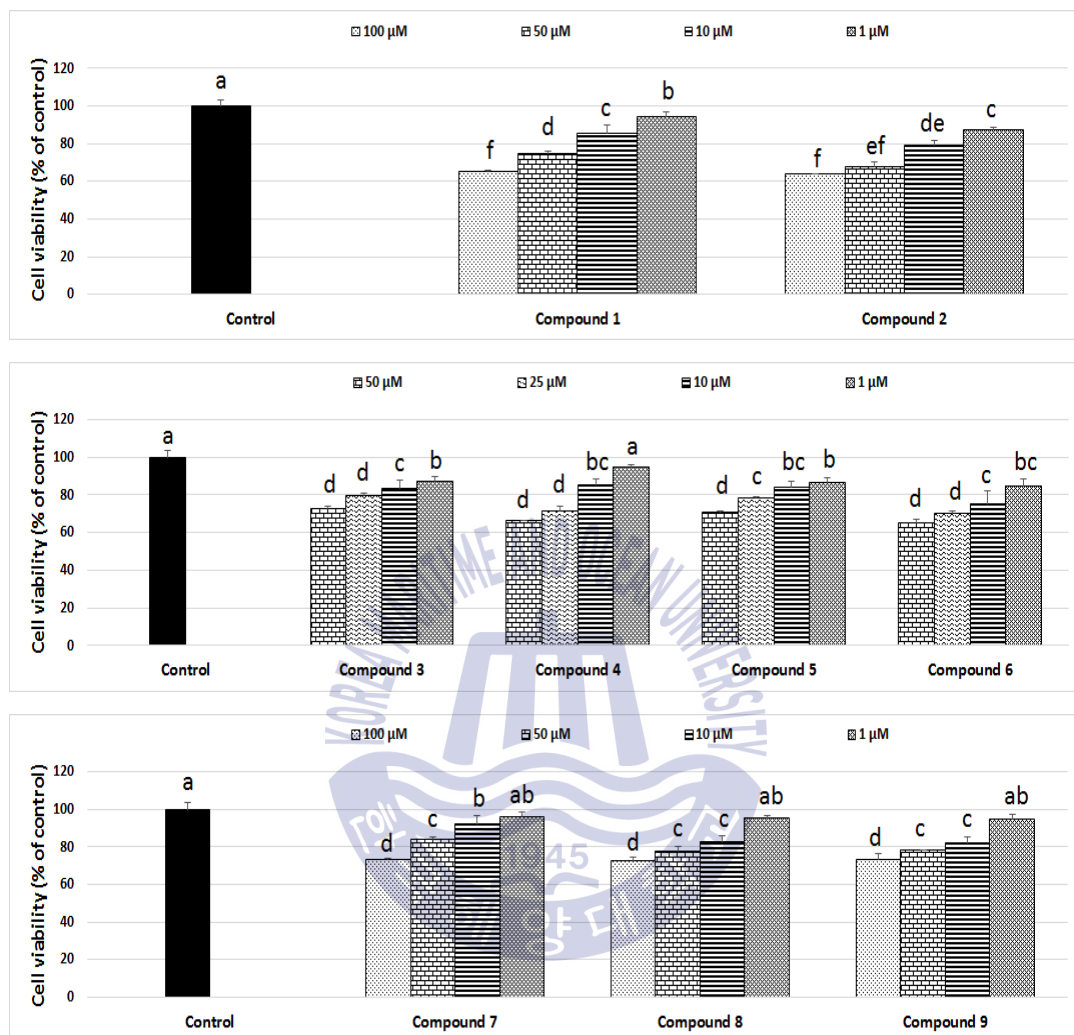


Fig. 26. Antiproliferative effect of compounds 1–9 from the sponge *Coscinoderma* sp. on viability of AGS cells. ^{a–f}Means with the different letters are significantly different ($p < 0.05$) by Duncan's multiple range test.

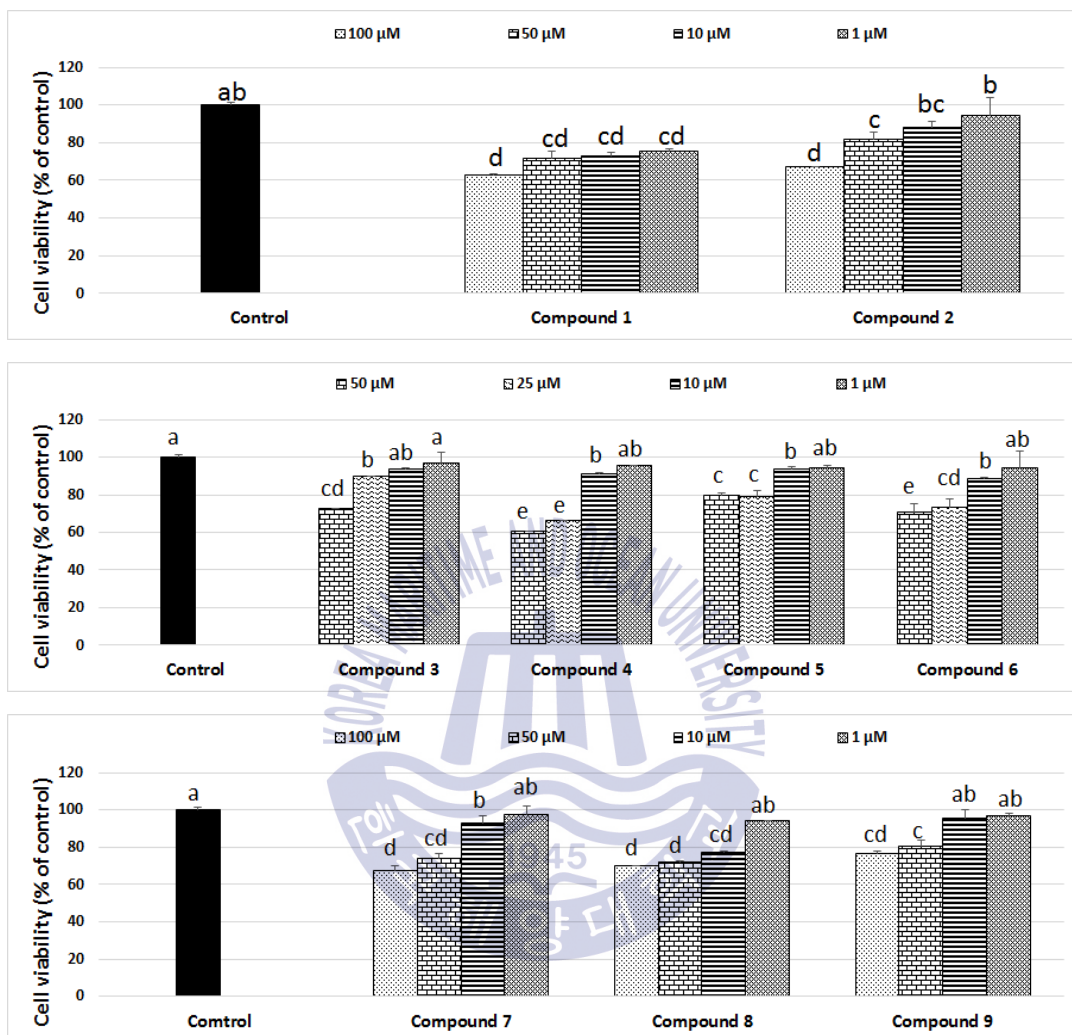


Fig. 27. Antiproliferative effect of compounds 1-9 from the sponge *Coscinoderma* sp. on viability of HT-29 cells. ^{a-e}Means with the different letters are significantly different ($p < 0.05$) by Duncan's multiple range test.

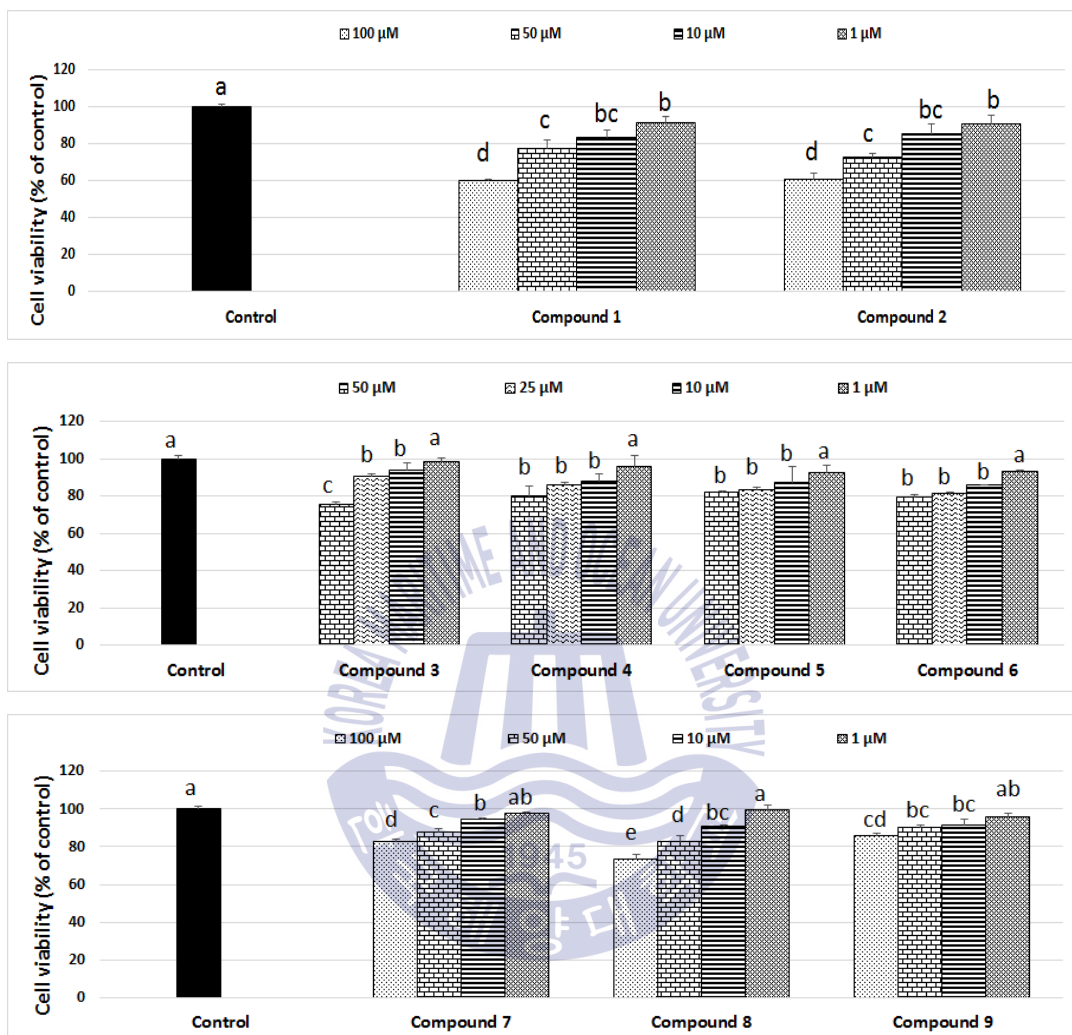
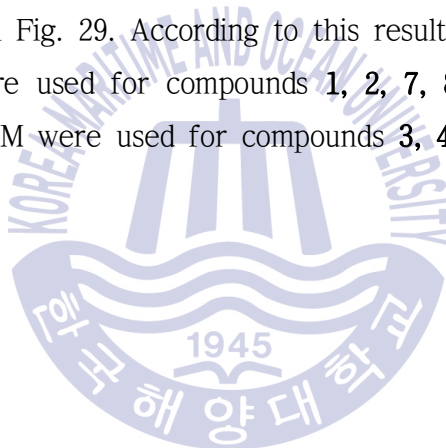


Fig. 28. Antiproliferative effect of compounds 1-9 from the sponge *Coscinoderma* sp. on viability of MCF-7 cells. ^{a-e}Means with the different letters are significantly different ($p < 0.05$) by Duncan's multiple range test.

3.7. Antiinflammatory effects of compounds 1-9

3.7.1 Measurement of cell viability by compounds 1-9 in Raw 264.7 cells

To avoid cytotoxic interference of compounds 1-9, the influence of the sample on cell viability of Raw 264.7 cells was determined using MTT assay. The cells were treated with 100 and 50 μ M of the sample for 1 h. Compounds 1, 2, 7, 8 and 9 showed a survival rate of 80% or more at 100 μ M and compounds 3, 4, 5 and 6 showed a survival rate of 80% or more at 50 μ M. This result is shown in Fig. 29. According to this result, concentrations of 100, 50, 10 and 1 μ M were used for compounds 1, 2, 7, 8 and 9. concentrations of 50, 25, 10 and 1 μ M were used for compounds 3, 4, 5 and 6.



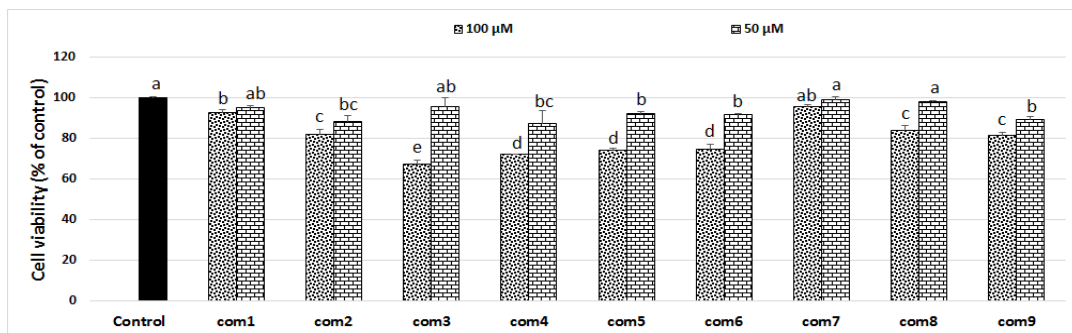
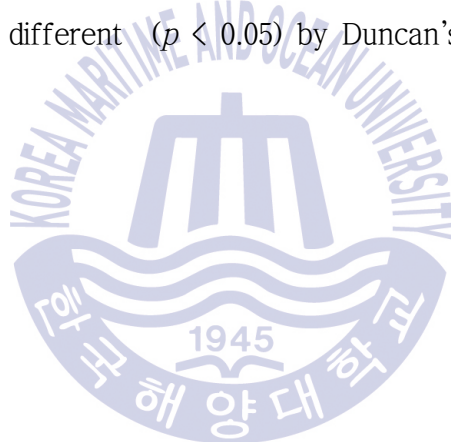


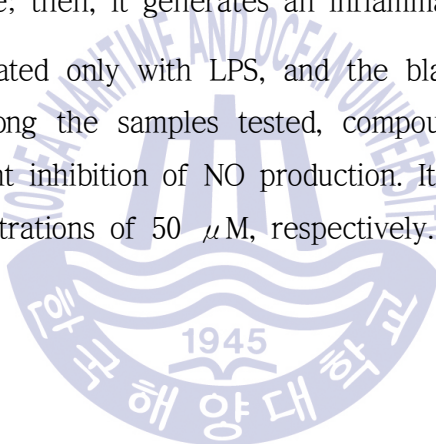
Fig. 29. Effect of compounds 1-9 from the sponge *Coscinoderma* sp. on viability of Raw 264.7 cells. ^{a-e}Means with the different letters are significantly different ($p < 0.05$) by Duncan's multiple range test.



3.7.2. Determination of nitric oxide (NO) production.

The anti-inflammatory effect of compounds **1-9** on NO production was investigated on Raw 264.7 cells by treating LPS. LPS is the cell envelope constituents of gram-negative bacillus; it has a strong stimulating effect on various cells such as monocytic cells and macrophages. In particular, macrophages are activated by LPS stimulation; after that; release and produce inflammatory mediators, such as NO. Excessive secretion of NO is changed to a reactive nitric oxide by the reaction of O_2 , O_2^- in vivo. It leads to oxidative stress and DNA damage; then, it generates an inflammatory disease.

The control was treated only with LPS, and the blank wasn't treated both samples and LPS. Among the samples tested, compounds **3**, **5** and **6** had a comparatively significant inhibition of NO production. Its ratios of 77.6%, 70.6% and 80.0% at a concentrations of 50 μ M, respectively. This result is shown in Fig. 30.



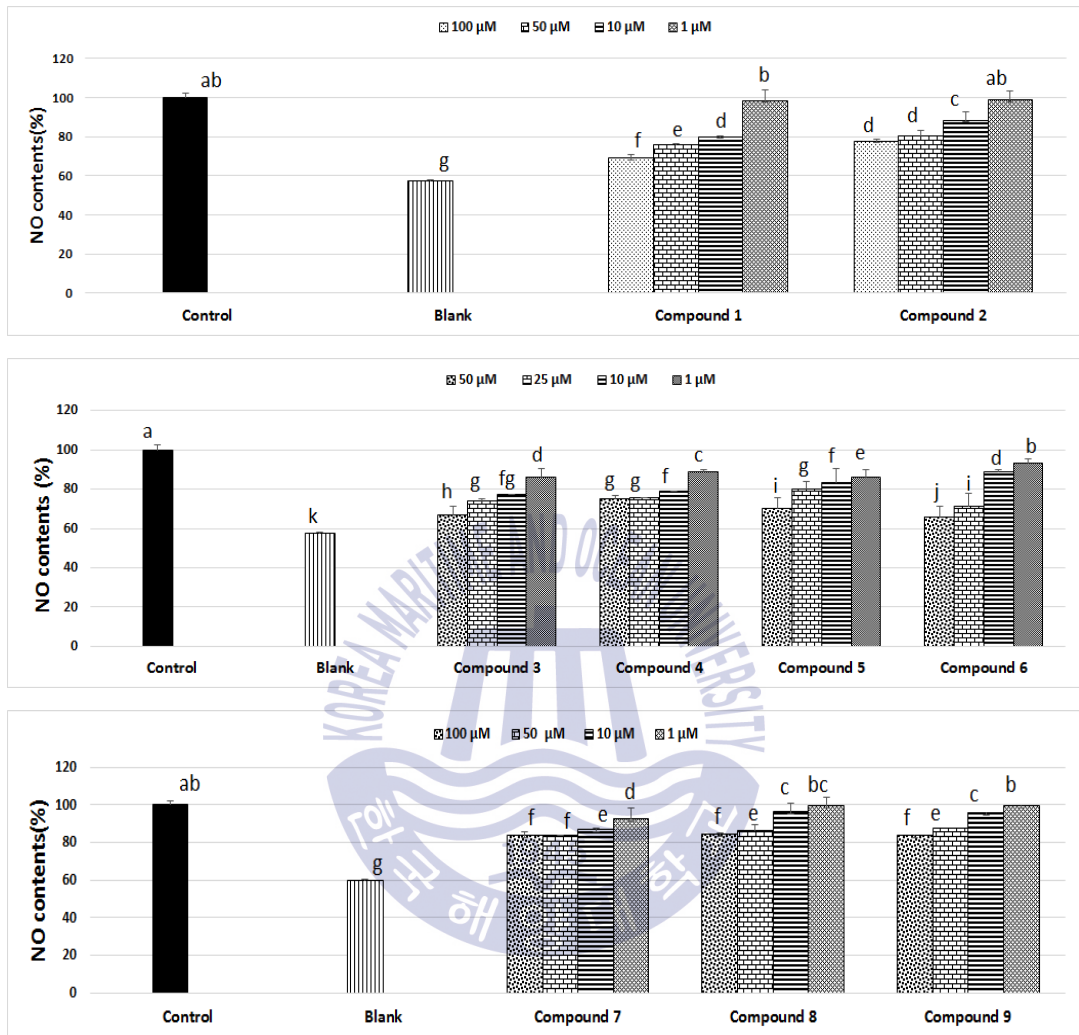


Fig. 30. Effects of compounds 1-9 from the sponge *Coscinoderma* sp. on nitrite production in Raw 264.7 cells. ^{a-k}Means with the different letters are significantly different ($p < 0.05$) by Duncan's multiple range test.

4. Conclusion

Since chemical investigation on marine organisms began in the 1960s, intensive research on them has been mainly conducted by developed countries. As a result, many biologically interesting substances have been isolated from marine organisms. Although the numbers of drugs developed from the sea are less than those of terrestrial plants and microbes, the published papers on marine natural products are already greatly surpassing the number of studies of terrestrial sources, a traditional repository of medicines. Among marine organisms, sponges are the richest source of structurally unique and biologically active substances which have been found until now.

The sponge *Coscinoderma* sp. was collected from off the shore of Chuuk Island, Federated States of Micronesia. The dried samples of the sponge were extracted with organic solvent. The crude extract was successively fractionated into *n*-hexane, 85% aq.MeOH, *n*-BuOH and water fractions by solvent polarity. Antioxidant activities of the crude extracts and their solvent fractions were evaluated by four different assay systems: scavenging power on DPPH radical, peroxy nitrite, and intracellular ROS produced in HT-1080 cells; ferric reducing antioxidant power (FRAP). In DPPH radical and FRAP assays, *n*-BuOH fraction showed the highest activity. In peroxy nitrite assay, all the fractions except water fraction showed the significant scavenging effect on authentic peroxy nitrite while the 85% aq.MeOH and *n*-BuOH fractions exhibited the significant scavenging effect on peroxy nitrite derived from SIN-1. For intracellular ROS produced in HT-1080 cells, *n*-BuOH fraction revealed the strongest scavenging effect on it, compared with the blank at a concentration of 50 $\mu\text{g/mL}$. To summarize, *n*-BuOH fraction showed the most

potent antioxidant activity in four different assay systems.

Antiinflammatory effect of the crude extract and its solvent fractions was investigated by measuring NO contents and protein expression of pro-inflammatory mediators produced in Raw 264.7 cells stimulated with LPS. The 85% aq.MeOH and *n*-BuOH fractions significantly inhibited production of nitric oxide and suppressed expression levels of proinflammatory mediators (iNOS, COX-2, IL-1 β , IL-6, and TNF- α) at a concentration of 50 μ g/mL. In cytotoxicity assay, *n*-BuOH fraction exhibited the good inhibition effect against four types of human cancer cells: 40.4% for HT-1080; 31.7% for AGS; 34.7% for HT-29; 43.1% for MCF-7 at a concentration of 100 μ g/mL.

Nine compounds were isolated from *Cosciniderma* sp. and their chemical structures were determined by extensive 2D NMR experiments and by comparison with published spectral data. Halisulfate 1 (1), 2' -deoxyadenosine (7), 2' -deosyridine (8) and thymidine (9) were separated from *n*-BuOH fraction. Halisulfate 2 (2) was separated from 85% aq.MeOH fraction. Four epidioxy steroids, (24S)-5,8-epidioxy-24-methylcholest-6-en-3 β -ol (3), 5 α ,8 α -epidioxycholesta-6,22-dien-3 β -ol (4), 5 α ,8 α -Epidioxycholesta-6-en-3b-ol (5), and 5 α ,8 α -Epidioxycholesta-6,9(11)-dien-3b-ol (6) were separated from *n*-hexane fraction.

Antioxidant, antiinflammatory and cytotoxic effect were also evaluated for the isolated compounds. In antioxidant assay systems, compounds **1** and **2** showed their scavenging ratios of 65.7% and 70.4% on authentic peroxy nitrite at a concentration of 100 μ M, respectively; 72.3% and 62.4% on peroxy nitrite from SIN-1 at the same concentration, respectively. In addition, compounds **1** and **2** exhibited the potent scavenging activity of 98.4% and 96.4% on intracellular ROS produced in HT 1080 cells at a concentration of 50 μ M, respectively. On the other hand, compounds **1**, **2** and **4** inhibited significantly growth against four types of human cancer cells (HT-1080, AGS, HT-29 and MCF-7) while compounds **3**, **5** and **6** inhibited significantly production of NO in LPS-stimulated Raw 264.7 cells.

Reference

Anderson C. D., Goodman L. & Baker B. R., Showing metabocard for Deoxyadenosine (HMDB00101) [Online] (2016-02-13 02:07:07 UTC) Available at : <http://www.hmdb.ca/metabolites/HMDB00101>.

Kim Y.J. & Son D.Y., 2014. Inflammatory mediator regulation of the *Zizyphus jujube* leaf fractions in the LPS-stimulated Raw264.7 mouse macrophage. *Korean J. Food Preserv*, 21, pp.114-120.

Kim Y.S. et al., 2011. Effect of hotwater extract of *Undaria pinnatifida* on the activities of antioxidant and nitrite scavenging. *KSBB J.*, 26, pp.151-156.

Beda N. & Nedospasov A., 2005. A spectrophotometric assay for nitrate in and excess of nitrite. *Nitric Oxide*, 13, pp.93-97.

Blois M.S., 1958. Antioxidant determinations by the use of a stable free radical. *Nature*, 181, pp.119-1200.

Crews P., Manes L.V. & Boehler M., 1986. Jasplakinolide, a cyclodepsipeptide from the marine sponge, *Jaspis*. sp. *Tetrahedron Letters*, 27, pp.2797-2800.

Faulkner D.J., 1997, Marine natural products. *Nat. Prod. Rep.*, 14, pp.259-302.

Gunatilaka A.A.L., Gopichand Y., Schmitz F.J. & Djerassi C., 1981. Minor and Trace Sterols in Marine Invertebrates. 26. Isolation and Structure Elucidation of Nine New 5α , 8α -Epidioxy Sterols from Four Marine Organisms. *J. Org. Chem*, 46, pp.3860-3866.

Greca M.D. et al., 1990. 5β , 8β -Epidioxyergosta-6, 22-dien-3 β -ol from *Typha latifolia*. *Gazz. Chim. Ital.*, 120, pp.391-392.

Green L.C. et al., 1982. Analysis of Nitrate, Nitrite, and [^{15}N] Nitrate in

Biological Fluids. *Anal. I Biochem*, 126, pp.131-138.

Hansen M.B., Nielsen S.E. & Berg K., 1989. Re-examination and further development of a precise and rapid dye method for measuring cell growth/cell kill. *J.Immunol. Meth*, 119, pp.203-210.

Hirata Y. & Uemura D., 1986. Halichondrins - antitumor polyether macrolides from a marine sponge. *Pure and Applied Chemistry*, 58, pp.701-710.

Ioannou E. et al., 2009. 5α , 8α -Epidioxysterols from the gorgonian *Eunicella cavolini* and the ascidian *Trididemnum inarmatum*: Isolation and evaluation of their antiproliferative activity. *Elsevier Inc*, 74, pp.73-80.

Kernan M.R. & Faulkner D.J. 1988. Sesterterpene sulfates from a sponge of the family halichondriidae. *J. Org. Chem*, 53, pp.4574-4578.

Kazuo I., Hiromi S., Zhi Y & Yasuji Y., 1993. A new 5α , 8α -epidioxy sterol from the Okinawan marine sponge of the *Axinyssa* genus. *Steroids*, 58, pp.410-413.

Kooy N.W., Royall H., Ischiropoulos H. & Beckman J.S., 1994. Peroxynitrite-mediated oxidation of dihydrorhodamine 123. *Free Radicic. Biol. Med*, 16, pp.149-156.

Martin M.J. et al., 2013. Isolation and First Total Synthesis of PM050489 and PM060184, Two New Marine Anticancer Compounds. *J. Am Chem. Soc*, 135, pp.10164-10171.

Molinski T.F., Dalisay D.S., Lievens S.L. & Saludes J.P., 2009. Drug development from marine natural products. *Drug Discovery*, 8, pp.69-85.

Newman D.J. & Cragg G.M., 2016. Drugs and Drug Candidates from Marine Sources: An Assessment of the Current "State of Play". *Planta Med*, 82, pp.775-789.

Okimoto Y. et al., 2000. A novel fluorescent probe diphenyl-1-1-pyrenylphosphine to follow lipid peroxidation in cell membranes.

FEBS Lett, 474, pp.137-140.

Oyaizu M., 1986. Studies on products of browning reaction. Antioxidative activities of products of browning reaction prepared from glucosamine. *Jpn. J. Nutr.* 44, pp.307-315.

Qiu C. et al., Spectral peak data for bmse000320, 2'-Deoxyuridine, 1D 1H, pH: 7.4 [Online] Available at : http://www.bmrwisc.edu/metabolomics/mol_summary/show_data.php?molName=2_Deoxyuridine&id=bmse000320.

Qiu C. et al., Assigned Chemical shifts for bmse000244, Thymidine [Online] Available at : http://bmrwisc.edu/metabolomics/mol_summary/show_data.php?molName=thymidine&id=bmse000244&whichTab=1.

Sera Y., Adachi K. & Shizuri Y., 1999. A New Epidioxy sterol as an Antifouling Substance from a Palauan Marine Sponge, *Lendenfeldia chondrodes*. *J. Nat. Prod.* 62, pp.152-154.

Shin J. et al., 2000. New Bromotyrosine Metabolites from the Sponge *Aplysinella rhax*. *Tetrahedron*, 56, pp.9071-9077.

Silva E.D. & Scheuer P.J., 1980. Manoalide, an antibiotic sesterterpenoid from the marine sponge *Luffariella variabilis* (polejaeff). *Tetrahedron Letters*, 21, pp.1611-1614.

Twentyman P.R & Luscombe M., 1987. A study of some variables in a tetrazolium dye (MTT) based assay for cell growth and chemosensitivity, *British Journal of Cancer*, 56, pp.279-285.

Zabriskie T.M. et al., 1986. Jaspamide, a modified peptide from a Jaspis sponge, with insecticidal and antifungal activity. *J. Am. Chem. Soc.* 108, pp.3123-3124.

Appendix

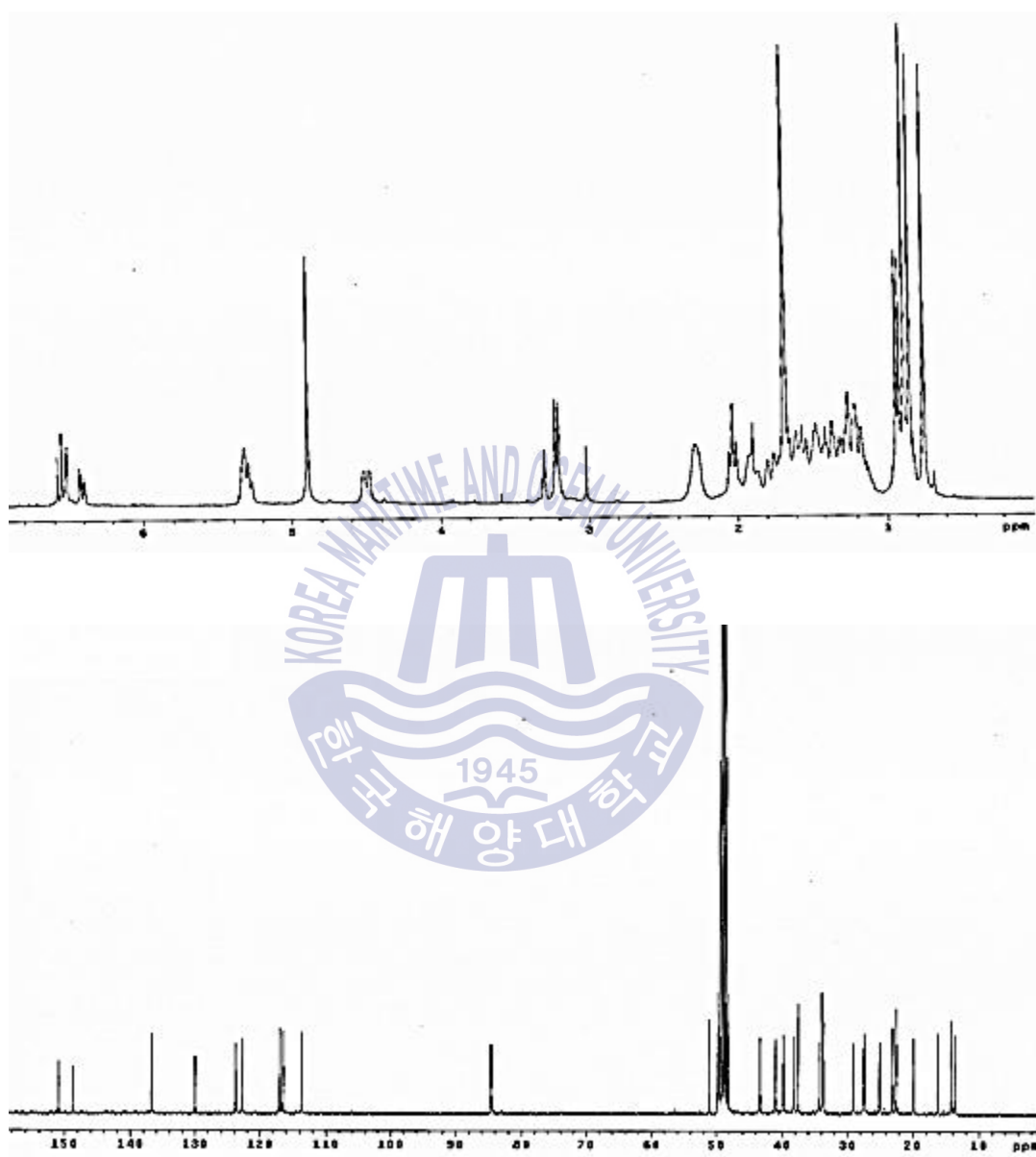


Fig. 31. ^1H and ^{13}C NMR spectrum of compound **1** isolated from the sponge *Coscinoderma* sp. in CD_3OD .

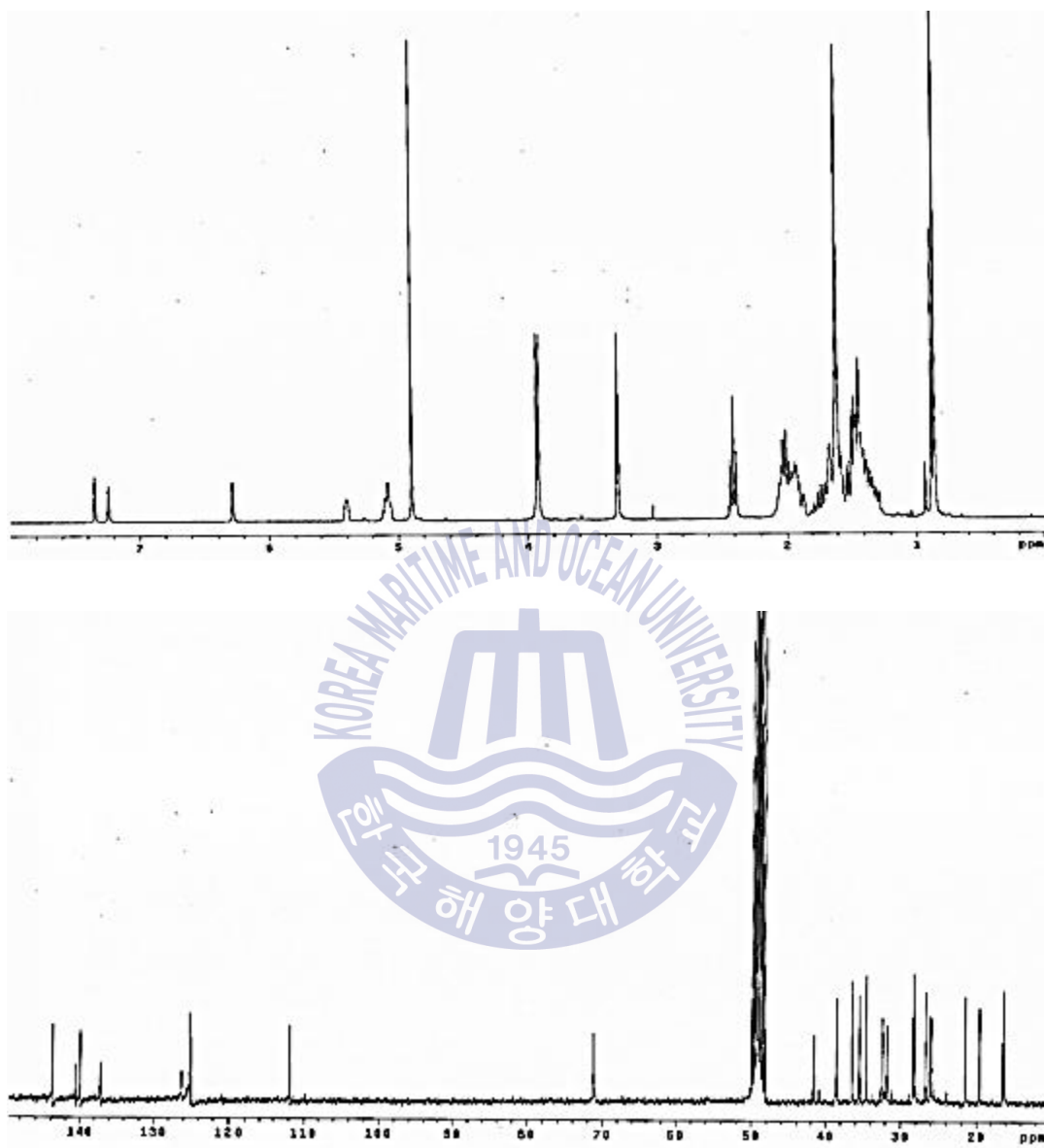


Fig. 32. ^1H and ^{13}C NMR spectrum of compound 2 isolated from the sponge *Coscinoderma* sp. in CD_3OD .

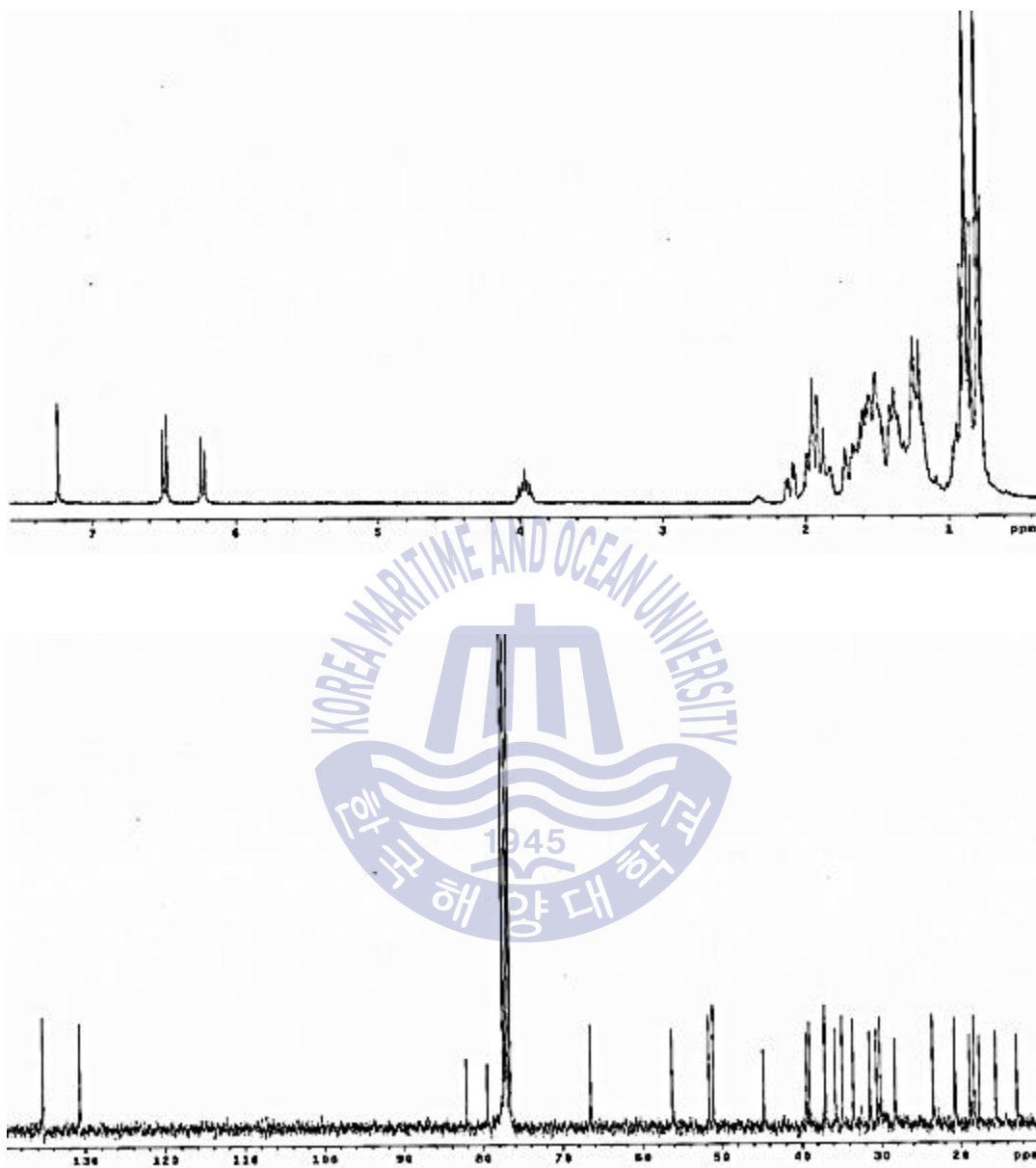


Fig. 33. ^1H and ^{13}C NMR spectrum of compound **3** isolated from the sponge *Coscinoderma* sp. in CDCl_3 .

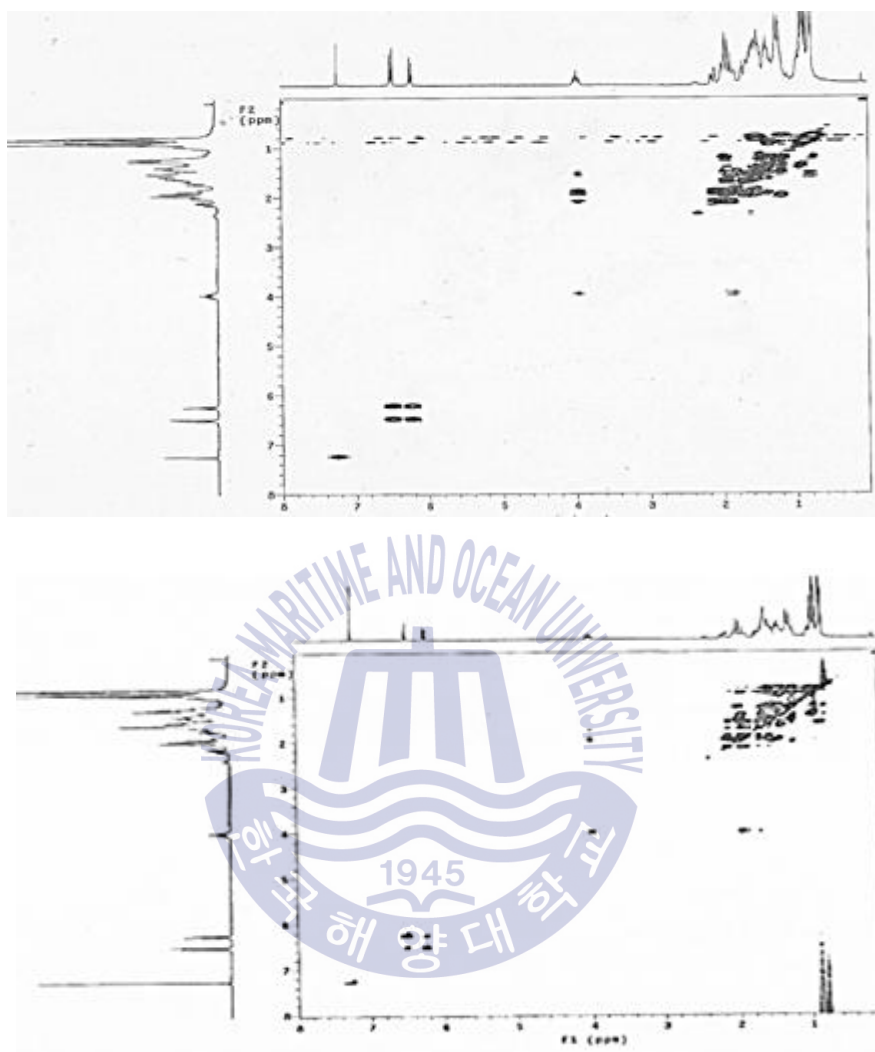


Fig. 34. ^1H COSY and TOCSY spectrum of compound **3** isolated from the sponge *Coscinoderma* sp. in CDCl_3 .

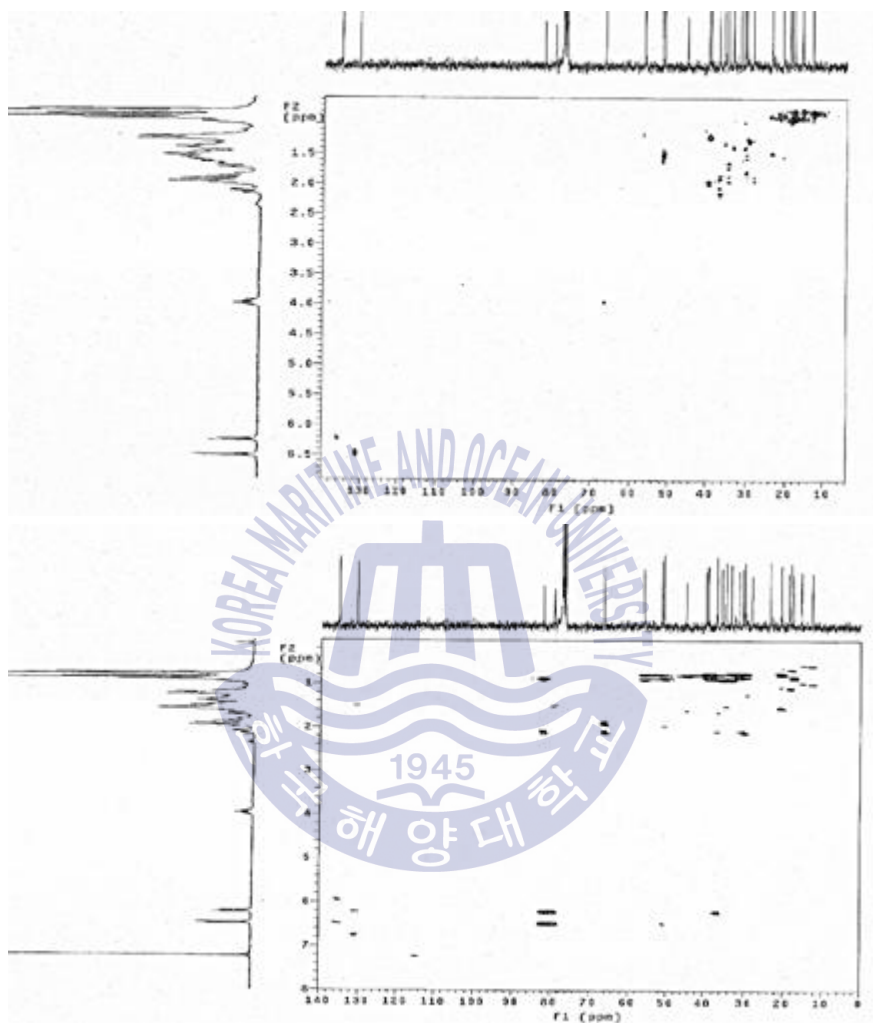


Fig. 35. gHMQC and gHMBC spectrum of compound **3** isolated from the sponge *Coscinoderma* sp. in CDCl₃.

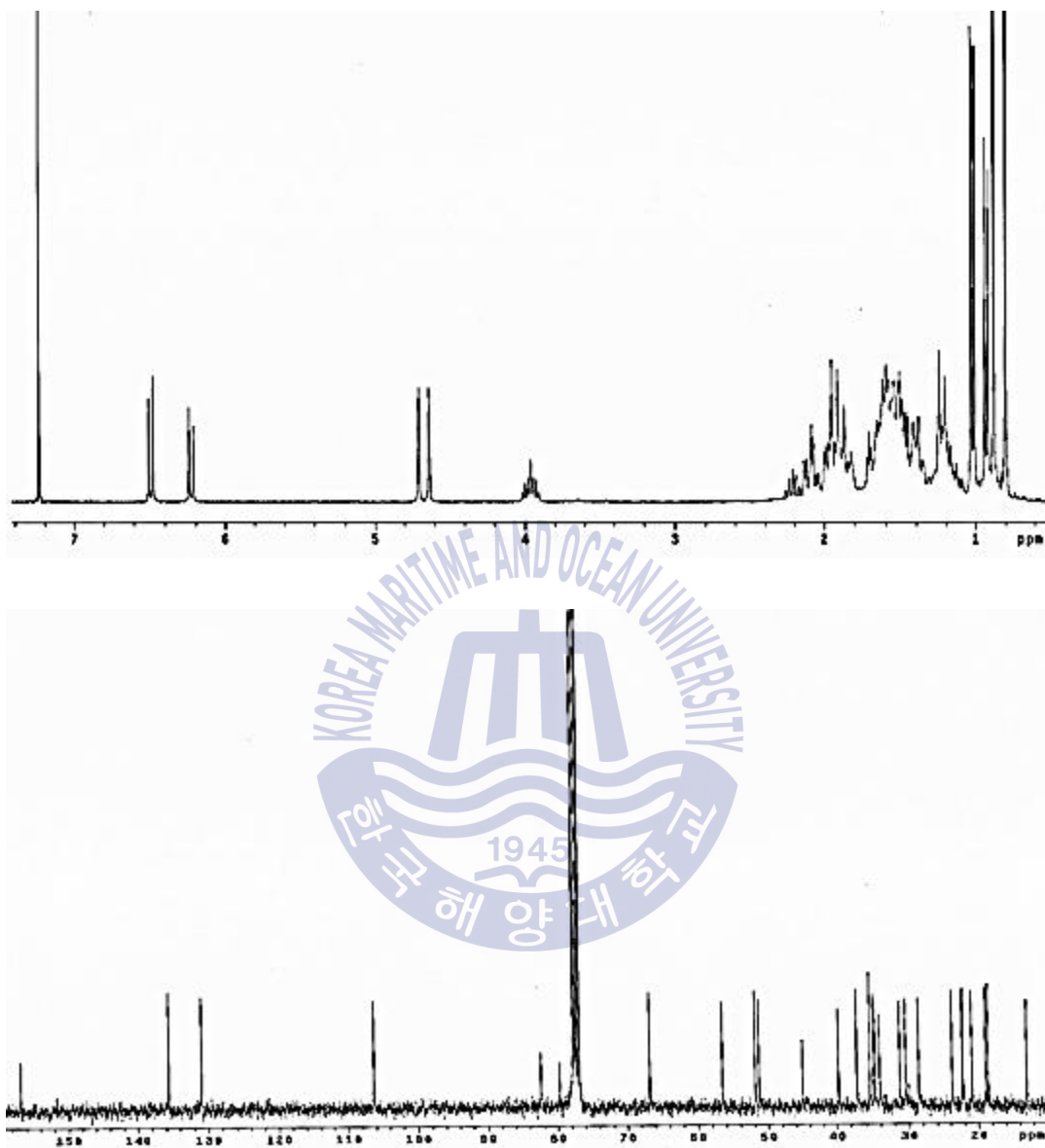


Fig. 36. ^1H and ^{13}C NMR spectrum of compound **4** isolated from the sponge *Coscinoderma* sp. in CDCl_3 .

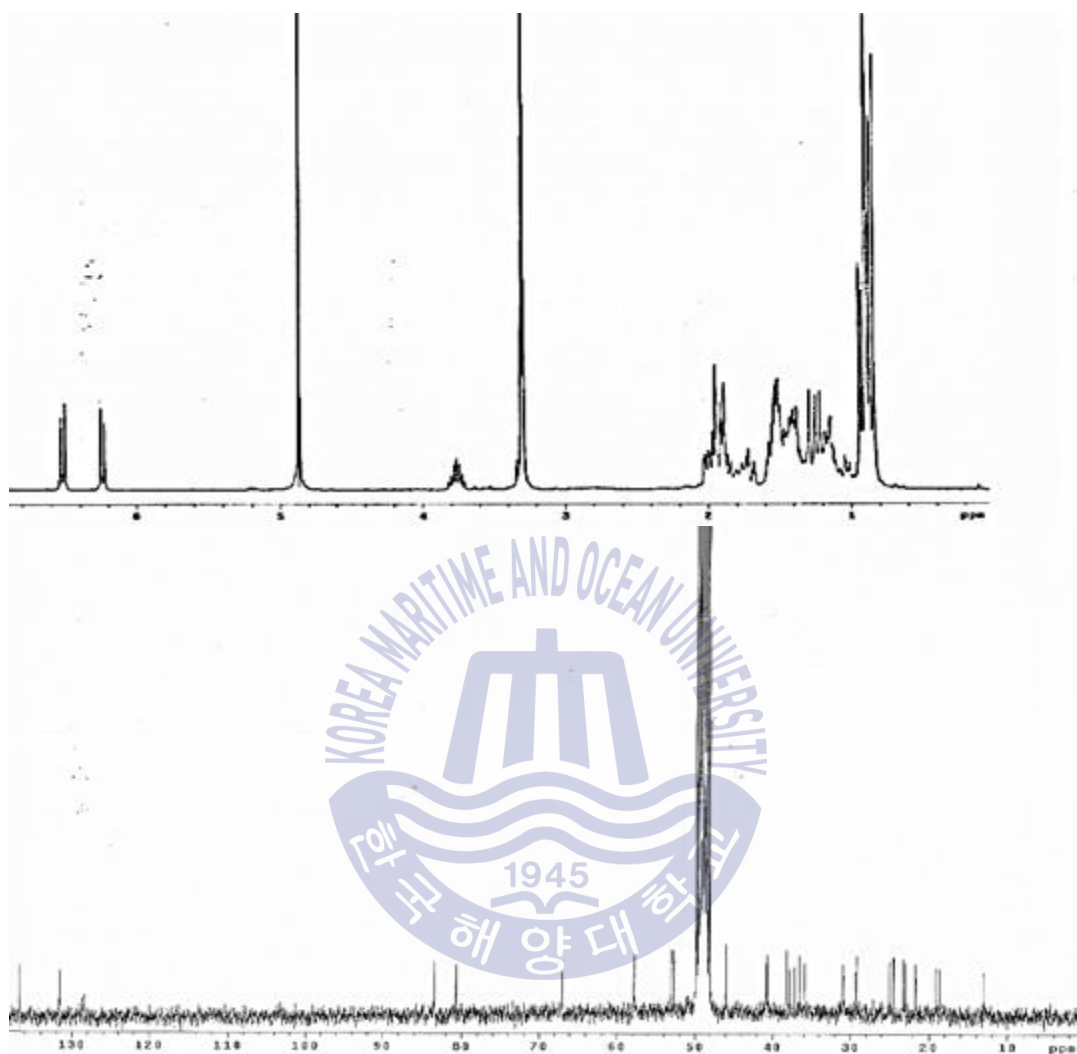


Fig. 37. ^1H and ^{13}C NMR spectrum of compound 5 isolated from the sponge *Coscinoderma* sp. in CD_3OD .

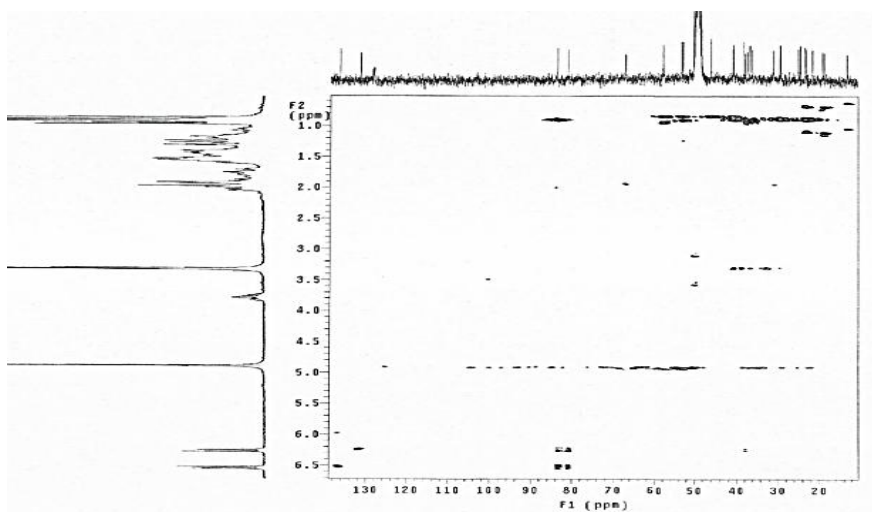
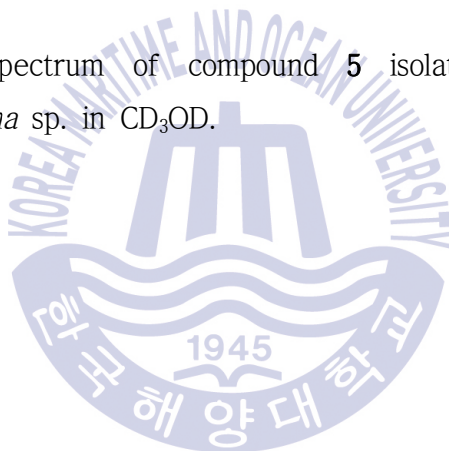


Fig. 38. gHMBC spectrum of compound **5** isolated from the sponge *Coscinoderma* sp. in CD₃OD.



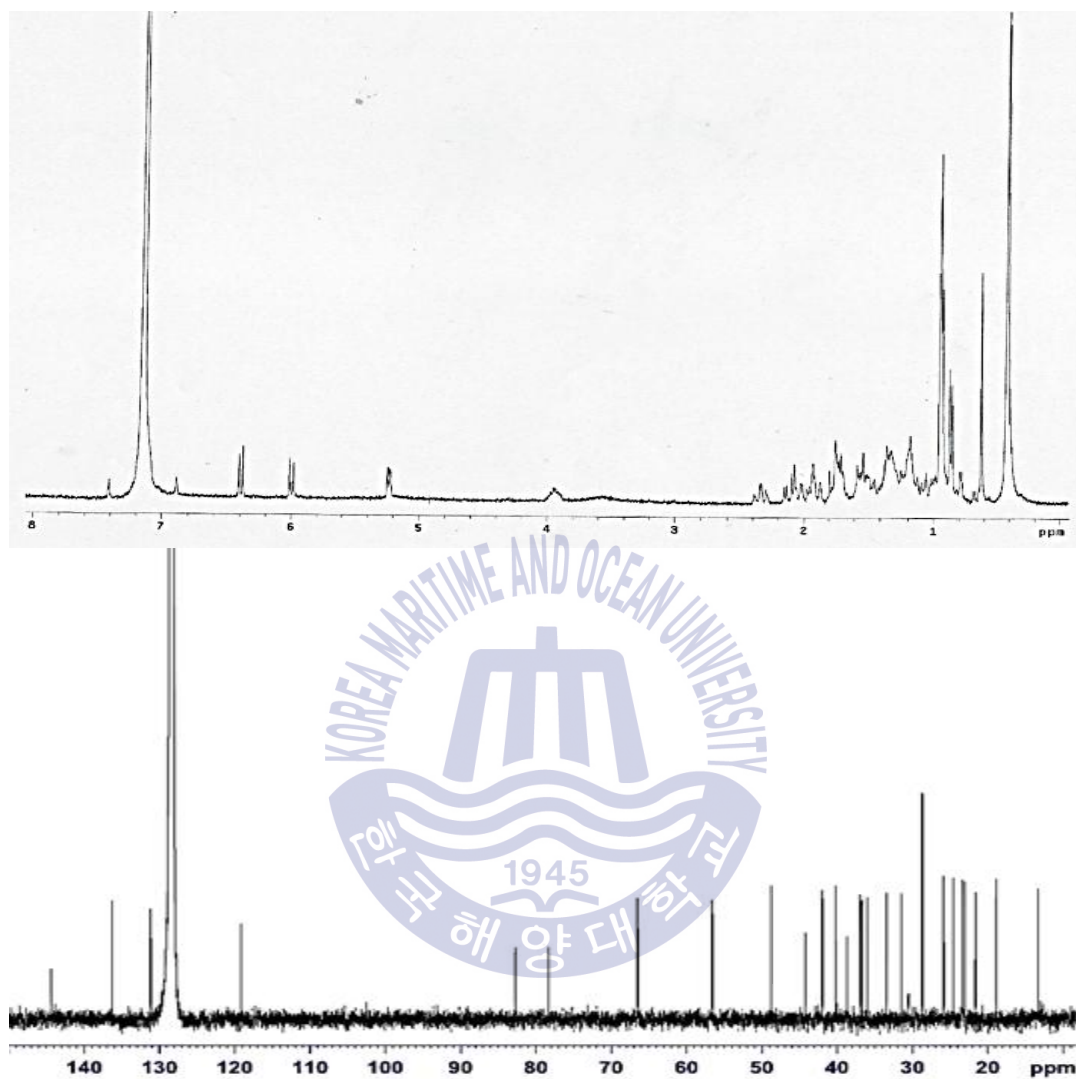


Fig. 39. ^1H and ^{13}C NMR spectrum of compound **6** isolated from sponge the *Coscinoderma* sp. in benzene- D_6 .

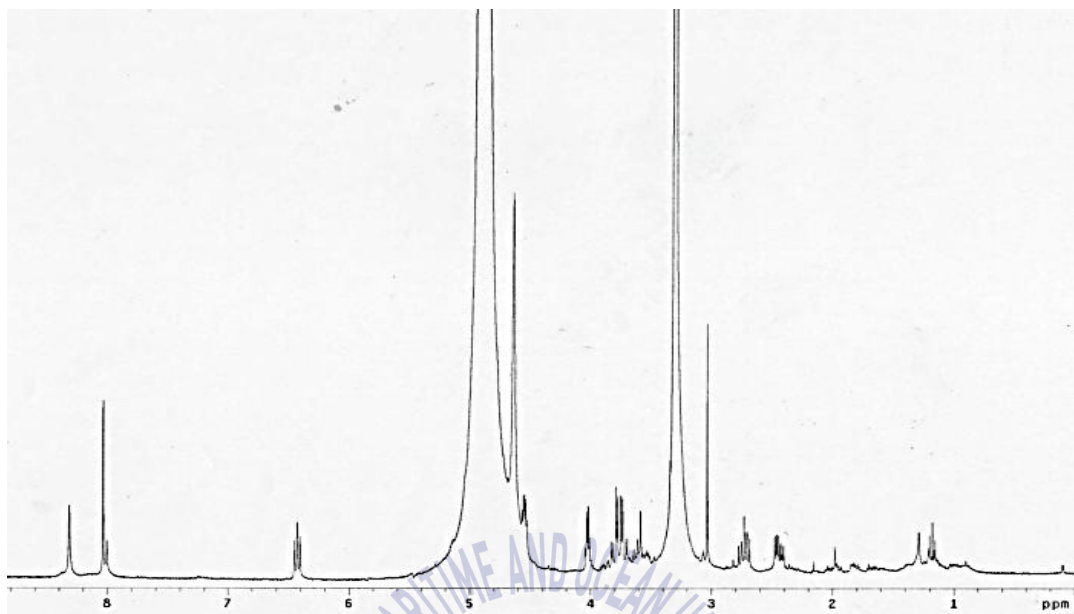
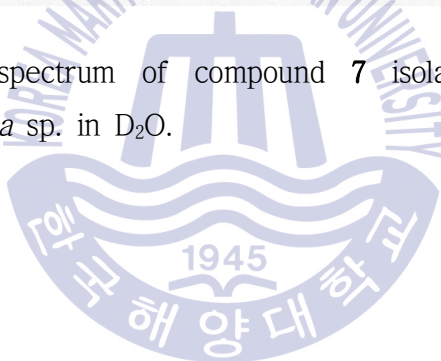


Fig. 40. ^1H NMR spectrum of compound **7** isolated from the sponge *Coscinoderma* sp. in D_2O .



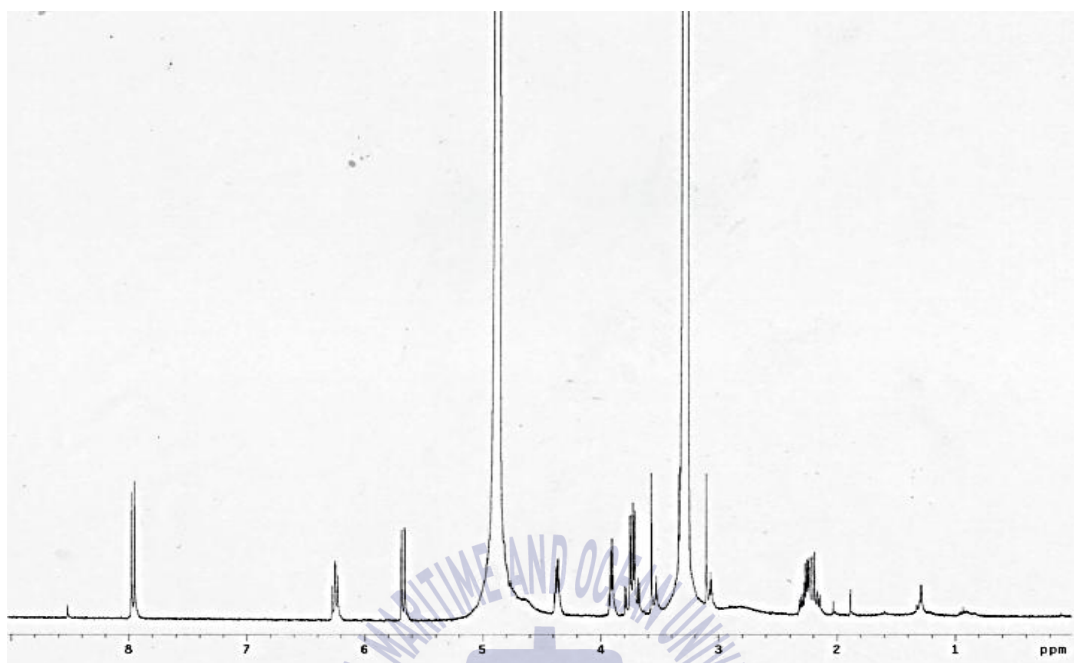


Fig. 41. ^1H NMR spectrum of compound **8** isolated from the sponge *Coscinoderma* sp. in D_2O .

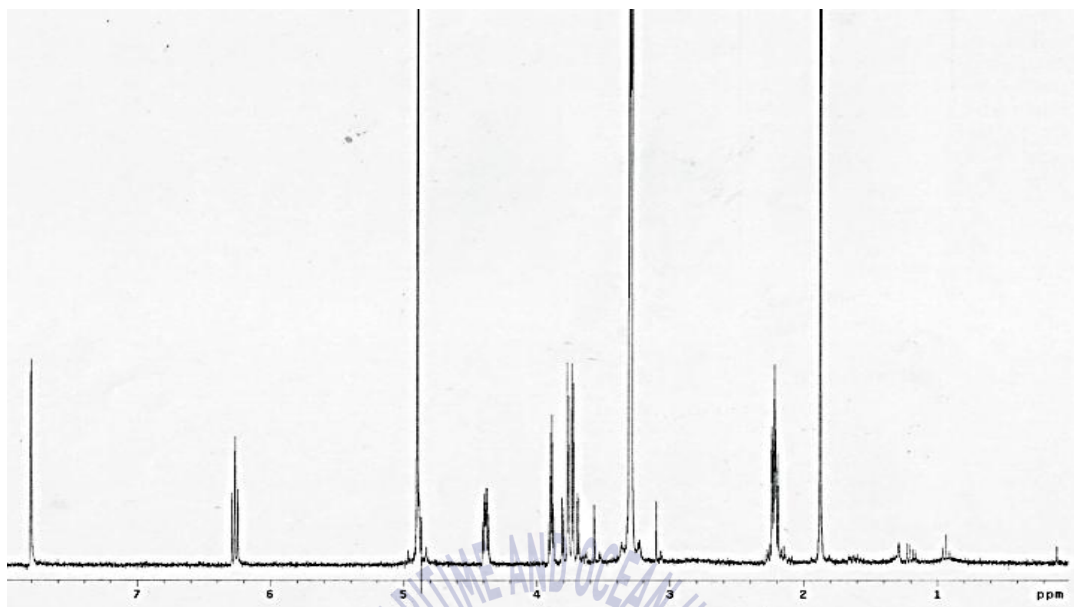
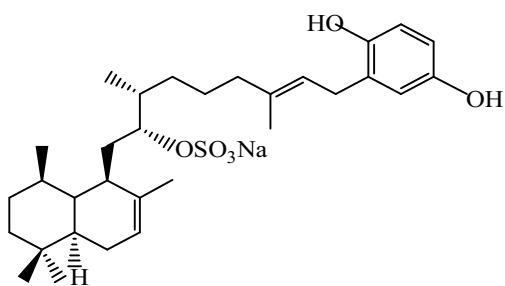
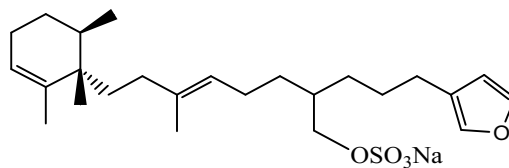


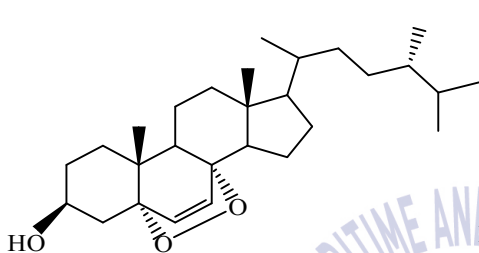
Fig. 42. ¹H NMR spectrum of compound **9** isolated from sponge *Coscinoderma* sp. in D₂O.



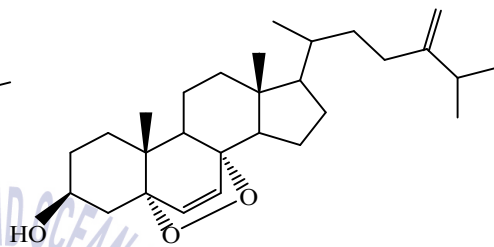
Compound 1



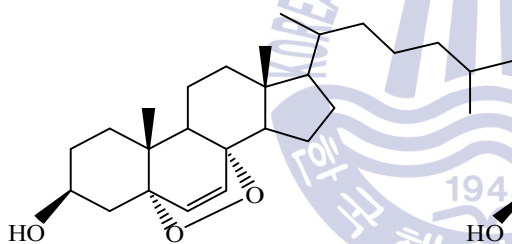
Compound 2



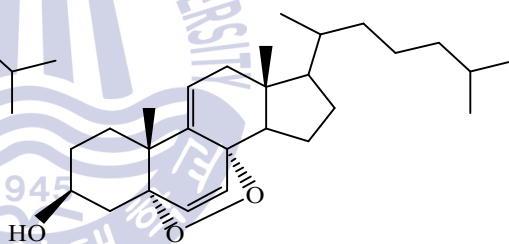
Compound 3



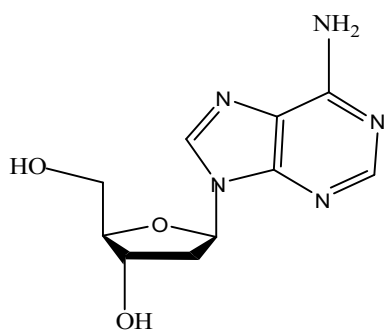
Compound 4



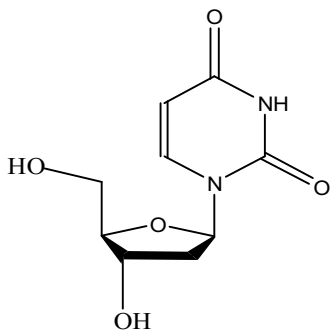
Compound 5



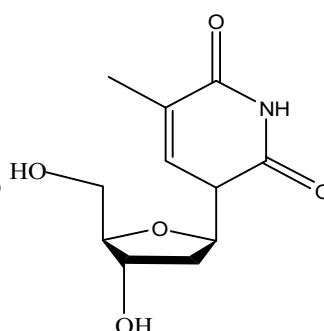
Compound 6



Compound 7



Compound 8



Compound 9